MASS. INST. OF TECHNOLOGY
JUN 27 1960
LIBRARY

CONTROLLED EXTERNALLY PRESSURIZED BEARINGS

by

John Erdmond Mayer, Jr.

B. S., Illinois Institute of Technology
(1952)

S. M., Massachusetts Institute of Technology
(1954)

Mech. E., Massachusetts Institute of Technology
(1957)

SUBMITTED IN PARTIAL FULFILLMENT
OF THE REQUIREMENTS FOR THE
DEGREE OF DOCTOR OF
SCIENCE

at the

MASSACHUSETTS INSTITUTE OF
TECHNOLOGY

June, 1960

Signature of Author. .....
Department of Mechanical Engineering
May 14, 1960

Certified by.. .....
Thesis Supervisor
Professor of Mechanical Engineering

Accepted by.....
Chairman, Departmental Committee
on Graduate Students

CONTROLLED EXTERNALLY PRESSURIZED BEARINGS

by

ohn Erdmond Mayer, Jr.

Submitted to the Department of Mechanical Engineering on May 14, 1960, in partial fulfiliment of the requirements for the degree of Doctor of Science.

ABSTRACT

This investigation is concerned with the improvement of the static stiffness of externally pressurized fluid bearings. The bearing considered was the radial type bearing. The term static stiffness refers to the slope of the journal static load versus displacement curve for the bearing. A variable external flow restriction was employed in place of the conventional fixed external flow restriction as a means for improving the bearing static stiffness. The flow resistance of the variable external flow restriction was automatically adjusted by the internal pressures of the bearing and hence, this device was a load sensing control. The variable external flow restriction employed was a spool valve with variable flow length.

The bearing static stiffness was determined by experimental and analytical means for the case of fixed external flow restrictions and the case of variable external flow restrictions for both incompressible and compressible fluid supplies. The experimental determinations for the incompressible fluid case were made for the non-rotational journal condition and for the compressible fluid case they were made for both the non-rotational and rotational journal condition. The incompressible fluid and compressible fluid which were employed were water and air respectively.

The results show that the variable external flow restriction offers a means of greatly improving the bearing static stiffness for incompressible fluid supplies and shows promise for a similar result for compressible fluid supplies. The results for the former case show that the bearing static stiffness can be increased by a factor of at least 25. The maximum bearing static stiffness attained for this case was at least 50×10^6 lb./in. which is comparable with the stiffness of rolling contact bearings. The results for the latter case show that the bearing static stiffness can be increased by a factor of 2; however, greater static stiffnesses should also be possible. The maximum bearing static

stiffness attained for this case was 13,400 lb./in. Before employing the variable external flow restriction in the compressible fluid supply case, the bearing had to be first stabilized by means of fixed orifice restrictions which were placed in the bearing feed ports. The rotational tests show that the journal rotation improves the bearing static stiffness. The tests were carried out up to 6000 rpm and at this speed the improvement was 10% compared to the non-rotational condition. The presence of the variable external flow restriction did not cause bearing instability for either the non-rotational or rotational journal condition.

Design procedures are given for the fixed external restriction bearing and the variable external restriction bearing for both the incompressible fluid supply and the compressible fluid supply. For the variable external restriction bearing with incompressible fluid supply, the design provides a specific bearing static stiffness. For the case of the compressible fluid supply the design provides the optimum variable external restriction for a particular stabilized bearing, but not a specific bearing static stiffness.

Thesis Supervisor: Milton C. Shaw

Title: Professor of Mechanical Engineering

TABLE OF CONTENTS

Subject	Page
Abstract	ii-iii
List of Figures	vi-ix
List of Tables	x
List of Symbols	xi-xviii
Biographical Note	xix-xxi
Acknowledgements	xxii-xxiii
Dedication	xxiv
Chapter I Introduction	1-8
Chapter II Externally Pressurized Bearing with Incompressible Fluid Supply	9-47
A. Externally Pressurized Bearing with Fixed External Restriction	9-27
1. Theoretical Bearing Static Stiffness (Square Bearing)	9-14
2. Theoretical Bearing Static Stiffness (Round Bearing)	14-15
3. Experimental Bearing Static Stiffness (Round Bearing)	16-21
4. Design Procedure for Maximum Bearing Stiffness	21-27
B. Externally Pressurized Bearing with Variable External Restriction (Load Sensing)	28-43
1. Theoretical Bearing Static Stiffness (Square Bearing)	28-33

Subject	Page
2. Experimental Bearing Static Stiffness (Round Bearing)	33-40
3. Design Procedure for Maximum Bearing Stiffness	41-43
C. Externally Pressurized Bearing with Variable External Restriction (Position Sensing)	44
D. Rotational Effects	45-47
Chapter III Externally Pressurized Bearing with Compressible Fluid Supply	48-102
A. Externally Pressurized Bearing with Fixed External Restriction	48-77
1. Theoretical Considerations	48-62
2. Experimental Investigations	63-75
3. Design Procedure	76-77
B. Externally Pressurized Bearing with Variable External Restriction (Load Sensing)	78-102
1. Theoretical Considerations	78-86
2. Experimental Investigations	87-99
3. Design Procedure	99-102
Chapter IV Conclusions	103-109
Chapter V Future Investigations	110-111
Figures	112-148
Appendices	149-161
Bibliography	162-163

LIST OF FIGURES

Figure Number	Title
1.	Self-acting fluid bearing.
2.	Internal composition of externally pressurized fluid bearing.
	(a) Pressure pad type.
	(b) Axial exhaust groove type.
3.	Arrangement of externally pressurized fluid bearing with external flow restrictions.
4.	Analytical model (square bearing) of externally pressurized fluid bearing with external flow restrictions.
5.	Theoretical journal load-displacement plot for fixed external orifice (no circumferential flow, non-rotating round bearing, incompressible fluid).
6.	Test apparatus (single radial bearing, incompressible fluid supply).
7.	Experimental journal load-displacement plot for fixed external orifice (non-rotating round bearing, incompressible fluid).
8.	Theoretical journal load-displacement plot for fixed external orifice (circumferential flow - Raimondi and Boyd Correction, non-rotating round bearing, incompressible fluid).
9.	Raimondi and Boyd bearing stiffness correction for circumferential flow (fixed external orifice restriction, incompressible fluid).
10.	Variable external restriction (load sensing) concept - (general case of fixed external restriction plus variable external restriction).
11.	Theoretical journal load-displacement plot for fixed external linear restriction plus variable external spool valve restriction (constant β_3, non-rotating square bearing, no circumferential flow in bearing, incompressible fluid).

Figure Number	Title
12.	Effect of β_2 on journal load-displacement plot in Fig. 11 for constant β_3 and C_c.
13.	Effect of β_3 on journal load-displacement plane surface for $\beta_2 = 0$ and variable C_c in Fig. 11 (surface abod).
14.	Controller limitation on journal load-displacement plot in Fig. 11.
15.	Variable external restriction (load sensing) concept - (special case of variable external spool valve restriction without fixed external restriction).
16.	Experimental journal load-displacement plot for variable external spool valve restriction with and without spool valve stop (non-rotating round bearing, incompressible fluid).
17.	Experimental journal load-displacement plot for variable external spool valve restriction ($\beta_3 = 1.49$, C_c = variable, non-rotating round bearing, incompressible fluid).
18.	Experimental journal load-displacement plot for variable external spool valve restriction (β_3 = variable, $C_c = 4.37$, non-rotating round bearing, incompressible fluid).
19.	Experimental journal load-displacement plot for variable external spool valve restriction (β_3 = variable, $C_c = 2.32$, non-rotating round bearing, incompressible fluid).
20.	Experimental load capacity ($\frac{W}{A_b P_s}$) at $\frac{\epsilon}{h_o} = 0.1$ versus C_c and β_3 for variable external spool valve restriction (non-rotating round bearing, incompressible fluid).
21.	Effect of circumferential flow on the theoretical non-circumferential flow journal load-displacement plot for variable external spool valve restriction

Figure Number	Title
	(β_3 = constant, non-rotating bearing, incompressible fluid).
22.	Transition to turbulent flow for flow through a thin annulus with relative rotation between surfaces (for condition of test bearing, incompressible fluid).
23.	Stability ratio for a parallel surface gas bearing with fixed orifice external resistance for non-choked and choked operation.
24.	Static stiffness for a parallel surface gas bearing with fixed orifice external resistance for non-choked and choked operation.
25.	Developed view of one internal sector of exhaust groove type bearing and pressure distribution through sector.
26.	Test apparatus (single radial bearing, compressible fluid supply).
27.	Proximity meter calibration curve.
28.	Fixed external orifice restriction calibration curve.
29.	Theoretical bearing flow through 1/4 bearing (fluid = air).
30.	Experimental journal load-displacement plot for fixed external orifice restriction (p_s = constant, β_3 = constant, fluid = air, non-rotating and rotating bearing).
31.	Variable external restriction (load sensing) concept- (special case of variable external spool valve restriction with stabilizing fixed external orifice restriction for compressible fluids).
32.	Variable external spool valve restriction calibration curve.
33.	Experimental journal load-displacement plot for variable external spool valve restriction (β_3 = 2.1, C_c = variable, non-rotating round bearing, fluid = air).
34.	Experimental journal load-displacement plot for variable external spool valve restriction (β_3 = 2.5, C_c = variable, non-rotating round bearing, fluid = air).

Figure Number	Title
35.	Experimental journal load-displacement plot for variable external spool valve restriction ($\beta_3 = 4.1$, C_c = variable, non-rotating round bearing, fluid = air).
36.	Experimental load capacity ($\frac{W}{A_b P_s}$) at $\epsilon/h_o = 0.2$ versus C_c and β_3 for variable external spool valve restriction (non-rotating round bearing, fluid = air).
37.	Experimental journal load-displacement plot for variable external spool valve restriction (p_s = constant, C_c = constant, β_3 = constant, fluid = air, non-rotating and rotating bearing).

LIST OF TABLES

Table No.	Title	Page
I.	Effect of β_3 on Point (f) of the Curved Surface for $\beta_2 = (\beta_3 - 1)$ and Variable C_c in Fig. 11 (Surface fbod).	32
II.	Values of $W_{in}/(Cd_o^2 P_s)$	58
III.	Computation of Raimondi and Boyd Bearing Stiffness Correction for Circumferential Flow	153

LIST OF SYMBOLS

A_b = effective bearing area referred to the pad pressure, $in.^2$

= the area of the pressure pad plus the area of the pressure pad exit path out one end of the bearing. These are projected areas which are projected on a plane perpendicular to the direction of the load, $in.^2$

A_c = controller spool valve cross-sectional area, in^2.

A_o = orifice area, in^2.

A_{oj} = the inherent (fixed orifice-journal) orifice area, in^2.

A_{pj} = the inherent (feed port-journal) orifice area, in^2.

B = bearing flow exit path width for one pad, inch.

$B_A = (\pi D/n) - wg$, inch.

$B_B = L_b$, inch.

B_c = width of controller flow path = πd_c, inches.

c_p = specific heat of fluid at constant pressure, Btu/lb.°F.

C = sharp-edged orifice discharge coefficient.

C_c = controller constant = $(A_c p_s)/(2K_c \ell)$.

C_g = depth of exhaust groove, inch.

C_p = depth of the bearing pressure pad, inch.

$C_1 = C_2 A_o$, in.-sec.

$C_2 = C C_3$, sec./in.

$$C_3 = \left(\frac{223.7}{R g}\right) \left(\frac{c_p}{T_s}\right)^{1/2}, \text{ sec./in.}$$

d_c = controller spool valve diameter, inch.

d_o = orifice diameter, inch.

d_p = feed pad or port diameter, inch.

d_t = capillary tube diameter, inch.

D = bearing journal diameter, inch.

E = modulus of elasticity of journal material, psi.

F_b = bearing factor = $(L_p L_e)/(Dw_c)$.

$$F_c = \left[1 + \left(\frac{\gamma}{2\beta}\right) \frac{\left(1 - \left(\frac{q}{z}\right)^{\beta}\right)}{\left[(z)^{\gamma} - 1\right]} - \frac{\left(1 - \left(\frac{q}{z}\right)^{\beta}\right)}{(k+1)} \right].$$

q = acceleration due to gravity = 386 in./sec.^{2}.

h = pressure pad exit path height, inch.

h_c = controller spool valve radial clearance, inch.

h_p = the clearance between fixed orifice and journal, inch.

h_o = pressure pad exit path height when journal is concentric
= radial clearance of bearing, inch.

h_1 = pressure pad exit path height in direction opposite to the direction of the load, inch.

h_2 = pressure pad exit path height in direction of the load, inch.

I = area moment of inertia of journal in bending, inch^4.

k = gas constant of fluid (ratio of constant pressure specific heat to constant volume specific heat).

K = bearing static stiffness = $\frac{\partial W}{\partial \epsilon}$, lb./in.

K_c = spring constant of controller spool valve compression springs, lb./in.

ℓ = flow length through one side of controller spool valve for central valve position, inch.

ℓ_a = distance between rear pivot bearing and front test bearing (compressible fluid supply test apparatus), inch.

ℓ_b = distance between front test bearing and loading bearing (compressible fluid supply test apparatus), inch.

ℓ_j = length of the journal, inch.

ℓ_1 = flow length through controller spool valve at low pressure end of spool valve, inch.

ℓ_2 = flow length through controller spool valve at high pressure end of spool valve, inch.

L_b = length of bearing, inch.

L_c = total controller spool valve length, inch.

L_e = length of bearing pressure pad exit path, inch.

L_p = length of bearing pressure pad, inch.

L_t = capillary tube length, inch.

$L_1 = d_p/2$, inch.

$L_2 = B_B/2$, inch.

$L_3 = B_A/2$, inch.

m_c = mass rate of flow through one side of spool valve controller for central spool valve position, $\frac{\text{lb.-sec.}}{\text{in.}}$.

m_{in} = fluid mass flow rate into the bearing pad or feed port from the external restriction, lb.-sec./in.

m_{out} = fluid mass flow rate out from the bearing pad or feed port through the bearing clearance, lb.-sec./in.

m_T = total bearing mass rate flow = $4m_{out}$, lb.-sec./in.

n = number of bearing sectors.

N = journal rotational speed, rpm.

N_{crit} = journal rotational speed for onset of turbulent flow in the bearing exit paths, rpm.

$N_{Inversion}$ = journal inversion point critical speed, rpm.

$N_{Mech.\ Crit.}$ = journal mechanical critical speed, rpm.

N_{trans} = journal rotational speed for transition flow region, rpm.

N_{whirl} = journal whirl speed, rpm.

$N_{Whirl\ Crit.}$ = journal whirl critical speed, rpm.

p_b = pressure pad pressure, psig.

p_{bo} = pressure pad pressure for concentric, no load journal condition, psig.

p_{bo}' = bearing pressure drop or bearing pad pressure for the no-load journal condition for the rotational journal case, psig.

p_{b1} = pressure in pad which is located in the direction opposite to the direction of the load, psig.

p_{b2} = pressure in pad which is located in the direction of the load, psig.

p_o'' = pressure drop across controller spool valve when it is centrally located (journal no-load condition), psig.

p_o''' = pressure drop across fixed external restriction, R, for journal no-load condition, psig.

p_s = overall supply pressure, psig.

p_s' = the back pressure of the controller, psig.

p_{so}' = the back pressure of the controller for the concentric, no-load journal condition, psig.

$(p_s-p_{bo})_o/(p_s-p_{bo})_t$ = the ratio of pressure drop for the fixed

orifice restriction by itself to the pressure drop for the fixed orifice restriction plus the inherent orifice restrictions for the same weight rate flow through each.

P_a = ambient exhaust pressure, psia.

P_b = bearing pad pressure, psia

P_{bo} = bearing pad or feed port pressure for concentric, no-load journal condition, psia.

P_s = overall supply pressure, psia.

P_s' = the back pressure of the controller, psia.

P_{so}' = the back pressure of the controller for the concentric, no-load journal condition, psia.

q = the pressure ratio P_a/P_s.

q' = the pressure ratio P_a/P_{so}'.

Q_b = the volumetric flow rate through one pressure pad, $in.^3/sec.$

Q_{bo} = the volumetric flow rate through one pressure pad for concentric, no-load journal condition, $in.^3/sec.$

Q_{b1} = the volumetric flow rate through the pressure pad which is located in a direction opposite to the direction of the load, $in.^3/sec.$

Q_{b2} = the volumetric flow rate through the pressure pad which is located in the direction of the load, $in.^3/sec.$

Q_T = total bearing flow, $in.^3/sec.$

r_t = capillary tube radius, inch.

R = specific gas constant of fluid, ft.-lb./lb.-°F abs.

R_e' = bearing Reynolds number = $(2h_o v')/\nu$.

$R_{e\ crit}'$ = bearing Reynold's number for onset of turbulent flow in bearing exit paths = 1500 to 2500.

R_o = flow resistance of fixed orifice restriction, sec./in.^{2}.

R_{oj} = flow resistance of inherent (fixed orifice-journal) orifice restriction, sec./in^2.

R_{pj} = flow resistance of inherent (feed port-journal) orifice restriction, sec./in^2.

R_t = total flow resistance of external restriction, sec./in^2.

R_w = whirl ratio = $N_{Whirl\ Crit.}/N_{whirl}$.

S = non-dimensional bearing static stiffness = $\dfrac{\partial \frac{W}{A_b P_s}}{\partial \frac{\epsilon}{h_o}}$.

T_s = supply tank fluid temperature, °F abs.

v = bearing axial flow velocity for N = 0, in./sec.

v' = bearing mean resultant velocity in the bearing exit paths due to rotation and axial flow, in./sec.

v'_{crit} = value of v' for onset of turbulent flow in the bearing exit paths = $(R_{e\ crit}'\ \nu)/(2h_o)$, in./sec.

V_c = internal volume of the controller including the volume of the connecting flow passages, in^3.

V_p = volume of pressure pad or feed port, in^3.

w_b = effective width of bearing, inch.

w_c = width of separation between pressure pads, inch.

w_g = width of exhaust groove, inch.

w_{gc} = controller spool valve inlet annular groove width, inch.

W = journal load, lb.

W_c = weight rate of flow through one side of spool valve controller for central spool valve position, lb./sec.

W_{CB} = journal counter-balance weight for test apparatus for compressible fluid supply.

$W_{in} = m_{in}(g)$, lb./sec.

W_j = weight of the journal, lb.

W_L = loading bearing load (compressible fluid supply test apparatus), lb.

$W_{out} = m_{out}\, g$, lb./sec.

W_T = total bearing weight rate flow = $4\, W_{out}$, lb./sec.

x = axial displacement of controller spool valve from its central position in direction away from high pressure controller side, inch.

x_b = distance along bearing flow path, inch.

x_c = distance along the controller flow path, inches.

z = the pressure ratio P_{bo}/P_s.

z' = the pressure ratio P_{bo}/P_{so}'.

z_{crit} = value of z for critical orifice condition.

z_{opt} = value of z which yields maximum S value.

$\beta = (k + 1)/k$.

β_2 = the pressure ratio p_o''/p_{bo}.

β_3 = the pressure ratio p_s/p_{bo}.

β_4 = the pressure ratio p_o'''/p_{bo}.

$\gamma = (k - 1)/k$.

$$\Delta_a = \frac{\partial m_{in_1}}{\partial P_{b1}} - \frac{\partial m_{out_1}}{\partial P_{b1}}$$

$$\Delta_b = \frac{\partial m_{in_1}}{\partial h_1} - \frac{\partial m_{out_1}}{\partial h_1}$$

ϵ = journal eccentricity, inch.

μ = fluid absolute viscosity, lb.sec./in^2.

ν = kinematic viscosity of fluid, in^2/sec.

ρ = fluid mass density, lb.sec.^{2}/in^4.

ρ_a = ambient exhaust mass density, lb.sec.^{2}/in^4.

ρ_{bo} = mass density of fluid in the bearing pad for concentric, no-load journal condition, lb.sec.^{2}/in^4.

τ_a / τ_b = stability ratio.

BIOGRAPHICAL NOTE

The author was born in Crystal Lake, Illinois on January 8, 1931. He attended the public elementary and high schools of that city. While attending Community High he earned membership to the National Honor Society, was awarded the Bausch and Lomb Science Award, was a member of the Student Council and a senior class officer, played on the school football team and intramural basketball team and was graduated in June, 1948.

His undergraduate study was obtained at the Illinois Institute of Technology, Chicago, Illinois. While at Illinois Tech, the author was elected to Pi Tau Sigma and Tau Beta Pi, was an officer in Pi Tau Sigma, received a two year John Morse Memorial Tuition Scholarship and was graduated on June, 1952, with the degree of Bachelor of Science in Mechanical Engineering.

He began his graduate study at M.I.T. in the following fall and received the Master of Science degree in September, 1954. During that time he was a research assistant in the Metals Processing Division of the Mechanical Engineering Department, was elected to membership in The Society of Sigma Xi and also married Patricia Joan Thomas of Crystal Lake, Illinois.

During the months of December, 1954, to September, 1956, the author served a tour of duty with the U. S. Army at the Quartermaster Research and Development Command, Natick, Mass. His assignment was as a mechanical engineer and was concerned

mainly with the design and testing of mobile baking equipment. Also during this time he was an Instructor in the graduate evening school at Worcester Polytechnic Institute, Worcester, Massachusetts. On February 9, 1955, his first child, Valerie Ann, was born.

After release from the Army in September, 1956, he returned to graduate study at M.I.T. as a research assistant in the Metals Processing Division of the Mechanical Engineering Department and received the degree of Mechanical Engineer in June 1957. The author's second daughter, Leslie Ann, was born April 24, 1957.

On July 1, 1957, the author received an appointment as Instructor in Mechanical Engineering at M.I.T. and continued his graduate study. He has held this appointment from that date until the present writing of this thesis. During this period his research investigation at M.I.T. has been mainly concerned with the topic of this thesis. Also within the span of the last three years he has been consulting engineer for Controls For Radiation, Inc., Cambridge, Massachusetts, where he developed the automation of chemical dosimeter manufacturing and has been a research engineer at the Whirlpool Research Laboratories, St. Joseph, Michigan, where he analyzed dielectric measurements of liquids.

The author's publications include an ASME Paper (1955) entitled "The Role of Chip Thickness in the Grinding Process" which was co-authored with Dr. George S. Reichenbach,

Dr. Milton C. Shaw and Mr. S. Kalpakcioglu; an ASLE Paper (1957) entitled "Grinding Temperatures" which was co-authored with Dr. Milton C. Shaw; reports for sponsored research in the Mechanical Engineering Department entitled: Externally Pressurized Spindle Bearing" (1958) and "External Dampers for Gas Bearings" (1959) and a Whirlpool Research Laboratory report entitled "Dielectric Properties of Liquids" (1959).

ACKNOWLEDGMENTS

The author wishes to express his deepest gratitude to Professor Milton C. Shaw (Chairman), Professor Norman C. Dahl, and Professor Lowen J. Shearer for their willingness to serve as the author's thesis committee and for their helpful advice and guidance.

The author also wishes to express everlasting appreciation to:

Professor Milton C. Shaw who has been an inspiration to the author throughout the author's graduate research investigations.

The Warner and Swasey Company of Cleveland, Ohio. for their generous support which made the first half of this study possible.

The Instrumentation Laboratory of M.I.T. and the Whirlpool Research Laboratories of St. Joseph, Michigan, for their generous and timely support which made the completion of this study possible.

Dr. Ernest B. Dane, Jr., Mr. John J. McCarthy and other members of the Instrumentation Laboratory who were instrumental in the manufacturing of the apparatus for the second half of this study to the fine precision required.

Mr. Lester V. French of the Whirlpool Research Laboratories who was instrumental in making possible the generous grant from

his company.

Professor Prescott A. Smith and his staff of the Machine Tool Laboratory of the Mechanical Engineering Department for their able assistance. In particular to Mr. John Leach and Mr. Frederick H. Anderson for the manufacturing of necessary components and Mr. Evans G. Arnold for his design detailing of all major apparatus parts.

Professor Nathan H. Cook, Professor Brandon G. Rightmire and Mr. Robert R. Donaldson of the Materials Processing Division of the Mechanical Engineering Department for their helpful consultations.

DEDICATION

The author wishes to dedicate this thesis to his wife, Patricia Joan, whose encouragement and love have given the author the necessary energy to advance through the trials of this research study. It is, without a doubt, only fitting to also dedicate this thesis to the author's precious daughters who were born during the period of the author's graduate studies.

CHAPTER I

INTRODUCTION

The use of the fluid bearing has been steadily decreasing since the development of commercial rolling contact bearings. For example, the Machine Tool Exhibition of 1955 in the United States indicated that American machine tools had at that time been converted almost 100% to rolling contact bearings.[1,2] Here the term "fluid bearing" refers to a bearing where the journal or shaft is supported by means of direct fluid pressure where the fluid is pressurized by internal self-acting means (the hydrodynamic bearing) or by external means (the externally pressurized bearing). The term rolling contact bearing refers to a bearing where the journal or shaft is supported by means of direct contact with metal balls or rollers. Such factors as availability and economics entered into the widespread adoption of the rolling contact bearing for most applications. However, from a technical viewpoint one would single out these three factors: (1) low frictional torque required by bearing, (2) very high stiffness of bearing, (3) load supportability when bearing is not rotating. The term "stiffness of the bearing" refers to the load-displacement characteristic of the journal or shaft in the plane of the bearing and is similar to the definition of the stiffness of a coil spring.

A major disadvantage of the rolling contact bearing is the chatter which is imparted to the journal by minute inaccuracies in the components of the bearing. Hirshfeld[3] and Helmke[4] indicate that this chatter causes poorer surface finishes on workpieces when rolling contact bearings are employed on machine tool spindles instead of fluid bearings. They state that the fluid bearing produces better surface finishes and contend that this is due to the smooth characteristics of the fluid bearing which is brought about by the damping properties of the fluid within the bearing. More recently, this chatter has proved troublesome to designers of missile guidance systems which employ rolling contact bearings on gyroscope rotors. This fact becomes quite obvious when one is aware of the elaborate program in existence at the Instrumentation Laboratory of M.I.T. to produce very precise rolling contact bearings. They have succeeded in producing rolling contact bearings with tolerances of 20 millionths of an inch.[5] Chatter of the gyroscope rotor caused from the rolling contact bearings will, of course, lead to errors in guidance of a missile.

Now if it were possible to produce a fluid bearing which possesses the advantages of the rolling contact bearing, then this bearing would have the following desirable characteristics: (1) low frictional torque, (2) very high stiffness, (3) load supportability when not rotating, and (4) smooth operation. A bearing of these characteristics would, indeed, be welcomed by the machine tool, gyroscope and many other manufacturers. To

produce such a bearing has been the concern of this research. However, the vastness of this problem necessitated that the investigation for this thesis be confined to only a specific area of this problem. In accordance with this the specific goal of this thesis is: TO IMPROVE THE STATIC STIFFNESS OF A FLUID BEARING. This thesis is mainly concerned with the static stiffness of radial fluid bearings rather than thrust fluid bearings.

The fluid bearing of the self-acting (hydrodynamic) type has been in existence for a long time. This bearing is also sometimes referred to as a plain journal bearing or a sleeve bearing. The self-acting bearing is described and analyzed by Fuller[6] and by Shaw and Macks.[7] This bearing consists simply of a round journal rotating within a cylindrical hole which is slightly larger in diameter than the journal. The fluid is supplied to the inner clearance of the bearing by means of a feed (usually gravity) through an inlet hole. The load carrying ability of the bearing is derived from the pumping action of the rotating journal which pumps fluid into the wedge formed by the eccentricity of the journal as it is loaded. This action forms a pressure distribution similar to that shown in Fig. 1. This pressure distribution, which is sometimes referred to as a pressure wedge, supports the load placed on the journal. Theory reveals that the displacement of the journal within the bearing is a function of load, fluid viscosity, fluid temperature, and rotational speed of the journal. Hence, it is seen that the

self-acting bearing cannot support a load by means of fluid pressure when the journal is not rotating and when the journal is rotating the journal eccentricity must be relatively large for larger journal loads which means that the bearing will have a low stiffness.

The fluid bearing of the externally pressurized type provides a bearing whose stiffness is independent of fluid viscosity, fluid temperature and rotational speed of the journal. This means that a fluid of low viscosity can be employed so that bearing frictional torque will be as minimum as possible. Also a fluid of high heat capacity can be employed to more readily remove heat from the bearing. Since the bearing stiffness is also independent of journal rotational speed, this bearing can be operated with equal effectiveness in the non-rotational case and in the rotational case. The externally pressurized fluid bearing is a fluid bearing where the fluid is supplied under pressure to inlet ports which are spaced symmetrically around the circumference of the bearing. As the fluid flows from the inlet ports through the bearing to exhaust out the bearing ends, a pressure distribution is established in the sector of the bearing about each inlet port. Hence, it is seen that pressure wedges somewhat similar to the pressure wedge of a self-acting bearing are established within this bearing by external means. Figure 2 illustrates the internal composition of two variations of the externally pressurized bearing and pertinent internal bearing dimensions are identified. The design of Fig. 2a has

four inlet ports which feed four pockets. Here theoretically the fluid flows axially from the pockets out both ends of the bearing. This bearing is primarily for incompressible fluids. The design of Fig. 2b has four inlet ports and each inlet port sector is separated by means of axial exhaust grooves. Here the fluid flows from each inlet port axially out both ends of the bearing and also circumferentially to the exhaust grooves. This bearing is primarily for compressible fluids.

The externally pressurized fluid bearing also provides a very important possibility. This bearing offers a means for obtaining a very stiff fluid bearing. The load carrying action of this bearing is rather obvious. By increasing the supply pressure to one inlet feed port while keeping it unchanged to the other inlet feed ports, a net pressure difference across the journal will exist which will allow the journal to support a load that is directed toward the higher supply pressure inlet feed port and that has a magnitude equal to the product of the net pressure difference across the journal times the projected area of the feed port bearing sector. Of course, load carrying action can also be obtained by lowering the supply pressure to one of the inlet feed ports rather than increasing its supply pressure. In this case, the direction of the load that can be supported is away from the lower supply pressure inlet feed port. Another possibility is to adjust the supply pressure to directly opposite inlet feed ports. Here one supply pressure is raised and the other is lowered. These adjustments in supply

pressure to the various inlet feed ports can be accomplished automatically by placing a fixed external flow restriction (or resistance) in the feed duct to each inlet feed port and providing a constant overall supply pressure to the input side of these flow restrictions. This idea is not new, but has been discussed by Shaw and Macks[7] and by Raimondi and Boyd.[8] This externally pressurized bearing arrangement is illustrated in Fig. 3. In this figure a pad type bearing is shown which has four equally spaced pads. The external flow restriction is represented in each feed duct by the letter R and is assumed to be a restriction of constant flow resistance. In an actual application the fixed restriction would be a capillary tube or an orifice. The load carrying action of this bearing can be easily explained by referring to Fig. 3. The external journal load W causes the journal to displace from the bearing center by the eccentricity, ϵ, and in the direction of the applied load. In this case the displacement of the journal is upward. This causes the axial exit path from the upper pressure pad (or pocket) to become thinner and the axial exit path from the lower pressure pad to become larger. The greater resistance through the upper part of the bearing causes the flow to be reduced and hence, less pressure drop occurs across the upper pad external resistance. This causes the upper pad pressure to increase compared to its initial no load value. By similar reasoning it can be seen that the lower pad pressure will be decreased compared to its initial no load value. This results in a net downward pressure difference

which balances the applied external load W and causes the journal to reach equilibrium at some specific eccentricity. The same procedure follows for a downward applied external load. Similarly the side pressure pads support horizontal loads and, of course, all four pads act to support a randomly acting external load in the plane of the bearing.

The externally pressurized bearing with fixed external restrictions described above provides a relatively stiff bearing. However, its stiffness can be greatly increased. This is accomplished by employing variable external restrictions rather than fixed external restrictions. The desirability of variable external restrictions can be quite evident by again referring to Fig. 3. If the functioning of the externally pressurized bearing with fixed external restrictions is recalled, it will be seen that an improvement will be obtained if the upper pressure pad external restriction is adjusted so that its flow resistance is decreased and the lower pressure pad external restriction is adjusted so that its flow resistance is increased. This improvement means that the journal will come to an equilibrium eccentricity of lesser value or it may even be possible to obtain equilibrium with the journal remaining always at the central or concentric position. This would, indeed, provide a very stiff bearing. The adjustments of the flow resistance of the external restriction can be made to occur automatically. One method is to employ a load sensing control which makes use of the pressure differential across opposite pressure pads. Another method is to employ a

positional sensing control which makes use of continuous journal eccentricity measurements. This thesis is concerned mainly with the load sensing type control.

The research study presented in this thesis is divided into two parts: the control of externally pressurized bearings with incompressible fluid supply and the control of externally pressurized bearings with compressible fluid supply. In each part the static stiffness for various externally pressurized bearing systems is presented as determined by analytical means and also by experimental means. The conclusions regarding both parts of the study are collectively presented in the Conclusions.

CHAPTER II

EXTERNALLY PRESSURIZED BEARING WITH INCOMPRESSIBLE FLUID SUPPLY

A. EXTERNALLY PRESSURIZED BEARING WITH FIXED EXTERNAL RESTRICTION

1. Theoretical Bearing Static Stiffness (Square Bearing)

For simplicity in analyzing this system a square bearing as illustrated in Fig. 4 is assumed rather than the round bearing pictured in Fig. 3. This allows one to deal with pressure pad exit paths of uniform height instead of non-uniform height which the round bearing possesses. In other words, parallel surface bearing exit flow paths are assumed. Later a correction will be given to convert square bearing results to round bearing results. However, for small journal eccentricities this correction is relatively small. In Fig. 4 a pad-type bearing is assumed which is the most efficient type for incompressible fluid supplies. Here the pad provides a large region or pad of uniform pressure which allows greater load capacity for a given supply pressure. Also the great radial clearance in the pad results in low viscous friction drag at the regions of the pads and hence, provides a net reduction of bearing frictional torque compared to the externally pressurized bearing without pressure pads.

In order to obtain an expression for the static stiffness of this bearing system, the journal load, W, must be expressed in terms of the pad pressures, p_D, and these in turn in terms of the bearing eccentricity, ϵ . From the assumed pressure distribution shown in Fig. 4, one can write the following expression

for W for the static case from a force equilibrium consideration:

$$W = A_b (P_{b2} - P_{b1}) \qquad (1)$$

where P_{b2} = the pressure in the pad which is located in the direction of the load, psig.

P_{b1} = the pressure in the pad which is located in the direction opposite to the direction of the load, psig.

A_b = effective projected bearing area = $(L_p + L_e)w_b$, in^2.

See Fig. 2 and Fig. 4 for the identification of L_p, L_e and w_b. The area A_b is the effective projected bearing area referred to the pad pressure and is illustrated in Fig. 4. More rigorously the area A_b is the integral of the pressure distribution with respect to bearing area divided by the pad pressure.

a. Linear External Flow Resistance (Capillary Tube)

If the external restriction is assumed to be a linear flow resistance, such as a capillary tube, and the flow is assumed to be laminar and incompressible, only out the ends of the bearing (that is, no circumferential flow occurs), and not effected by the journal rotational speed, then

$$P_{b2} = P_s - \frac{Q_{b2}}{Q_{b0}}(P_s - P_{b0}) \qquad (2)$$

$$P_{b1} = P_s - \frac{Q_{b1}}{Q_{b0}}(P_s - P_{b0}) \qquad (3)$$

where $\frac{Q_{b2}}{Q_{b0}} = \frac{P_{b2}}{P_{b0}} \left(\frac{h_2}{h_0}\right)^3$ and $\frac{Q_{b1}}{Q_{b0}} = \frac{P_{b1}}{P_{b0}} \left(\frac{h_1}{h_0}\right)^3$. (4) (5)

Here the second term of the expression for p_{b2} and p_{b1} is the pressure drop across the external restriction, R. It should also be noticed the p_s has been assumed constant. Also:

p_s = overall supply pressure, psig.

Q_{bo} = volumetric flow rate through one pressure pad for the concentric, no load journal condition, in^3/sec.

Q_{b2} = volumetric flow rate through the pressure pad which is located in the direction of the load, in^3/sec.

Q_{b1} = volumetric flow rate through the pressure pad which is located in the direction opposite to the direction of the load, in^3/sec.

h_o = pressure pad exit path height when journal is concentric = radial clearance of bearing, inch.

h_2 = pressure pad exit path height in direction of the load, inch.

h_1 = pressure pad exit path height in direction opposite to the direction of the load, inch.

Furthermore $$h_2 = h_o - \epsilon \qquad (6)$$

and $$h_1 = h_o + \epsilon \; . \qquad (7)$$

Thus for $\epsilon \ll h_o$, $$\left(\frac{h_2}{h_0}\right)^3 \approx 1 - 3\frac{\epsilon}{h_0} \; . \qquad (8)$$

and $$\left(\frac{h_1}{h_0}\right)^3 \approx 1 + 3\frac{\epsilon}{h_0} \; . \qquad (9)$$

By substitution of equations (2), (3), (4), (5), (8), and (9) into equation (1), the following expression for W is obtained:

$$W = 6 \frac{A_b P_s \epsilon}{h_o} \frac{|\beta_3 - 1|}{\beta_3^2} \qquad (10)$$

where $\beta_3 = \frac{P_s}{P_{bo}}$. Equation (10) is an expression for W which has been linearized about $\epsilon \approx 0$, hence it should not be used for values of ϵ/h_o larger than 0 to 0.3.

The static stiffness of the bearing, K, can be obtained by taking the partial derivative of W with respect to ϵ, hence

$$K = \frac{\partial W}{\partial \epsilon} = 6 \frac{A_b P_s}{h_o} \frac{|\beta_3 - 1|}{\beta_3^2} \qquad (11)$$

The expression for K has a maximum with respect to β_3 and occurs for:

$$\beta_3 = 2 \qquad \text{or} \qquad \frac{1}{\beta_3} = 0.5$$

and this $K_{max} = 1.5 \frac{A_b P_s}{h_o}$. (12)

Now if a non-dimensional static stiffness is defined as

$$S \equiv \frac{K}{\left(\frac{A_b P_s}{h_o}\right)} = \frac{\partial \frac{W}{A_b P_s}}{\partial \frac{\epsilon}{h_o}}, \qquad (13)$$

then $S_{max} = 1.5$ (14)

and it occurs for $\beta_3 = 2$.

b. Non-Linear External Flow Resistance (Orifice)

An analysis similar to that for the linear external flow resistance can be carried out for the case of a non-linear external flow resistance. An orifice is a non-linear flow resistance in that the pressure drop across an orifice varies as the square of the volumetric flow rate. The bearing static stiffness when the external restriction is an orifice has been determined (See Appendix A) and the results are as follows:

$$K = \frac{\partial W}{\partial \epsilon} = 12 \frac{A_b P_s}{h_o} \frac{\left(1 - \frac{1}{\beta_3}\right)}{(2\beta_3 - 1)} \tag{15}$$

This expression for K is a maximum for $\beta_3 = 1.71$ or $1/\beta_3 = .586$ and

$$K_{max} = 2.05 \frac{A_b P_s}{h_o} \tag{16}$$

Thus $S_{max} = 2.05$ (17)

and it occurs for $\beta_3 = 1.71$.

It is seen from the above analyses that the optimum bearing static stiffness is greater for the orifice external restriction than for the capillary external restriction and that it occurs for approximately the same value of β_3. It should be recalled that the above analyses assumed that the fluid is incompressible,

that p_s = constant, that $\epsilon << h_o$, that no circumferential flow occurs, that the bearing has parallel surface exit flow paths (that is, it is a square bearing), and that the journal rotational speed does not effect the bearing stiffness.

2. Theoretical Bearing Static Stiffness (Round Bearing)

The bearing exit flow paths of the round bearing cannot be approximated as parallel surface flow paths except when $\epsilon = 0$. When the ϵ is not zero, the exit flow paths are non-uniform in height. However, there is fortunately a simple correction for the round bearing referred to the results of the square bearing (See Appendix B). This correction only effects the value of K and S and does not change the optimum value of the pressure ratio β_3. This correction is simply:

$$K_{RD.BRG.} = K_{SQ.BRG.} \left(\frac{1}{1.13}\right) \qquad (18)$$

or

$$S_{RD.BRG.} = S_{SQ.BRG.} \left(\frac{1}{1.13}\right) \qquad (19)$$

When this correction is applied to the results of the square bearing analyses, the following is obtained:

a. Capillary External Restriction

$$K = 5.3 \frac{A_b P_s}{h_o} \frac{(\beta_3 - 1)}{\beta_3^2} \tag{20}$$

and $S_{max} = 1.33$ (21)

and it occurs for $\beta_3 = 2.0$.

b. Orifice External Restriction

$$K = 10.6 \frac{A_b P_s}{h_o} \frac{\left(1 - \frac{1}{\beta_3}\right)}{(2\beta_3 - 1)} \tag{22}$$

and $S_{max} = 1.81$. (23)

and it occurs for $\beta_3 = 1.71$.

These results assume that the fluid is incompressible, that p_s = constant, that $\epsilon << h_o$, that no circumferential flow occurs, and that the journal rotational speed does not effect the bearing stiffness.

Equation (22) has been plotted in Fig. 5 in the form of a non-dimensional load, $(W/A_b p_s)$, versus the eccentricity ratio, (ϵ/h_o). Here the relationship is assumed linear out to $(\epsilon/h_o) = 0.3$. The slope of a constant β_3 curve is the bearing stiffness, S. The effect of β_3 is clearly seen in this figure.

3. Experimental Bearing Static Stiffness (Round Bearing)

a. Experimental Apparatus

In order to see if the preceding analyses agree with the real bearing, experimental testing was carried out for the externally pressurized bearing with fixed external orifice restrictions. In these experiments the bearing journal was not rotated. The bearing chosen for this testing was that illustrated in Fig. 2a. The bearing internal dimensions are as follows:

MATERIALS
JOURNAL = HARDENED STEEL BEARING = BRASS.

$D = 6$ inches

$L_b = 3.5$ inches

$L_p = 1.5$ inches

$L_e = 1.0$ inches

$h_o = 0.0015$ inches

$2h_o$ = diametral clearance = 0.003 inches

$C_p = 0.032$ inches

$w_c = 0.5$ inches

$$w_b = \frac{D}{\sqrt{2}} = 4.24 \text{ inches}$$

$$A_b = (L_p + L_e)w_b = 10.6 \text{ in.}^2$$

The number of pressure pads was four as seen from Fig. 2a. This selection was made by an analytical means. The bearing stiffness was maximized with reference to the number of pressure pads. It was found that four pressure pads were definitely better than 1, 2 or 3 pads. Four pressure pads were not quite as good as 5, 6, 7, or 8 pads, but the increase in bearing stiffness over that for four pads is no more than 15%. Four pressure pads were selected from this standpoint and also because of ease of

manufacture and reduction of the number of external restrictions required. One external restriction, of course, is required for each pressure pad employed.

The test bearing was held in a rigid test bearing support which was secured to a table and stand. The journal loading was accomplished by means of loading bearings which were located on each side of the test bearing. The loading bearings were also of the externally pressurized type and the external pressure for these bearings was also employed to provide loading to the load bearings through pressure cylinders. Figure 6 shows a cross-sectional view of the test apparatus. In order to achieve an initial no-load condition the test bearing journal and attached components were counter-balanced. The counter-balance weights are indicated by W_1 and W_2 and act at the loading bearings. During testing the journal displacement was measured by means of dial gages as shown in the figure. The smallest division of these dial gages was 0.0001 inch, however, displacements were estimated to the nearest 0.00001 inch.

The external pressure for the test bearing was supplied from a Type QDH-3 Gerotor pump manufactured by the Gerotor May Corp., Baltimore, Maryland. The pump was driven by a variable speed electric motor. The fluid employed was White and Bagley cutting fluid mixed with water to grinding fluid proportions (80:1). Basically, this fluid can be considered as water with a rust inhibitor added. Using this fluid the pump developed a supply pressure of 300 psig for a flow of 2.5 gpm at the rated pump speed of 1200 rpm. The external pressure for the loading bearings

was supplied from a separate pump which was identical to the pump for test bearing. This pump was operated at a constant speed of 1200 rpm and the supply pressure was varied by means of a variable reducing valve. The fluid employed for the loading bearings was hydraulic oil. With this fluid the pump developes a supply pressure of 1500 psig for a flow of 2.5 gpm at the rated pump speed of 1200 rpm. A supply pressure of 400 psig on the loading bearing pressure cylinders corresponds to a total radial journal load of about 10,000 lb.

The flow resistance of the fixed external orifice restriction was changed by changing the orifice diameter. The orifice arrangement was made by placing a 0.003 inch shim stock disk, which had a hole very cleanly punched through it, within the assembly of a feed tubing and a Ermeto[9] tube fitting. This arrangement makes a very simple and easily changeable fixed orifice. It also conforms to the specifications of the VDI sharp edged orifice discussed by Hunsaker and Rightmire.[10] This orifice is convenient to use since exact coefficients are available without calibration. For this experimentation the orifice diameter was varied from 0.032 inch to 0.086 inch. This caused the overall supply pressure, p_s, to vary from 400 psig to 175 psig and consequently the maximum attainable journal load, W, varied from 2500 pounds to 1000 pounds.

b. Experimental Results

Experimental journal load versus journal displacement data was obtained for various β_3 pressure ratios. The pressure ratio

was varied by changing the orifice diameter. In this experimentation it was found that a single test bearing would not support a bending moment. The bearing would cock readily when a moment was applied. To eliminate error due to cocking the journal was manually pushed into alignment, thus making both dial indicators shown in Fig. 6 read the same deflection. The experimental results are shown plotted in Fig. 7. The general trend does seem to agree with the theoretical curves of Fig. 5. The maximum bearing stiffness occurs at approximately $\beta_3 = 1.71$ as predicted. The curves are fairly linear up to $(\epsilon/h_o) = 0.3$. However, it is seen that the magnitude of the stiffness is not in agreement with the theoretical prediction. The experimental bearing stiffness is consistently less than the theoretically predicted value. The value of experimental S_{max} is about 60% of the theoretical S_{max} value. For β_3 greater than 1.71, the reduction in S is greater than this and for β_3 less than 1.71, the reduction in S is less than this. The net result is that the experimental S_{max} is not as sensitive to β_3 as the theoretical S_{max}. Figure 7 indicates that S_{max} occurs for the range of $\beta_3 = 1.11$ to 2 rather than just for $\beta_3 = 1.71$. This means that the fixed orifice diameter is not critical as long as it yields a β_3 ratio which remains within the optimum range. For the condition of K_{max} in this investigation p_s was about 200 psig, hence K_{max} was approximately 1.4×10^6 lb./in.

c. Circumferential Flow Effect

The discrepancy between the magnitude of theoretical and experimental bearing stiffness has been found to be due to the

circumferential flow effect. No circumferential flow was assumed in the above analyses, however, there will be circumferential flow in the actual bearing. Circumferential flow will take place from the pressure pads of higher pressure to the pressure pads of lower pressure. This will cause the bearing to have less load carrying capacity due to the reduction of the net pressure differential across the bearing effective area than that predicted by the non-circumferential flow theory. Raimondi and Boyd[8] give a comparison between theoretical and experimental results for conditions similar to those under investigation here. They give theoretical results based on the assumption of no circumferential flow and experimental results which of course will have circumferential flow. They also give theoretical results which take circumferential flow into account. This latter theory does compare well with their experimental results. Their experiments were for the non-rotating journal case which is also the case being considered here. Making use of their findings Figure 5 can be corrected to account for circumferential flow. In this connection the difference between their bearing internal composition and that of the bearing employed in this study was also taken into account. This corrected plot is shown in Fig. 8. (See Appendix C for correction procedure). Now from a comparison of the corrected plot with the experimental results of Fig. 7, it is seen that very good agreement does exist. It exists not only for the general trend, but also for the bearing stiffness magnitudes. The bearing stiffness magnitudes are in agreement

within an accuracy of about 20%. Thus, without a doubt, the reduction in bearing stiffness compared to the non-circumferential flow theoretical value is due to the circumferential flow effect and this effect has a considerable influence.

Although the non-circumferential flow analysis yields bearing stiffness magnitudes which are in error, it does portray the bearing stiffness trends with respect to β_3 and it does single out a correct optimum β_3 value. It was also useful in another respect. It pointed out the important dimensionless parameters. This was very helpful as a guide for experimental work.

4. Design Procedure For Maximum Bearing Stiffness

In order so others can easily profit from the results of this study, this section is offered as a guide to the design of externally pressurized bearings with fixed external restrictions which will provide the maximum bearing stiffness for this arrangement. The work of Raimondi and Boyd[8] shows that the same correction for the fixed external orifice bearing also applies to the fixed external capillary bearing. One would expect this to be so, since the circumferential flow is a characteristic of the internal composition of the bearing itself. Hence, the same percentage reduction in the actual bearing stiffness compared to the theoretical non-circumferential flow value can be used for both external restriction types. In some applications where very small flow rates are desired a capillary external restriction must be used because the functioning of an orifice for very small flow rates is questionable. For this reason design procedure is

presented for both external restriction types.

Before listing the design steps it is well to point out that the designed bearing must have the same percentage circumferential flow as the bearing employed in this investigation in order to yield the same stiffness value. In order to insure the same percentage circumferential flow a bearing factor is here defined as

$$F_b = \text{BEARING FACTOR} = \frac{L_p L_e}{D\ w_c} \qquad (24)$$

and the designed bearing should have the same bearing factor as the bearing employed herein which is $F_b = 0.5$. This bearing factor is a ratio of the flow resistance circumferentially between adjacent pressure pads and of the flow resistance axially out from the pressure pad. This is not a ratio of the actual flow since the pressure drop between adjacent pressure pads is different than the pressure drop from the pressure pad axially out to ambient pressure. However, the ratio of the actual flow should be a direct function of F_b.

a. Design Steps for Fixed Capillary External Restriction

(1) Use a four pocket bearing as illustrated in Fig. 2a.

(2) Select L_p, L_e, D and w_c so that $F_b = \frac{L_p L_e}{D\ w_c} = 0.5$.

(3) Select a minimum practical value for the bearing diametral clearance, $2h_o$, in accordance with the D to be employed (A minimum is usually $2h_o/D = 0.0005$).

(4) Make $C_p \gg h_o$. This means that $C_p \geq 10\ h_o$.

(5) Calculate $w_b = D/\sqrt{2}$.

(6) Calculate $A_b = (L_p + L_e)w_b$.

(7) The maximum non-dimensional stiffness for this bearing will be $S_{max} = 0.73$ and it will occur for $\beta_3 = 2.0$. (For the fixed orifice external restriction the ratio of the experimental S_{max} to the non-circumferential theoretical S_{max} was 0.552. This correction was also applied here for this case).

(8) Determine the maximum journal load to be encountered, W_{max}.

(9) Calculate the necessary supply pressure, p_s, from the following relation:

$$P_s = \frac{W_{max}}{A_b\ S_{max} \left(\frac{\epsilon}{h_o}\right)_{max}} = \frac{W_{max}}{.073\ A_b} .$$

(This relation makes the maximum ϵ/h_o ratio equal to 0.1).

(10) Select a convenient capillary tube internal diameter, $d_t = 2r_t$.

(11) Calculate the capillary tube length, L_t, per pressure pad which is required to provide the optimum β_3 value of 2.0. Use the following relation for this calculation:

$$L_t = 3 \frac{L_e r_t^4}{D h_o^3} (\beta_3 - 1) \qquad (25)$$

$$= 3 \frac{L_e r_t^4}{D h_o^3} \text{ for optimum } \beta_3 .$$

(See Appendix D for derivation of equation 25).

(12) Calculate the bearing pressure pad no-load pressure $P_{bo} = P_s / \beta_3$.

(13) Calculate the total flow required by the bearing, Q_T, from:

$$Q_T = \frac{\pi D b_o^3 P_{bo}}{6 \mu L_e} . \qquad (26)$$

where μ is the fluid absolute viscosity in $\frac{\text{lb. sec.}}{\text{in}^2}$ units. (See Appendix D for derivation of equation 26).

For the above detemined values of L_p, L_e, D, w_c, h_o, C_p, A_b, W_{max}, P_s, r_t, P_{bo}, and Q_T, the resulting design provides:

$$\beta_3 = 2.0$$

$$S = 0.73$$

$$K = W_{max}/(0.1\ h_o)$$

$$\left(\frac{\epsilon}{h_o}\right)_{max} = 0.1$$

This procedure will provide a relatively high value of K. However, as an alternate method of calculation it might be desired

to specify K. To do this replace Step (9) with the following procedure:

Alternate Step (9)

(a) Specify K

(b) Calculate $(\frac{\epsilon}{h_o})_{max} = \frac{W_{max}}{K\ h_o}$ . . . (Should not exceed 0.3).

(c) Calculate $p_s = \frac{W_{max}}{A_b\ S_{max}\ (\frac{\epsilon}{h_o})_{max}} = \frac{W_{max}}{0.73\ A_b\ (\frac{\epsilon}{h_o})_{max}}$.

After executing alternate Step (9) continue as before to obtain r_t, L_t, p_{bc}, and Q_b by means of Steps (10), (11), (12), and (13) respectively. The resulting design will provide:

$\beta_3 = 2.0$

$S = 0.73$

K = as specified

$(\frac{\epsilon}{h_o})_{max} = \frac{W_{max}}{K\ h_o}$ . . . (Should not exceed 0.3)

b. Design Steps for Fixed Orifice External Restriction

(1) through (6) - Same as Steps (1) through (6) above.

(7) The maximum non-dimensional stiffness for this bearing will be $S_{max} = 1.0$ and it will occur for $\beta_3 = 1.71$.

(8) Determine the maximum journal load to be encountered, W_{max}.

(9) Calculate the necessary supply pressure, p_s, from the following relation:

$$p_s = \frac{W_{max}}{0.1\ A_b}$$

(This relation makes the maximum $\frac{\epsilon}{h_o}$ ratio equal to 0.1)

(10) Calculate the orifice diameter, d_o, which is required to provide the optimum β_3 value of 1.71 Use the following relation for this calculation:

$$d_o = \left(\frac{D\ h_o^3}{6 \mu L_e C} \sqrt{\frac{\rho\ p_s}{2.42}} \right)^{\frac{1}{2}} \qquad (27)$$

where C = coefficient of discharge for V.D.I. sharp edged orifice determined from Ref. 10.

ρ = mass density of fluid, lb. sec.^{2}/in.^{4}

(See Appendix D for derivation of equation 27).

(11) through (12) - Same as Steps (12) through (13) above.

For the above determined values of L_p, L_e, D, w_c, h_o, C_p, A_b, W_{Max}, p_s, d_o and Q_T, the resulting design provides:

$$\beta_3 = 1.71$$

$$S = 1.0$$

$$K = W_{max}/(0.1\ h_o)$$

$$\left(\frac{\epsilon}{h_o}\right)_{max} = 0.1$$

Again it might be desired to specify K. To do this replace Step (9) with the following:

Alternate Step (9)

(a) Specify K

(b) Calculate $(\frac{\epsilon}{h_o})_{max} = \frac{W_{max}}{K\ h_o}$ ... (should not exceed 0.3)

(c) Calculate $p_s = \frac{W_{max}}{A_b\ S_{max}\ (\frac{\epsilon}{h_o})_{max}} = \frac{W_{max}}{A_b\ (\frac{\epsilon}{h_o})_{max}}$

After executing alternate Step (9) continue as before to obtain d_o, p_{bo}, and Q_T by means of Steps (10), (11), and (12) respectively. The resulting design will provide:

$\beta_3 = 1.71$

$S = 1.0$

K = as specified

$(\frac{\epsilon}{h_o})_{max} = \frac{W_{max}}{K\ h_o}$ . . . (should not exceed 0.3)

B. EXTERNALLY PRESSURIZED BEARING WITH VARIABLE EXTERNAL RESTRICTION (LOAD SENSING).

1. Theoretical Bearing Static Stiffness (Square Bearing).

As it was pointed out in the INTRODUCTION, the variable external restriction offers a means of improving the static stiffness as compared to the static stiffness of the bearing with fixed external restriction. The variable external restriction should be designed so that it will decrease in flow resistance when its connecting bearing pressure pad increases in pressure due to external journal loading and so that it will increase in flow resistance when its connecting bearing pressure pad decreases in pressure due to external journal loading. This should yield a stiffer bearing than one with fixed external restrictions. This type control of the variable external restriction is of the load sensing variety, in that the external flow resistance is adjusted by the bearing pad pressure, which, of course, is a function of journal load. For this arrangement, the variable restrictions for pressure pads which are located opposite each other can be considered as a controller for displacement in the direction of these particular pads. For a bearing with four pressure pads, two such controllers are necessary.

The controller design which was selected and which conforms to the above description is a spool valve type flow resistance with valve position dependent upon the pressure difference between opposite bearing pressure pads. This controller concept is illustrated in Figure 10. Here the flow path length through the spool valve on the high pressure side decreases, hence decreasing its flow resistance, and the flow path length through the spool valve on the low pressure side increases, hence increasing its flow resistance. In Figure 10 the general case of a fixed external restriction, R, plus a variable external restriction is shown. For this case the spool valve position is adjusted directly by the pad pressures; however, the flow through the spool valve clearance must pass through R before entering the pressure pad. This arrangement may be thought of as having a fixed external resistance and a variable input pressure to this fixed resistance.

The pertinent controller dimensions are identified in Figure 10. They are spool valve diameter, d_c; spool valve cross-sectional area, $A_c = \pi d_c^2/4$; spool valve radial clearance, h_c; flow length through one side of spool valve for central valve position, ℓ; spool valve inlet annular groove width, w_g; and total spool valve length, $L_c = (2\ell + w_g)$. Also illustrated are the spool valve compression springs of spring constant K_c.

In the analysis for bearing static stiffness of the above control system, the bearing is again assumed to be a square bearing, that is, the bearing is considered to have parallel surface exit flow paths. Other assumptions are: the fixed external restriction is a linear flow resistance, such as a capillary tube; the variable external restriction of the controller can be considered as a parallel surface restriction and hence as a variable linear flow resistance; the bearing flow is only out the ends of the bearing (that is, no circumferential flow exists) and is not affected by the journal rotational speed; the flow throughout is laminar and incompressible; the overall supply pressure, p_s, is constant and $\epsilon << h_o$.

The journal load, W, is again expressed for the static case by equation (1), that is:

$$W = A_b (p_{b2} - p_{b1}) \tag{1}$$

To determine an expression for the static bearing stiffness, the pad pressures, p_{b2} and p_{b1}, must be expressed in terms of the bearing eccentricity, ϵ. The procedure is as follows: The pressure pad pressures can be written as

$$p_{b2} = p_s - \frac{Q_{b2}}{Q_{b0}} \left(\frac{\ell - x}{\ell} \right) p_o'' - \frac{Q_{b2}}{Q_{b0}} p_o''' \tag{28}$$

and

$$p_{b1} = p_s - \frac{Q_{b1}}{Q_{b0}} \left(\frac{\ell + x}{\ell} \right) p_o'' - \frac{Q_{b1}}{Q_{b0}} p_o''' \tag{29}$$

where p_o'' = pressure drop across controller spool valve when it is centrally located (journal no-load condition), psi g.

p_o''' = pressure drop across fixed external restriction, R, for journal no-load condition, psi g.

x = axial displacement of controller spool valve in the direction away from high pressure controller side(See Figure 10), inch.

The bearing flow ratios Q_{b2}/Q_{bo} and Q_{b1}/Q_{bo} are again related to the bearing clearance ratios h_2/h_o and h_1/h_o by equations (4) and (5) respectively. And the bearing clearance ratios are related to the bearing eccentricity ratios by equations (8) and (9). The pressure ratios are defined as

$$\beta_2 = \frac{P_d}{P_{bo}} \tag{30}$$

and β_3 again as $\beta_3 = \frac{P_s}{P_{bo}}$ (31)

The axial displacement of the spool valve can be expressed as

$$x = \frac{A_c}{2K_c}\left(P_{b2} - P_{b1}\right) = \frac{A_c W}{2K_c A_b} \tag{32}$$

Now by substitution of equations (4), (5), (8), (9), (30), (31) and (32) into equations (28) and (29) and then by substitution of equations (28) and (29) into equation (1), the following relation is obtained:

$$\frac{\epsilon}{h_o} = \frac{\left(2C_c\beta_2 - \beta_3^2\right)\left(\frac{W}{A_b P_s}\right) + \left(C_c\beta_2\right)^2\left(\frac{W}{A_b P_s}\right)^3}{6C_c\beta_2\left(\frac{W}{A_b P_s}\right)^2 - 6\left(\beta_3 - 1\right)} \tag{33}$$

where C_c = controller constant $= \frac{A_c P_s}{2K_c \ell}$ (34)

This expression is a cubic equation in W. An expression for $K = \partial W/\partial\epsilon$ was obtained for $W = 0$ and this expression was maximized with respect to β_3 and β_2. This led to $K_{max} = (2.2\ A_b p_s)/h_o$, which is not much larger than K_{max} for the fixed external restrictions. However, it was noticed from the expression for $K = \partial W/\partial\epsilon$ that it is possible to obtain K values larger than the K_{max} value which was obtained by maximizing K with respect to β_3 and β_2. This can be understood if a three dimensional plot of K versus β_3 and β_2 is visualized. The maximized K value is that K value where the slope $\partial K/\partial\beta_3$ and $\partial K/\partial\beta_2$ are both equal to zero. It is conceivable that values of K exist which are higher than that at this maximized point. This is the case of $K = \partial W/\partial\epsilon$ at $W = 0$ for the expression (33), in fact for this case it is mathematically possible to obtain $K = \infty$ if the proper β_3, β_2, and C_c values are selected.

Since little was gained by dealing with $K = \partial W / \partial \epsilon$, it was decided to study instead W versus ϵ. A three dimensional plot of $W/(A_b p_s)$ versus ϵ/h_o and C_c with parameters β_3 and β_2 was constructed from equation (33). The appearance of this plot is shown in Figure 11. The relation is plotted only out to $C_c = 3.0$ and up to $W/(A_b p_s) = 0.5$. This particular plot is for $\beta_3 = 2.0$. The surfaces abod and fbod are the limiting surfaces of the plot and represent the surface for β_3 fixed at 2.0 and β_2 fixed at zero and the surface for β_3 fixed at 2.0 and β_2 fixed at the value $(\beta_3 - 1)$ respectively. In between these two limiting surfaces, lie a family of surfaces which represent the surfaces for β_3 fixed at 2.0 and β_2 fixed at various values between zero and $(\beta_3 - 1)$. Some idea of this may be gained by observing Figure 12, which illustrates a $W/(A_b p_s)$ versus ϵ/h_o cross section of Figure 11 at $C_c = 3.0$. Here in Figure 12 the effect of the variation of β_2 is seen when β_3 is held fixed. Again referring to Figure 11, surface abod is a plane surface of constant slope on the $W/(A_b p_s)$ and ϵ/h_o coordinates, that is constant K value. This surface, as has been pointed out, represents $\beta_2 = 0$. This case will always yield a plane surface, such as abod, for all values of β_3, since it is the case where there is no pressure drop across the controller spool valve. Hence this case reduces simply to the case of the externally pressurized bearing with fixed external linear restriction, R. The surface fbod is a curved surface. It is the surface for the case when $\beta_2 = (\beta_3 - 1)$. This is the case where there is no pressure drop across the fixed external restriction R. That is, it is the case when only a variable external restriction is employed. The family of surfaces for β_2 ranging from zero to $(\beta_3 - 1)$, which lies between the abod and fbod surfaces, will be curved surfaces and represent the cases when a pressure drop exists across both R and the controller spool valve. The effect of variation of β_2 for a fixed β_3 has already been seen. The influence of β_3 on Figure 11 can be visualized by seeing the effect of β_3 on the two limiting surfaces abod and fbod. The effect on the family of surfaces between these limiting surfaces will be obvious and need not be mentioned. The influence of β_3 on the surface abod is seen in Figure 13, where an end-view of the plane surface is shown and

the variation of K can easily be seen. Hence for β_3 other than the optimum β_3 value, the plane surface abod is inclined more to the right and thus has a smaller K value. This of course is nothing new, since it was discussed earlier for the case of fixed external linear restrictions and was depicted by equation (10). The influence of β_3 on the surface fbod can be seen from Table I. The location of (o) and (d) of the fbod surface is unchanged, but the location of (f) is affected by β_3. From Table I it is seen that the surface fbod becomes curved more to the left as β_3 is increased, since point (f) moves more to the left. Also, the location of (b) moves more to the right or left in accordance with Figure 13.

TABLE I

Effect of β_3 on Point (f) of the Curved Surface for $\beta_2 = (\beta_3 - 1)$ and Variable C_c in Figure 11 (Surface fbod).

β_2	β_3	ϵ/h_o for point (f) of Figure 11
$(\beta_3 - 1)$	1.5	−0.88
$(\beta_3 - 1)$	2	−1.42
$(\beta_3 - 1)$	3	−2.00
$(\beta_3 - 1)$	4	−2.47

Of course, ϵ/h_o values greater than plus or minus unity are not possible, since this would mean that the journal had exceeded the radial clearance in the bearing. This limitation must be kept in mind when observing Figure 11. The plot is not valid for $|\epsilon/h_o|$ greater than 1.0.

There is another limitation which must be placed on Figure 11. The controller spool valve displacement, x, must not exceed length ℓ. If x is made to exceed ℓ, then the equations indicate an increase in pressure through the controller spool valve, which of course is impossible. Therefore, the variables should be so limited to insure that $x \leq \ell$. From equations (32) and (34), this is the same as the following limitation:

$$C_c \left(\frac{W}{A_b P_s} \right) \ell \leq \ell$$

or that

$$\frac{W}{A_b P_s} \leq \frac{1}{C_c} \quad . \tag{35}$$

Equation (35) is shown plotted in Figure 14a and its limitation on Figure 11 is shown in Figure 14b. Here it is seen that surface qtrz limits the $W/(A_b p_s)$ values as C_c is increased.

As a summary of the findings of the analysis, it can be said that it seems possible that a very stiff bearing should be attainable. Also, there is the possibility of instability which would lead to oscillation of the bearing journal. This instability would arise when a negative bearing stiffness is encountered. This is possible here, as may be seen from Figure 11, 12 or 14. Furthermore, it is seen that there is no need to employ the fixed restriction, R. If a stiff bearing can be attained, it can be attained just as well with or without the R. Of course, construction of the system is simplified if R is not employed. For this case, the controller spool valve end seals are not required and the controller simply can be of the design illustrated in Figure 15. This controller design is represented in Figure 14b by the surface zqbod where $\beta_2 = (\beta_3 - 1)$.

It is well to recall that the above analysis assumed that the fluid is incompressible, that p_s is constant, that the bearing is a square bearing (that is, the bearing is considered to have parallel surface exit flow paths), that R is a linear flow restriction, that the controller is a parallel surface restriction, that the flow is laminar, that $\epsilon << h_o$, that the bearing flow is not affected by the journal rotational speed, and that no circumferential flow exists in the bearing.

In order to correct the above analysis for the square bearing to that of the round bearing, it is merely necessary to multiply all calculated ϵ/h_o values by 1.13. This is an accordance with equations (18) and (19). This means that the right-hand side of equation (33) should be multiplied by the constant 1.13.

2. Experimental Bearing Static Stiffness (Round Bearing).

a. Experimental Apparatus

In order to see if the preceding analysis agrees with the actual bearing, an experimental investigation was carried out for the externally pressurized bearing with variable external spool valve restrictions. In this experimental investigation the bearing journal was not rotated. The bearing chosen for this testing was exactly the same four pressure pad bearing which was employed

in the experimental investigation for the fixed external orifice restrictions. This bearing is fully described in Chapter II-A-3 of this thesis. Also described in Chapter II-A-3 is the test fixture for supporting the test bearing and loading the test bearing journal, the pressure supply unit for loading the journal, the pressure supply unit for the test bearing, the means of counter-balancing the weight of the bearing journal and attached components and the means of measurement of the journal displacement. The variable external spool valve restriction arrangement is as depicted in Figure 15. The pertinent controller internal dimensions are as follows:

$d_c = 0.515$ inches
$\ell = 0.283$ inches
$w_{gc} = 0.250$ inches
$L_c = 2\ell + w_{gc} = 0.816$ inches
$A_c = (\pi d_c^2)/4 = 0.208$ in^2
$h_c =$ varied
$K_c =$ varied

MATERIALS
SPOOL VALVE = MILD STEEL
CONTOLLER HOUSING = MILD STEEL

For this investigation the pressure ratio, β_3, was varied by changing h_c. Here β_3 was varied from 3.33 to 1.43 as h_c was changed from 0.00085 to 0.0043 inches. For this controller-bearing arrangement without the fixed external restriction, R, of Figure 10, the pressure ratio β_2 is not an independent variable, since it is equal to $(\beta_3 - 1)$. Hence there is no need to include β_2 in this discussion. The controller constant, C_c, was varied by changing the spring constant, K_c, of the controller compression springs. The controller would accomodate compression coil springs of 1/4" minimum I.D., of 1/2" maximum O.D., and of 1 1/2" to 3" in length. Standard "Wickwire" compression coil springs were employed. They were obtained from the Hardware Products Co., Boston, Massachusetts. Here C_c was varied from approximately 1.0 to 7.0 as K_c was changed from 92 to 14.2 lb/in. The supply pressure, p_s, was held constant so that it would not influence C_c. The pressure chosen for p_s was 270 psig.

Since the loading in these tests is in the direction of two opposite bearing pressure pads, the bearing pressure pads perpendicular to the loading will be unaltered with respect to pressure difference. Hence, this set of pressure pads will not actuate its associated controller and the controller will then act as a fixed external restriction with a β_3 pressure ratio equal

to that for the controller no-load condition. Hence, while testing a particular controller for radial bearing loading, it is only necessary to provide the set of pressure pads perpendicular to the loading with fixed external restrictions. The test controller is only necessary for the pressure pads in line with the loading. Therefore, in order to save building of a duplicate controller in the controller tests reported herein, the set of pressure pads perpendicular to the loading were not fitted with a controller but instead were fitted with fixed external orifice restrictions of the same β_3 pressure ratio as that for the no-load condition for the controller under test.

b. Experimental Results

Experimental journal load versus journal displacement data were obtained for various β_3 pressure ratios and various C_c controller constant values. In obtaining this data, it was soon found that an instability exists for weak controller compression springs if a stop is not provided for the spool valve. If the spool valve happens to overshoot its equilibrium position when this position is such that the trailing edge of the spool valve is near the fluid inlet annulus, then the spool valve trailing edge may pass into the inlet annulus and be held there by the force of the supply pressure, p_s, on the end of the spool valve. In this case a negative loading is applied to the bearing journal by the controller through the bearing pressure pads. The typical journal load versus displacement data for this situation is shown in Figure 16. When a stop is provided for the spool valve which prevents its trailing edge from entering the inlet annulus, the negative loading is eliminated. Data are also shown in Figure 16 for the case where a stop is employed. For the remaining controller data, a spool valve stop was employed. The experimental journal load-displacement results are shown in Figures 17, 18, 19 and 20. Figure 17 shows the effect of C_c when β_3 is held constant at 1.49. Here C_c was varied from 1.06 to 6.86. It is seen that an optimum value of C_c does exist and for $\beta_3 = 1.49$ of this figure, this optimum value of C_c is 4.37. Figure 18 shows the effect of β_3 when C_c is held constant at 4.37, the optimum C_c value for Figure 17. Here β_3 was varied from 1.49 to 3.33. It is seen that an optimum value of β_3 also exists and for $C_c = 4.37$

of this figure this optimum value of β_3 is 1.79. Figure 19 shows the effect of β_3 when C_c is held constant at a value other than the optimum C_c value for Figure 17. Here the C_c value is 2.32 and β_3 is varied from 1.39 to 3.33. Here again there is an optimum value for β_3 and it is approximately the same value as the optimum β_3 value for Figure 18. The results of Figures 17, 18, and 19 are compiled in Figure 20 in order to obtain the precise optimum C_c and β_3 values. Figure 20a is a plot of $W/(A_b p_s)$ at $\epsilon/h_o = 0.1$ versus C_c with β_3 as a parameter for the family of curves. Figure 20b is a plot of $W/(A_b p_s)$ at $\epsilon/h_o = 0.1$ versus β_3 with C_c as a parameter for the family of curves. These are plots of non-dimensional load capacity at a specific ϵ/h_o value, hence they are an indication of the non-dimensional bearing static stiffness, S. From Figure 20a it is seen that the optimum C_c value seems to be 4.5 and from Figure 20b it is seen that the optimum β_3 value is 1.8. The controller which was tested that is closest to this optimum condition has $C_c = 4.37$ and $\beta_3 = 1.79$. For this controller K_c was 22.3 lb/in (spring-compression type 2" long x 1/2" O.D. x 0.062" wire diameter) and h_c was 0.0015 inches. The journal stiffness for this condition should not be significantly different from that at the optimum condition, since these two controllers are almost identical. The journal load-displacement data for $C_c = 4.37$ and $\beta_3 = 1.79$ can be seen in Figure 18. The bearing stiffness for this condition seems to be infinity for $W/(A_b p_s)$ from zero to 0.25, and for $W/(A_b p_s)$ greater than 0.25 the curve goes off at a bearing stiffness of about S = 1.0. For this controller, the controller spool valve will be just up against the spool valve stop when $W/(A_b p_s) = 1/C_c = 1/4.37 = 0.23$. This is the upper load limit for the controlling action of the controller. This relation was presented as equation (35) and was plotted in Figure 14a. For loads below $W/(A_b p_s) = 0.25$, the spool valve displacement, x, is less than ℓ and the controller does furnish controlling action. At $W/(A_b p_s) = 0.25$, the spool valve displacement, x, is equal to ℓ and the controller spool valve is against the spool valve stop. For $W/(A_b p_s)$ higher than 0.25, the controller does not provide control, but simply acts as a fixed external restriction in the low pressure side of the bearing. The external restriction in the high pressure side of the bearing when the spool valve is against the spool valve stop is almost completely removed from the flow path.

Thus it is seen that a variable external flow restriction can provide an externally pressurized bearing with an extremely high bearing stiffness. For the optimum β_3 and C_c values, the spool valve controller provided a bearing stiffness of $S = \infty$ for loads within its controlling range. If the accuracy of the journal displacement measurements is taken into account, then a more conservative value of maximum bearing stiffness might be $S_{max} \approx 25$. For the optimum controller condition the supply pressure, p_s, was 270 psig, hence this $S_{max} \approx 25$ corresponds to a value of $K_{max} \approx 50 \times 10^6$ lb/in. This bearing stiffness is comparable with the stiffness of a rolling contact bearing.

A comparison of the above experimental results with the theoretical results predicted by the preceding analysis which culminated into the equations (33) and (35) where $\beta_2 = (\beta_3 - 1)$ and the plot of Figure 14b where $\beta_2 = (\beta_3 - 1)$ shows a major discrepancy with regard to the bearing stiffness. The analysis predicted that a very stiff bearing could be produced by any β_3 value as long as C_c was properly selected, that is for every β_3 value there would be an optimum C_c value which would produce an extremely stiff bearing. The experimental results showed that there is only one combination of β_3 and C_c which will produce an extremely stiff bearing. Furthermore, the analysis indicated that it would be possible to obtain undesirable negative bearing stiffnesses. The experimental results showed that all bearing stiffnesses are positive (the exception to this was the case when the controller spool valve did not have a spool valve stop, however the negative stiffness in this case was due to an extraneous cause). These discrepancies are, without a doubt, due to the circumferential flow effect within the bearing. It was seen in Figures 5, 7 and 8 that the bearing circumferential flow has a very significant effect in reducing the bearing stiffness as compared to the theoretical non-circumferential result for the case of the fixed external restriction. Therefore, it should be expected that the circumferential flow will have an even greater effect in reducing the bearing stiffness as compared to the theoretical non-circumferential result for the case of the variable external restriction. Here an even greater pressure difference is forced across the bearing by the controller, hence a greater quantity of circumferential flow should occur. By the reduction of the bearing stiffness the circumferential flow is stabilizing the bearing against negative bearing stiffnesses, however, it is doing so at the expense of the overall

bearing stiffness except for the condition of the optimized controller. The effect of the circumferential flow on the theoretical non-circumferential flow analysis is illustrated in Figure 21. Here the journal load-displacement surface for $\beta_3 = 2.0$ is shown for the theoretical non-circumferential flow case (Surface zuqbod) and for the experimental case (Surface f'b'od) which of course will have circumferential flow. The theoretical non-circumferential flow journal load-displacement surface is merely the surface for $\beta_2 = (\beta_3 - 1)$ in Figure 14b (Surface zqbod) plus the surface zuq which represents the theoretical non-circumferential flow controller result with the spool valve up against the spool valve stop (that is, the result when $W/(A_b p_s)$ exceeds the value given by Figure 14a or Equation (35)). The experimental surface was determined from Figures 17, 18, and 19. From Figure 21, one can see that the spacing between the theoretical and experimental surfaces is fairly uniform for $\beta_3 = 2.0$ and $C_c = 0$ to 6.0. It is known that the reduction in bearing stiffness at $C_c = 0$ is due to the circumferential flow effect. Thus one is reasonably justified in stating that the discrepancy between the theoretical and experimental surfaces for $C_c = 0$ to 6.0 must also be due entirely to the circumferential flow effect. It should be realized that the uniform spacing between the two surfaces does not indicate a uniform reduction in bearing stiffness. The maximum reduction in bearing stiffness occurs in the vicinity of the optimum C_c value ($C_c = 4.5$).

Although the foregoing theoretical non-circumferential flow analysis for bearing stiffness did lead to a considerable error when it was compared to the actual bearing where circumferential flow does occur, it did serve a useful purpose in this investigation. It did point out the important non-dimensional parameters $W/(A_b p_s)$, ϵ/h_o, β_2, β_3, and C_c. This was very useful in carrying out the experimental investigation. The analysis also pointed out that there was no benefit to be gained by including a fixed external restriction in the system in addition to the variable external restriction. This eliminated needless complexity in the controller design. Incidently, it is doubted that the extreme bearing stiffness which was obtained for the optimum controller condition would have been possible if the fixed external restriction had been included in the system. It can be seen from the experimental results that the controller at the optimum condition just barely had enough controlling action to yield the result that it did, a fixed

external restriction in addition to the controller would have decreased the controller's effectiveness within the bearing. Furthermore, the theoretical results are perfectly usable for the case where no circumferential flow is present. A bearing with only two opposite 1/4 circumference pressure pads would be a bearing with little circumferential flow.

No mention has been made so far as to the dynamic response of the controlled bearing. It was not the goal of this investigation to study the dynamic properties of the bearings, however the following observations were made: at no time did the controlled bearing become unstable so as to cause vibration of the journal; the controlled bearing remained stable when the journal was loaded rapidly with the loading pressure supply, when the journal was cocked back and forth, when the journal was tapped, and when the controller was tapped.

As a variation of the above spool valve controller, a controller with a second spool valve connected to the original spool valve (primary spool valve) was investigated in an effort to extend the controller's controlling range to load capacities higher than $W/(A_b p_s) = 0.25$ for the optimum primary controller. It will be recalled that the optimum controller was active only below this load capacity. In this investigation the second spool valve was so arranged so that it was active only when the primary spool valve had nearly completed its stroke and so that it only engaged on the low pressure side of the controller. The idea of this arrangement was to increase the flow resistance to the low pressure side of the bearing in an effort to further decrease the pad pressure on the low pressure side. The primary spool valve by itself causes the high pressure pad of the bearing to achieve a pressure of p_s. However, it does not cause the low pressure pad of the bearing to reach zero pressure, as the simplified theory predicts. The reason for this discrepancy comes from the fact that circumferential flow does exist in the bearing and from the fact that the controller does not completely shut off the fluid supply to the low pressure side of the bearing. An analysis which assumes circumferential flow for the case when the low pressure pad supply is completely shut off was carried out. This analysis showed that the maximum value of $W/(A_b p_s)$ which will cause no displacement of the journal is approximately 0.7. An experiment with a non-operative controller for this

same condition experimentally revealed that this maximum value of $W/(A_b p_s)$ is 0.6. Hence it is theoretically possible to increase the controller's controlling range by 100% by employing a secondary spool valve. The difficulty of this arrangement is that the secondary spool valve must be capable of, or very nearly capable of, completely shutting off the low pressure side of the bearing. Hence the secondary spool valve must produce a very large flow resistance. Thus, if the secondary flow resistance is not engaged at the proper time or at the proper rate, then it is possible for this controller to apply negative loading to the bearing journal which leads to a negative bearing stiffness. Of course, the rate of engagement of the secondary spool valve must be controlled by means of a secondary spool valve compression spring which only engages when the secondary spool valve is engaged. For the various conditions tested, the following secondary spool valve specifications lead to the maximum increase in the controller's controlling range without leading to negative bearing stiffnesses: spring constant of secondary spool valve compression spring = 185 lb/in, engagement of this spring at $x = 0.75\ell$, engagement of secondary spool valve at $x = 0.67\ell$, secondary spool valve diameter = 0.515 inch, and secondary spool valve diametral clearance = 0.001 inch. This secondary spool valve arrangement coupled to the spool valve of the previously optimized controller increases the upper limit of the controlling range from $W/(A_b p_s) = 0.25$ to 0.35. The bearing stiffness within the controlling range is again infinity and above the controlling range, $S \approx 1.0$. This investigation did not exhaust all possibilities. It is believed that a further increase in the upper limit of the controlling range could have been achieved if the diametral clearance of the secondary spool valve had been decreased. In this investigation only the spring constant of the secondary spool valve compression spring and the time of the engagement of this spring were varied. The other variables were held constant at the above given values. Further investigation along the lines of a secondary spool valve were abandoned since it was felt that the added complexity of the secondary spool valve and its secondary compression spring was not warranted. It was felt that the single spool valve controller is much more desirable and that for a particular application the value of $A_b p_s$ can be so adjusted so that the maximum $W/(A_b p_s)$ value lies within the controller's controlling range. (For further details of the secondary spool valve investigation, see reference 11.)

3. Design Procedure for Maximum Bearing Stiffness

This section is offered as a guide to the design of externally pressurized bearings with variable external spool valve restrictions which will provide the maximum bearing stiffness for this arrangement. This design procedure is based on the experimental results for the optimized single spool valve controller, that is, the controller shown in Figure 15 for optimum β_3 and C_c values. The experimental results are reliable for design purposes, since the circumferential flow effect is incorporated into the result. Care is taken in the design procedure to insure a circumferential flow effect in the designed bearing which is equivalent to that of the tested bearing. If this condition were not placed on the designed bearing, then its bearing stiffness would not necessarily be that which is indicated in the design procedure. If the bearing internal arrangement were such as to have more circumferential flow, then the bearing stiffness would be less than the design value; and if the bearing internal arrangement were such as to have less circumferential flow, then the bearing stiffness will be greater than the design value.

a. Design Steps for Variable External Spool Valve Restriction (Spool Valve Controller)

(1) Use a four pocket bearing as illustrated in Figure 2a.

(2) Select L_p, L_e, D and w_c so that $F_b = L_p L_e / D w_c = 0.5$.

(3) Select a minimum practical value for the bearing diametral clearance, $2h_o$, in accordance with the D to be employed (A minimum is usually $2h_o/D = 0.0005$).

(4) Make $C_p >> h_o$. This means that $C_p \geq 10h_o$.

(5) Calculate $w_b = D/\sqrt{2}$.

(6) Calculate $A_b = (L_p + L_e)w_b$.

(7) Use one spool valve controller to feed each set of opposite bearing pressure pads. In this case two controllers are required. The spool valve controller should be of the design shown in Figure 15. It should be connected directly to the bearing pads as also shown in this figure. The spool valve should be provided with a spool valve stop on each side so that the spool valve ends cannot pass into the spool valve inlet annulus. The controller body should be designed so that the spool valve cannot close off the flow at the end of its stroke (that is, the only flow restriction within the controller should be that through the diametral clearance of the

spool valve). The maximum non-dimensional stiffness for the designed bearing will be $S_{max} \geq 25$ and it will occur for $\beta_3 = 1.8$ and $C_c = 4.5$.

(8) Determine the maximum journal load to be encountered, W_{max}.

(9) Calculate the necessary supply pressure, p_s, to keep the controller within its operating range throughout the entire loading up to W_{max} from the following relation:

$$p_s = \frac{W_{max}}{0.25\ A_b} \quad .$$

(If this p_s is unreasonable, then another value of A_b must be selected which will yield a reasonable p_s. The reselection of A_b will usually mean a reselection of L_p, L_e, D and w_c, since the value of F_b must also be maintained at 0.5.)

(10) Select a practical spool valve diameter, d_c.

(11) Calculate $A_c = (\pi d_c^2)/4$.

(12) Select a value for the overall spool valve length, L_c, so that $L_c \geq 1.5\ d_c$.

(13) Select a value for the spool valve inlet annulus groove width, w_{gc}, so that the inlet annulus will offer little flow resistance.

(14) Determine the value of ℓ from $\ell = (L_c - w_{gc})/2$.

(15) Calculate the spool valve radial clearance, h_c, which is necessary to produce the optimum β_3 pressure ratio of 1.8. Use the following relation for this calculation:

$$h_c = \left(\frac{D\ell}{1.6\ d_c\ L_e} \right)^{\frac{1}{3}} h_0 \quad . \tag{36}$$

(See Appendix E for derivation of equation (36).)

(16) Calculate the spring constant, K_c, of the spool valve compression springs which is necessary to produce the optimum C_c value of 4.5. Use the following relation for this calculation:

$$K_c = \frac{A_c\ p_s}{9\ell} \quad . \tag{37}$$

(If K_c thus determined is not practical or is non-standard, then the values of A_c and ℓ should be adjusted to provide a desirable K_c. This reselection of A_c and ℓ will usually change h_c as seen from equation (36).)

(17) Select a depth for the spool valve inlet annulus groove so that it will be at least ten times the value of h_c.

(18) Calculate the bearing pressure pad no-load pressure $p_{bo} = p_s/\beta_3$.

(19) Calculate the total flow required by the bearing, Q_T, from:

$$Q_T = \frac{\pi D h_o^3 P_{bo}}{6 \mu L_e} \tag{26}$$

where μ is the fluid absolute viscosity in lb-sec/in^2 units. (See Appendix D for derivation of equation (26).) For the above determined values of L_p, L_e, D, w_c, h_o, C_p, A_b, W_{max}, p_s, d_c, A_c, ℓ, h_c, K_c, p_{bo}, and Q_T, the resulting design provides:

$$\beta_3 = 1.8$$
$$C_c = 4.5$$
$$S \geq 25$$
$$K \geq W_{max}/(0.01\ h_o)$$

C. EXTERNALLY PRESSURIZED BEARING WITH VARIABLE EXTERNAL RESTRICTION (POSITION SENSING).

Scher[12] employed positional feedback control to increase the stiffness of an externally pressured journal bearing. A complete linearized dynamic analysis of this system was made. A laboratory model of the system was constructed and tested. This was a non-rotating model with journal diameter of 1 inch and diametrical clearance of .003 inches. The fluid used was hydraulic oil of 155 SSU at 100°F.

The operation of this controller is as follows: Displacement of the journal is sensed by an orifice which is formed between the journal surface and a hole in the sensing device. This causes a pressure change in a transducer feed line which in turn moves a flapper valve. This motion of the flapper valve changes the orifice area of exhaust orifices which are located in the bearing pressure pad feed lines. Hence a controlled pressure difference is developed across opposite bearing pressure pads which supports the load that initially caused the journal displacement. Since the journal displacement sensing devise is continually measuring and adjusting for the error in journal position by adjusting the bearing pressure differential, the controller is a positional feedback control system.

The results obtained for the positional controller are comparable to those reported herein for the load sensing controller. However, the positional feedback controller is more complex in design, and hence, manufacture, than the load sensing controller.

D. ROTATIONAL EFFECTS

The experimental results for the externally pressurized bearing with incompressible fluid supply for this investigation were all for the case when the bearing journal was not rotating. Also the experimental results of Shaw and Macks[7] and Raimondi and Boyd[8], which dealt with the case of the fixed external restriction, were for the case of a non-rotating journal. And the experimental results of Scher[12], which dealt with the case of the position sensing controller, were also for the case of the non-rotational journal. Hence the effect of the journal rotation on the bearing stiffness and stability is not exactly known. However, Raimondi and Boyd[8] predict that the journal rotation will increase the bearing stiffness due to some self-acting bearing action in addition to the externally pressurized bearing action. Their idea is that the rotating journal will pump fluid from the low pressure pad to the high pressure pad. This, of course, produces an effect which is opposite to that of the pressure-induced circumferential flow. Thus the bearing stiffness should be improved by the journal rotation.

Another effect which the journal rotation may produce, if the rotational speed is increased high enough, is turbulent flow in the bearing. From the work of Tao and Donovan[11,13], which was concerned with the flow through a concentric annulus of fine clearance with rotation, the journal rotational speed, N_{crit}, for the onset of turbulent flow in the bearing exit paths can be estimated as:

$$N_{crit} = \frac{120}{\pi D} v'_{crit} \sqrt{1 - \left(\frac{v}{v'_{crit}}\right)^2} \quad , \text{rpm} \tag{38}$$

where $v'_{crit} = \dfrac{R'_{e_{crit}} \nu}{2 h_o}$, in/sec

$R'_{e_{crit}} = 1500$ to 2500

ν = kinematic viscosity of fluid, in^2/sec.

v = axial flow velocity for $N = 0$.

or $v = \dfrac{2 Q_B}{\pi D h_o}$, in/sec.

Equation (38) is shown plotted in Figure 22 where v is the variable. The onset of turbulent flow was taken as $R'_{e_{crit}} = 1500$ and the condition of

fully developed turbulent flow was taken as $R'_{e_{crit}} = 2500$. Figure 22 is plotted for the case of the four-pad bearing employed in this thesis investigation, that is for D = 6 inches, $h_o = 0.0015$ inches and $\nu = 88.5 \times 10^{-5}$ in^2/sec (fluid = water). Also it should be noticed that v is plotted in ft/sec units instead of in in/sec units as defined above. Included on Figure 22 is the data from Cornish which was reported by Croft[14]. It is seen that there is agreement between the results of Tao and Donovan and the results of Cornish. The work of Cornish was carried out prior to 1938, whereas the work of Tao and Donovan was as recent as 1955. It is believed that Cornish had difficulty determining the exact point at which turbulence began and thus his data spreads throughout the transition region as determined by the curves of Tao and Donovan. Equation (38) is a theoretical expression with the exception that $R'_{e_{crit}}$ was experimentally determined. Hence from Figure 22, it is seen that for journal rotational speeds of the test bearing which are higher than about 5000 rpm, the bearing flow will be entirely turbulent. Below about 5000 rpm the bearing flow may be turbulent, may be in the transition region or may be laminar, depending on the fluid axial flow velocity. Of course, for a bearing of smaller diameter and smaller diametral clearance, the value of N_{crit} is increased since it varies as $1/(Dh_o)$ for constant v and the same fluid. Thus for a bearing of D = 1 inch, $h_o = 0.0005$ inch and fluid = water, the value of v would be very small and thus the transition region would occur from about 50,000 rpm to 88,000 rpm (the result for $v \approx 0$).

Tao and Donovan[11,13] also presented information which gives an indication of the effect of turbulent flow in the bearing on the bearing stiffness. These results are expressible for the rotational case as:

$$\frac{p'_{bo}}{p_{bo}} = 1 \qquad \text{for laminar flow} \qquad (39)$$

$$\frac{p'_{bo}}{p_{bo}} = \left(\frac{v'}{v}\right)^{0.79} \qquad \text{for turbulent flow} \qquad (40)$$

where p'_{bo} = bearing pressure drop for no-load journal condition for the rotational journal case.

p_{bo} = bearing pressure drop for no-load journal condition for the non-rotational journal case.

v = axial flow velocity for N = 0.

or $$v = \frac{2\,Q_B}{\pi D\, h_c}\ , \text{ in/sec}$$

v' = mean resultant velocity due to rotation and axial flow.

or $$v' = \sqrt{v^2 + \left(\frac{\pi DN}{120}\right)^2}\ , \text{ in/sec} \qquad (41)$$

N = journal rotational speed, rpm.

Hence it is seen that the bearing pressure drop is unchanged from its non-rotational value for the rotational case as long as laminar flow exists in the bearing. Also it is seen that the bearing pressure drop is increased from its non-rotational value for the rotational case when turbulent flow exists in the bearing, since (v'/v) will always be unity or larger. Thus, if the journal speed is high enough to cause turbulent flow in the bearing, then the bearing flow resistance will increase. The flow resistance of the external restriction will remain unchanged. Hence for a constant pressure supply, p_s, the value of p_{bo} must increase. This means that β_3 will be decreased. This will be detrimental if the decrease in β_3 is large, since this will lower the bearing stiffness, as can be seen in Figures 7, 18, 19 and 20. However, Figures 7 and 20 indicate that a decrease in β_3 by 15% from its optimum value will not greatly influence the bearing stiffness. Hence turbulent flow in the bearing due to journal rotation should not greatly influence the bearing stiffness unless β_3 is significantly decreased.

CHAPTER III

EXTERNALLY PRESSURIZED BEARING WITH COMPRESSIBLE FLUID SUPPLY

A. EXTERNALLY PRESSURIZED BEARING WITH FIXED EXTERNAL RESTRICTION

1. Theoretical Considerations

a. Bearing Stability for Fixed External Restriction

An important effect that must be considered for the case of the compressible fluid supply which was not important for the case of the incompressible fluid supply is the stability of the bearing. Here an unstable bearing is defined as a bearing which exhibits self-excited journal vibration. For the case of the compressible fluid supply the fluid compressibility plus the fact that this type fluid usually offers very little squeeze-film damping may lead to an unstable bearing. For the case of the incompressible fluid supply the fluid does not possess the detrimental compressibility characteristic and usually offers high squeeze-film damping. Hence this type fluid supply leads to a stable bearing.

A criterion for bearing stability for the case of a compressible fluid supply can be obtained from the work of Richardson[15] and from the work of Rightmire[16]. This criterion can be expressed in terms of the following stability ratio (τ_a / τ_b),

$$\frac{\tau_a}{\tau_b} = \frac{h_0}{k P_{b0}} \left(\frac{\Delta_b}{\Delta_a} \right) \left(1 + \frac{V_p}{A_b h_0} \right) \tag{42}$$

where the new symbols are

P_{bo} = bearing pad or feed port pressure for concentric, no-load journal condition, psia.

k = gas constant of fluid (ratio of constant pressure specific heat to constant volume specific heat).

V_p = volume of pressure pad or feed port, in^3.

$$\Delta_b = \frac{\partial m_{in_1}}{\partial h_1} - \frac{\partial m_{out_1}}{\partial h_1} \tag{43}$$

$$\Delta_a = \frac{\partial m_{in_1}}{\partial P_{b1}} - \frac{\partial m_{out_1}}{\partial P_{b1}} \tag{44}$$

where the subscript (1) refers to a specific bearing pad or feed port and

m_{in} = fluid mass flow rate into the bearing pad or feed port from the external restriction, lb-sec/in.

m_{out} = fluid mass flow rate out from the bearing pad or feed port through the bearing clearance, lb-sec/in.

P_b = bearing pad or feed port pressure, psia.

This expression for (τ_a/τ_b) assumes that the fluid is compressible, neglects the inertia of the fluid and the squeeze-film damping of the fluid, and assumes a linear pressure distribution through the bearing. The condition for stability is

$$\frac{\tau_a}{\tau_b} < 1.0 \tag{45}$$

This condition states that the network of the fluid on the journal during one cycle of sinusoidal journal displacement must be negative for stable journal behavior. Furthermore, from equations (42), (43) and (44) it is seen that this condition exists when the change in fluid mass storage rate with respect to pad pressure is greater than the change in fluid mass storage rate with respect to journal displacement. Also from equation (42) it is seen that greatest stability is achieved for small pad or feed port volumes relative to the effective bearing internal volume. These are indeed important factors to be considered when designing the internal composition of a bearing for use with an incompressible fluid supply.

(1) Fixed External Capillary Restriction

An expression for the ratio $(\Delta b/\Delta a)$ and hence for (τ_a/τ_b) has been worked out by Rightmire[16] and this expression is as follows:

$$\frac{\tau_a}{\tau_b} = \frac{3}{k+1}\left(1 - \left(\frac{q}{z}\right)^{\beta}\right)\frac{\left(1 - z^{\beta}\right)}{\left(1 - q^{\beta}\right)}\left(1 + \frac{V_p}{A_b h_0}\right) \tag{46}$$

where the new symbols are

$$z = \frac{P_{bo}}{P_s}$$

$$q = \frac{P_a}{P_s}$$

$$\beta = \frac{k+1}{k}$$

and

P_s = overall supply pressure, psia.

P_a = ambient exhaust pressure, psia.

In addition to the assumptions for equation (42) this expression for the stability ratio assumes that the bearing has parallel flow exit paths, that no circumferential flow occurs between bearing pads, that the bearing and capillary flows are laminar, that the expansion through the bearing and capillary is isentropic, and that sonic velocity is nowhere reached.

Equation (46) indicates that $(\mathcal{T}_a/\mathcal{T}_b)$ will be less than unity for any value of q when z is such as to provide maximum bearing stiffness, provided that $V_p/(A_b h_o)$ is small enough. Hence, for these conditions a stable bearing will be achieved. The condition for z to provide maximum bearing stiffness will be discussed later. Also for q approaching zero, sonic velocities may be achieved. Hence equation (46) is not valid for values of q which are close to zero.

(2) Fixed External Orifice Restriction.

(a) Choked Orifice Condition

The case when the fixed external orifice restrictions are in the choked condition occurs when[16,17]

$$z \leq \left(\frac{2}{k+1}\right)^{\frac{1}{\gamma}} \tag{47}$$

where $\gamma = \frac{k-1}{k}$. When the fluid is air, then k = 1.4 and the critical value of z is $z_{crit} = 0.528$.

An expression for the ratio $(\Delta b/\Delta a)$ and hence for $(\mathcal{T}_a/\mathcal{T}_b)$ for the choked orifice condition has been worked out by Rightmire[16] and this expression is as follows:

$$\frac{\mathcal{T}_a}{\mathcal{T}_b} = \frac{3}{k+1}\left(1 - \left(\frac{q}{z}\right)^{\beta}\right)\left(1 + \frac{V_p}{A_b h_o}\right) \tag{48}$$

In addition to the assumptions for equation (42) this expression assumes that the bearing has parallel surface flow exit paths, that no circumferential flow occurs between bearing pads, that the bearing flow is laminar, that the orifice has a fixed orifice area, that the supply tank temperature is constant,

that the expansion through the orifice and through the bearing is isentropic, that the orifice is operating in the choked condition, and that sonic velocities are not reached through the bearing.

A comparison of equations (46) and (48) shows that a more severe condition is placed on $V_p/(A_b h_o)$ for stability in the case of the choked external orifice restriction for the same choice of q and z. This statement assumes that q is always less than z.

(b) Non-Choked Orifice Condition

By employing the procedure of Rightmire[16], an expression for the ratio $(\Delta b/\Delta a)$ and for (τ_a/τ_b) can be obtained for the case of the non-choked orifice condition, that is, when $z \geq z_{crit}$. This procedure follows below.

In order to obtain an expression for the ratio $(\Delta b/\Delta a)$, expressions for m_{in} and m_{out} must be available. An expression for m_{in} for a non-choked orifice with isentropic expansion can be obtained from Faires[17] and is

$$m_{in} = C_1 P_s (z)^{\frac{1}{k}} \left(1 - (z)^{\gamma}\right)^{\frac{1}{2}} \qquad (49)$$

where the new symbols are

$C_1 = C_2 A_o$, in-sec.

$C_2 = CC_3$, sec/in.

$C_3 = \left(\frac{223.7}{R g}\right)\left(\frac{c_p}{T_s}\right)^{1/2}$, sec/in.

R = specific gas constant of fluid, ft-lb/lb°F abs.

g = acceleration due to gravity = 386 in/sec^2.

c_p = specific heat of fluid at constant pressure, Btu/lb°F.

T_s = supply tank fluid temperature, °F abs.

This expression for m_{in} is only valid for $z \geq z_{crit}$, and it assumes that the orifice area is fixed, that the supply tank temperature is constant and that the expansion through the orifice is isentropic. An expression for m_{out} for a parallel surface bearing with isentropic expansion can be obtained from Rightmire[16] and is as follows:

$$m_{out} = \frac{2}{\beta} \frac{\rho_a P_a h_o^3 B}{12 \mu L_e} \left(\left(\frac{z}{q}\right)^{\beta} - 1\right) \qquad (50)$$

where the new symbols are

ρ_a = ambient exhaust mass density, $\frac{\text{lb-sec}^2}{\text{in}^4}$.

B = bearing flow exit path width for one pad, inch.

This expression assumes that the bearing has parallel surface flow exit paths, that no circumferential flow occurs between bearing pads, that the bearing flow is laminar, that the expansion through the bearing is isentropic and that sonic velocities are not reached through the bearing.

By substitution of these expressions for $\dot{m}_{in}$ and $\dot{m}_{out}$ into equations (43) and (44), the following is obtained:

$$\Delta b = - \frac{\rho_a P_a h_0^2 B}{2\beta\mu L_e} \left(\left(\frac{z}{q}\right)^{\beta} - 1 \right) \tag{51}$$

and

$$\Delta a = C_1 \left(\frac{1}{k z^{\gamma}} - \frac{\gamma}{2} \right) \left(1 - z^{\gamma} \right)^{\frac{1}{2}} - \frac{\rho_{bo} h_0^3 B}{6\mu L_e} \tag{52}$$

where ρ_{bo} = mass density of fluid in the bearing pad for concentric, no-load journal condition, $\frac{\text{lb-sec}^2}{\text{in}^4}$

And by substitution of these expressions for Δb and Δa and the continuity condition of $\dot{m}_{in} = \dot{m}_{out}$ for steady state flow into equation (42), the following expression for (T_a / T_b) is obtained:

$$\frac{T_a}{T_b} = \frac{3}{k+1} \left(1 - \left(\frac{q}{z}\right)^{\beta} \right) \frac{\left(1 + \frac{V_p}{A_b h_0} \right)}{\left\{ 1 + \frac{\gamma}{2\beta} \frac{\left(1 - \left(\frac{q}{z}\right)^{\beta} \right)}{\left(z^{\gamma} - 1 \right)} - \frac{\left(1 - \left(\frac{q}{z}\right)^{\beta} \right)}{(k+1)} \right\}} \tag{53}$$

In addition to the assumptions for equation (42) this expression assumes that the bearing has parallel surface flow exit paths, that no circumferential flow occurs between bearing pads, that the bearing flow is laminar, that the orifice has a fixed orifice area, that the supply tank temperature is constant, that the expansion through the orifice and through the bearing is isentropic, that the orifice is operating in the non-choked condition, and that sonic velocities are not reached anywhere.

A comparison of equation (53) with equation (48) for the choked orifice case shows that

$$\left(\frac{\tau_a}{\tau_b}\right)_{\text{non-choked}} = \left(\frac{\tau_a}{\tau_b}\right)_{\text{choked}} \frac{1}{F_c} \tag{54}$$

where

$$F_c = \left\{ 1 + \frac{\gamma}{2\beta} \frac{\left(1 - \left(\frac{q}{z}\right)^{\beta}\right)}{(z - \gamma - 1)} - \frac{\left(1 - \left(\frac{q}{z}\right)^{\beta}\right)}{(k+1)} \right\} \tag{55}$$

Thus it is seen that the non-choked expression is the same as that for the choked case except that in the non-choked case it is divided by the term F_c.

(c) Air as the Compressible Supply Fluid

The stability ratio for the fixed external orifice restriction bearing when the supply fluid is air can be determined for various z and q values from equations (48) and (53) by employing the air constants, that is, $k = 1.4$, $\gamma = 0.286$, $\beta = 1.71$ and $\gamma/\beta = 0.167$. The stability ratio for air has been determined in this manner and is shown in Figure 23. In this figure $(\tau_a/\tau_b)\left[1/(1 + V_p/A_b h_o)\right]$ instead of the stability ratio (τ_a/τ_b) is plotted versus q with z as the parameter for the family of curves. In this case the stability condition is

$$\frac{\tau_a}{\tau_b} \frac{1}{\left(1 + \frac{V_p}{A_b h_o}\right)} < \frac{1}{\left(1 + \frac{V_p}{A_b h_o}\right)} \tag{56}$$

and is shown in Figure 23 as the horizontal dashed line for various $V_p/(A_b h_o)$ values. The region above each horizontal dashed line is unstable and the region below each horizontal dashed line is stable.

From Figure 23 it is seen that the choked orifice case tends to be more unstable than the non-choked orifice case. Instability will always occur for the choked orifice case if q is made small enough, that is, if P_s is increased high enough. For the critical orifice condition of $z = 0.528$, instability occurs for $q \leq 0.2$ when $V_p/(A_b h_o) = 0$ and this condition corresponds

to $P_s \geq 73.5$ psia or $p_s \geq 58.8$ psig for $P_a = 14.7$ psia. Whereas for the non-choked orifice case, if $z > .663$, then the bearing will be stable for all values of q if $V_p/(A_b h_o) = 0$. Also it is seen that as $(V_p/A_b h_o)$ is increased, it becomes more difficult to achieve a stable bearing, especially for the choked orifice case.

b. Bearing Static Stiffness for Fixed External Restriction

An expression for the bearing static stiffness for the case of a compressible fluid can be obtained from the work of Richardson[15] and from the work of Rightmire[16]. This expression can be written as:

$$S = \frac{2h_o}{(P_s - P_a)} \left(\frac{\Delta b}{\Delta a}\right) = \frac{2h_o}{P_s} \left(\frac{\Delta b}{\Delta a}\right) \tag{57}$$

This expression for S assumes that the fluid is compressible, neglects the inertia of the fluid, and assumes a linear pressure distribution through the bearing.

(1) Fixed External Capillary Restriction

An expression for the ratio $(\Delta b/\Delta a)$ and hence for S has been worked out by Rightmire[16] and the expression is as follows:

$$S = \frac{6z}{\beta} \frac{\left(1 - \left(\frac{q}{z}\right)^{\beta}\right)\left(1 - z^{\beta}\right)}{\left(1 - q^{\beta}\right)\left(1 - q\right)} \tag{58}$$

In addition to the assumptions for equation (57) this expression for S assumes that the bearing has parallel surface flow exit paths, that no circumferential flow occurs between bearing pads, that the bearing and capillary flows are laminar, that the expansion through the bearing and capillary is isentropic, and that sonic velocity is nowhere reached.

The maximum value of equation (58) for any given value of q is obtained when the value of z is as follows:

$$z_{opt} = \frac{1 + q^{\beta} + \sqrt{\left(1 + q^{\beta}\right)^2 + 4\left(\beta^2 - 1\right) q^{\beta}}}{2(1 + \beta)} \tag{59}$$

The value of S_{max} varies from 1.23 to 1.50 as q is varied from 0 to 1. The practical condition for q will be $q < 1$, hence $S_{max} < 1.50$. For the similar case for incompressible fluid supply, equation (14) indicated that $S_{max} = 1.50$, thus the compressibility reduces the stiffness slightly. For the compressible fluid supply the optimum value of β_3 is about 2.0 for all values of q except those near zero, where it approaches 1.79. For the incompressible fluid supply, the optimum value of β_3 was found to be 2.0. (See equation (14).)

(2) Fixed External Orifice Restriction

(a) Choked Orifice Condition

An expression for the ratio $(\Delta b/\Delta a)$ and hence for S for the choked orifice case has been worked out by Rightmire[16] and the expression for S is as follows:

$$S = \frac{6z}{\beta} \frac{\left(1 - \left(\frac{q}{z}\right)^{\beta}\right)}{(1-q)} \tag{60}$$

In addition to the assumptions for equation (57) this expression for S assumes that the bearing has parallel surface flow exit paths, that no circumferential flow occurs between bearing pads, that the bearing flow is laminar, that the orifice has a fixed orifice area, that the supply tank temperature is constant, that the expansion through the orifice and through the bearing is isentropic, that the orifice is operating in the choked condition, and that sonic velocities are not reached through the bearing.

The maximum value of S attainable occurs for z at the critical value. This value is $S_{max} \approx 1.9$ when the fluid is air and occurs for $z = z_{crit}$ and $q \approx 0.1$. It is seen from Figure 23 that this condition causes an unstable bearing. However, the S_{max} for a stable bearing still occurs for $z = z_{crit}$, but its value is slightly decreased.

(b) Non-Choked Orifice Condition

An expression for S for the case of the non-choked orifice condition can be obtained by substituting equations (51) and (52) into equation (57). This substitution results in the following expression:

$$S = \frac{6z}{\beta} \frac{\left(1 - \left(\frac{q}{z}\right)^{\beta}\right)}{(1-q)} \frac{1}{F_c} \tag{61}$$

In addition to the assumptions for equation (57) this expression assumes that the bearing has parallel surface flow exit paths, that no circumferential flow occurs between bearing pads, that the bearing flow is laminar, that the orifice has a fixed orifice area, that the supply tank temperature is constant, that the expansion through the orifice and through the bearing is isentropic, that the orifice is operating in the non-choked condition, and that sonic velocities are not reached anywhere.

A comparison of equation (61) with equation (60) for the choked orifice condition shows that:

$$S_{\text{non-choked}} = S_{\text{choked}} \frac{1}{F_c} \tag{62}$$

Here it is seen that the non-choked expression is the same as that for the choked case except that in the non-choked case it is divided by the term F_c.

The maximum value of S attainable for the non-choked condition (equation 61) is about 2.15 when the fluid is air. This S_{max} value can be achieved for q values ranging approximately from q = .8 to .2 by the proper choice of z. And for $V_p/(A_b h_o) = 0$, these conditions are all stable for $z \geq 0.663$. For the similar case for the incompressible fluid supply, equation (17) indicated that $S_{max} = 2.05$, thus the compressibility does not seem to greatly affect the magnitude of S_{max} for this case. For the compressible fluid supply the optimum value of β_3 varies from 1.56 to 1.82 and is dependent upon the supply pressure, p_s. For the incompressible fluid supply, the optimum value of β_3 was found to be 1.71 and is independent of the supply pressure, p_s. Hence even the optimum β_3 values are in fair agreement.

(c) Air as the Compressible Supply Fluid

The static stiffness for the fixed external orifice restriction bearing when the supply fluid is air can be determined for various z and q values from equations (60) and (61) by employing the air constants, that is, $k = 1.4$, $\gamma = 0.286$, $\beta = 1.71$ and $\gamma/\beta = 0.167$. The results of this procedure are shown in Figure 24. In this figure S is plotted versus q with z as the parameter for the family of curves. Also plotted in Figure 24 is a stable-unstable boundary line for $V_p/(A_b h_o) = 0$. This boundary line was plotted from the information of Figure 23. The boundary line applies only to those constant z curves which are circled at the intersection of the boundary line and the constant z curves. Stable-unstable boundary lines for $V_p/(A_b h_o) > 0$

are not shown in Figure 24, but if necessary they can be obtained from the information of Figure 23. In general as $V_p/(A_b h_o)$ increases the unstable region also increases in Figure 24 due to a shift of the stable-unstable boundary line to the right.

The maximum static stiffness for a stable bearing in the case of the choked orifice condition is seen to be 1.87 for $V_p/(A_b h_o) = 0$ and occurs for $z = z_{crit}$ and $q \approx 0.2$, whereas in the case of the non-choked orifice condition it is seen that the maximum static stiffness is 2.15 and instability is not a problem as long as $z > 0.663$ for $V_p/(A_b h_o) = 0$. For greater stability in the case of the choked orifice condition, a reduction in bearing static stiffness is necessary. Thus, when it is at all possible, the non-choked orifice condition should be employed since for this condition the maximum bearing static stiffness and stability can be attained for any particular value of $V_p/(A_b h_o)$. Also the value of the static stiffness is maintained at relatively high values over most of its active q-region.

A comparison of the results of Figure 24 with the results obtained in Chapter II for the fixed external orifice restriction with incompressible fluid shows that the compressibility does not decrease the value of S_{max} for the non-choked case, but it actually increases S_{max} slightly. The similar value for the incompressible fluid case for no circumferential flow is $S_{max} = 2.05$. The compressibility does, however, add another parameter, that is q. For each value of q there is an optimum value for z, hence a single z_{opt} value does not exist unless q is held constant. It should be realized that z is the ratio $1/\beta_3$ expressed in absolute pressure units and q for most cases is entirely determined by P_s. Hence if a comparison of various fixed external orifice restriction bearings for the compressible fluid case is to be made experimentally, it is very important to employ the same value of P_s for all testing because a change in P_s will affect the value of S as will a change in the pressure ratio $z = P_{bo}/P_s$. For the incompressible fluid case, β_3 has only one optimum value.

c. Flow Characteristics of Bearing Components

(1) Fixed External Restriction Flow Characteristics

The above sections showed that the maximum bearing stiffness is attained when the fixed external restriction is an orifice for the compressible fluid supply case. Also the best stability for a fixed external

orifice restriction bearing is attained when the orifice is operated in the non-choked condition. Hence the fixed external orifice restriction operating in the non-choked condition will only be considered here. An expression for the flow characteristics of this orifice was given by equation (49), however it might be desirable to have the expression in terms of weight rate flow instead of mass rate flow as in equation (49). The use of the following relation provides such an expression,

$$W_{in} = m_{in}(g), \text{ lb/sec.} \tag{63}$$

And when the fluid is air which is supplied at P_s and 70 F, then this expression can be written as,

$$W_{in} = .0703\, C d_o^2 P_s z^{.715} \left(1 - z^{.286} \right)^{\frac{1}{2}} \tag{64}$$

since $R = 53.3$ ft-lb/lb ^{o}F abs.

$T_s = 530^{o}$F abs.

$c_p = 0.24$ Btu/lb^{o}F

$A_o = (\pi/4)\, d_o^2$, in^2.

$1/k = 0.715$

$\gamma = (k - 1)/k = 0.286$

Values for $W_{in}/(C\, d_o^2\, P_s)$ are given below in Table II for various z values.

Table II Values of $W_{in}/(C\, d_o^2\, P_s)$

z	$W_{in}/(C\, d_o^2\, P_s)$, 10^{-2} sec^{-1}
.6	1.80
.7	1.70
.8	1.50
.9	1.12
.95	0.82
1.0	0

(2) Bearing Flow Characteristics

The flow characteristics of a bearing of the axial exhaust groove type shown in Figure 2b will be now presented for the concentric, no-load journal case. The flow is considered to be similar to the flow through parallel surfaces. Figure 25 shows a developed view of one of the bearing

internal sectors with pertinent dimensions illustrated. This figure also shows the assumed linear pressure distribution through the sector. The sector is divided into two equivalent flow paths like the one labeled (A) and two equivalent flow paths like the one labeled (B). The flow through each of these flow paths can be determined from the following expression for flow through parallel surfaces which assumes laminar sub-sonic flow,

$$m = \frac{h_0^3 B}{12\mu} \rho \frac{\partial P}{\partial x_b} \quad . \tag{65}$$

which can be obtained from Rightmire[16] and Shaw and Macks[7]. For flow through the flow path labeled (A), this expression becomes,

$$m_A = \frac{h_0^3}{12\mu} \left(\frac{B_A}{L_2} x_b \right) \rho \frac{\partial P}{\partial x_b} \tag{66}$$

where $B_A = (\pi D/n) - w_g$

$L_2 = B_B/2 = L_b/2$

n = number of bearing sectors.

x_b = distance along flow path as defined in Figure 25.

And if isothermal flow is assumed to exist, then

$$m_A \frac{dx_b}{x_b} = \frac{h_0^3 B_A \rho_a}{12\mu L_2 P_a} P\, dP \tag{67}$$

By integrating both sides of equation (67) as follows

$$m_A \int_{L_1}^{L_2} \frac{dx_b}{x_b} = \frac{h_0^3 B_A \rho_a}{12\mu L_2 P_a} \int_{P_a}^{P_{b0}} P\, dP \tag{68}$$

$$m_A \ln \frac{L_2}{L_1} = \frac{h_0^3 B_A \rho_a}{12\mu L_2 P_a} \left(\frac{P_{b0}^2}{2} - \frac{P_a^2}{2} \right) , \tag{69}$$

the following is obtained:

$$m_A = \frac{B_A}{L_2 \ln \frac{L_2}{L_1}} \frac{h_0^3 P_a \rho_a}{24\mu} \left(\left(\frac{P_{b0}}{P_a} \right)^2 - 1 \right) \tag{70}$$

where $L_1 = d_p/2$

d_p = feed pad or port diameter, inch.

In a similar fashion the following can be obtained:

$$m_B = \frac{B_B}{L_3 \ln \frac{L_3}{L_1}} \frac{h_0^3 P_a \rho_a}{24\mu} \left(\left(\frac{P_{b0}}{P_a} \right)^2 - 1 \right) \tag{71}$$

where $B_B = L_b$

$L_3 = B_A/2$

The total flow through the sector is the flow which is twice the sum of m_A and m_B, hence

$$m_{out} = \left\{ \frac{B_A}{L_2 \ln \frac{L_2}{L_1}} + \frac{B_B}{L_3 \ln \frac{L_3}{L_1}} \right\} \frac{h_0^3 P_a \rho_a}{12\mu} \left(\left(\frac{P_{b0}}{P_a} \right)^2 - 1 \right) \tag{72}$$

For the four sector exhaust groove bearing of Figure 2b, the total bearing flow is

$$m_T = n\, m_{out} = 4\, m_{out} \tag{73}$$

where $B_A = \frac{\pi D}{n} - w_g = \frac{\pi D}{4} - w_g$

$B_B = L_b$

$L_1 = d_p$

$L_2 = B_B/2 = L_b/2$

$L_3 = B_A/2$

Equations (72) and (73) also assume that no circumferential flow occurs between bearing pads (or sectors).

Equation (72) can be expressed in terms of weight rate of flow as follows:

$$W_{out} = m_{out}\, g \tag{74}$$

and equation (73) as

$$W_T = 4\, W_{out} \tag{75}$$

d. Rotational Effects

(1) Turbulence within the Bearing due to Journal Rotation

The journal rotational speed for transition from laminar to fully developed turbulent flow can be predicted from equation (38) in Chapter II. For onset of turbulence $R'_{e_{crit}}$ can be taken as 1500 and for fully developed turbulence $R'_{e_{crit}}$ can be taken as 2500. When the supply fluid is air with $D = 0.75"$ and $2h_o = .001"$, this expression yields for the transition region the following range of N:

$$N_{trans} = 187{,}000 \text{ to } 312{,}000 \text{ rpm}$$

when $W_T = 80 \times 10^{-6}$ lb/sec

$\nu = 2.45 \times 10^{-2}$ in^2/sec

(See Appendix F for details of this calculation.)

(2) Journal Critical Speeds

The important journal critical speeds for a gas bearing have been pointed out be Fischer, Cherubim and Fuller[18]. These journal critical speeds are presented in the following discussion.

(a) Mechanical Critical Speed

This critical speed is best given by the natural frequency of a "free-free" beam and is

$$N_{mech\ crit} = 214 \left(\frac{EIg}{W_j \ell_j^3} \right)^{\frac{1}{2}} \text{ rpm} \qquad (76)$$

where E = modulus of elasticity of journal material, psi.

I = area moment of inertia of journal in bending, in^4.

W_j = weight of the journal, lb.

ℓ_j = length of the journal, inch.

For a steel journal of $D = 0.75"$ and $\ell_j = 11.5"$, equation (76) yields $N_{mech.\ crit.} = 61{,}500$ rpm.

(b) Inversion Point Critical Speed

This is the journal speed where the journal ceases to spin about its geometric center and begins to spin about its center of gravity. This critical speed is given by

$$N_{Inversion} = \frac{30}{\pi}\left(\frac{K g}{W_j}\right)^{\frac{1}{2}} \quad \text{rpm} . \tag{77}$$

For journal speeds below $N_{Inversion}$, the balance of the journal is not important. The value of $N_{Inversion}$ is considerably lower than $N_{mech.\ crit.}$ For a steel journal of D = 0.75" and ℓ_j = 11.5" which is supported by an air bearing of minimum K = 3600 lb/in, equation (77) yields $N_{Inversion}$ = 9,460 rpm. For values of K higher than that used in this calculation, this critical speed will be higher.

(c) Whirl Critical Speed

This is the journal speed where the center of the journal moves in an orbital motion around the center of the bearing at a frequency that is equal to, or less than, N/2. For an externally pressurized bearing with compressible fluid supply, this speed can be determined from

$$N_{whirl\ crit} = \frac{30}{\pi} R_w \left(\frac{K g}{W_j}\right)^{\frac{1}{2}} \tag{78}$$

where R_w is the whirl ratio which is the ratio of the journal speed to the whirl or orbit speed = $N_{whirl\ crit.}/N_{whirl}$. Hence for R_w = 2, N_{whirl} = $N_{whirl\ crit.}/2$ which is referred to as the half-frequency whirl. The value of R_w can vary from 2 to 6.

A comparison of equation (78) with equation (77) shows that for an externally pressurized gas bearing the following relationship holds:

$$N_{whirl\ crit.} = R_w\ N_{Inversion} \tag{79}$$

Hence for the journal and air bearing given in the example of the above section (b), $N_{whirl\ crit.}$ = 18,900 to 56,700 rpm, since $N_{Inversion}$ = 9,460 rpm.

2. Experimental Investigations

a. Goal of Experimental Investigations

The experimental investigations for the fixed external restriction bearing had a specific goal. This goal was simply to provide a bearing which was stable up to a reasonable value of P_s and which possessed a typical bearing stiffness. This bearing was to be used as a standard for the further investigation in Part B of this Chapter. Hence this present investigation might be considered as a preliminary investigation. Therefore an extensive testing program was not carried out to varify the results of Figures 23 and 24, but instead a testing program was carried out only far enough to provide one satisfactory fixed external restriction bearing. The restriction employed was an orifice which is operating in the non-choked condition.

b. Experimental Apparatus

The experimental apparatus can be divided into the following components: test bearing, test bearing fixture, journal loading and counter-balancing devices, journal rotational drive mechanism, journal displacement measuring device, test bearing fluid supply, and fixed external restrictions. These components are discussed below.

(1) Test Bearing

The internal design of the test bearing was selected on the basis of the work of Fischer, Cherubim and Fuller[18] which presented some satisfactory designs. The design chosen is that shown in Figure 2b and is the four-sector exhaust groove type bearing. The pertinent internal dimensions are as follows:

$D = 0.75$ inch.
$L_b = 1.00$ inch
$h_o = 0.0005$ inch.
$w_g = 0.063$ inch.
$C_g = 0.063$ inch
$w_b = D/\sqrt{2} = 0.53$ inch
$A_b = 0.159$ in^2.
$d_p = 0.213$ inch
$n = 4$

The value of A_b was determined from the following relation,

$$A_b = \left[\frac{\pi d_p^2}{4} + \frac{1}{4}\left(L_b w_b - \frac{\pi d_p^2}{4}\right)\right] = \left[\frac{3\pi d_p^2}{16} + \frac{L_b w_b}{4}\right] \tag{80}$$

This expression is readily obtained if the pressure distribution of Figure 25 is assumed and the area is referred to p_{bo}.

The material of the journal was hardened tool steel and the bearing material was cast iron. The journal and bearing were lapped and honed to a tolerance of $\pm$ 0.00001 inch on the diameter. Hence the bearing diametral clearance was very accurate as well as being uniform.

(2) Test Bearing Fixture

The test bearing was housed integrally in a test bearing fixture. This arrangement is shown in Figure 26. The front end of the journal was supported by the test bearing and the rear end was supported by a precision angular contact ball bearing. The rear bearing served as a pivot for the journal. The journal length between the two bearings was much longer than the test bearing length, hence the bearing clearances remained fairly uniform through the length of the bearing as the journal pivoted about the rear bearing when the test bearing was loaded. The ball bearing stiffness was so much greater than the test bearing stiffness that little radial journal displacement occurred at the rear bearing. Also, because the angle of pivot was very small, the rear pivot bearing offerred essentially no bending moment on the rear end of the journal.

(3) Test Bearing Journal Loading and Counter-Balancing

The loading was applied to the journal by means of a radial ball bearing mounted on the very front end of the journal close to the test bearing. Loads were applied by hanging weights on the loading bearing. In order to achieve a no-load journal condition, the journal was counter-balanced by loading vertically upward by means of a frictionless pulley arrangement which is illustrated in Figure 26. The test bearing was then loaded vertically downward by hanging weights on the loading bearing. In both cases the loading was applied through a nylon string in series with a rubber section.

The rubber section was merely a "rubber band" and served to dynamically isolate the loading weights from the journal mass.

Since the loading was not applied directly to the center of the bearing length, the actual journal load had to be calculated from the load applied to the loading bearing. This calculation is

$$W = \frac{(\ell_a + \ell_b)}{\ell_a} W_L \tag{81}$$

The values of ℓ_a and ℓ_b in this investigation were 9.50" and 1.94" respectively, thus $W = 1.20\ W_L$.

(4) Journal Rotational Drive

The journal could be rotated up to rotational speeds of 6000 rpm. The rotational drive arrangement is illustrated in Figure 26. A variable speed Graham transmission which had a speed range of 0 to 3000 rpm was used to drive a jack shaft by means of an endless flat belt. The pulley diameters were such as to step up the rotational speed by a factor of two. The jack shaft was supported by two preloaded angular contact ball bearings. The jack shaft drove the bearing journal through a soft rubber coupling. The rubber coupling was merely a short length of low pressure rubber hose and it was held on the jack shaft and journal by its own elasticity.

(5) Journal Displacement Measurement

The radial displacement of the journal within the test bearing was measured by means of capacitance probes located symmetrically on each side of the test bearing. This arrangement can be seen in Figure 26. Each probe conformed to the curvature of the journal and was located at a distance of 0.005" from the journal surface. The surface area of each probe was 0.381 in^2. These probes were electrically connected in parallel to a Fielden Proximity Meter, Model PM.2, which was obtained from Fielden Electronics Limited, Manchester, England. This instrument indicated the displacement of the journal by the position of a pointer on an indicating meter. The Proximity Meter had a built-in modulator which allowed the instrument to indicate the static position of a stable journal or the mean position of a vibrating journal. The instrument could also be operated without the internal

modulator. In this case the instrument would indicate the total amplitude of vibration of a vibrating journal. Provision was made on the instrument so that the vibrating journal displacement waveform could be observed on a cathode ray oscilloscope (CRO). Hence the frequency of the vibrating journal could be determined.

The Fielden Proximity Meter and probes were calibrated by means of Johansson precision gage blocks. This calibration was carried out by placing the test bearing fixture on a surface plate and building up gage blocks under the journal immediately in front of the test bearing. The resulting calibration curve is shown in Figure 27. Here the journal displacement is that displacement at the location of the gage blocks, for this reason the total displacement is 0.0011" instead of $2h_o = 0.001"$. Since the journal pivots about the rear bearing, the journal displacement at the gage blocks will be greater than the journal displacement within the bearing. The journal displacement at the gage block location was estimated from the distances involved for a journal displacement of $2h_o$ at the front edge of the bearing and was found to be approximately 0.0011". This pivoting of the journal also caused the total journal displacement at the bearing central location along the length of the bearing to be less than $2h_o$. However, the deviation was only 5% of the diametral clearance or 5% of the radial clearance, that is, only 5% error in the ratio ϵ/h_o. Thus this deviation was neglected and the mean total journal displacement was taken as $2h_o$.

The calibration showed that the meter indication was linear with journal motion for journal eccentricity ratios of $\epsilon/h_o = +1.0$ to -0.8 where the journal central position is $\epsilon/h_o = 0$ and positive eccentricity ratios represent journal motion in the direction of the loading, that is, downward. Thus the meter indications could be directly employed because the eccentricity ratios encountered in this investigation were all within the linear region of the meter. For the calibration of this investigation the smallest meter division corresponded to 20×10^{-6} inches, however, the meter could easily be estimated to half divisions. This meter proved quite satisfactory for this investigation with regard to sensitivity and bridge balance stability with time. This testing was carried out in an air conditioned room where the room temperature was maintained at 70 F. This factor no doubt helped the meter stability.

In order for the Proximity Meter to function properly, the journal had to be grounded to the meter. This can be problematic when the journal is rotating. A satisfactory means of grounding the journal to the meter was found and is illustrated in Figure 26. First, electrical contact between the journal and jack shaft was attained by placing a fine wire within the rubber coupling between them. The rubber coupling held the wire in contact with the journal and the jack shaft. Next, a straight steel phonograph needle was press-fitted into a hole in the free end of the jack shaft. A carbon brush of the type used for electric motor brushes was then spring loaded against the needle point to provide the final electrical path for the ground lead. This arrangement was found to be satisfactory for the rotational speeds encountered in this investigation.

Error in the ratio ϵ/h_o was estimated for error in journal displacement measurements due to bending of the journal under the loading. For the maximum loadings employed in this investigation, the error caused by this journal bending would be only 1% of the ratio ϵ/h_o. Hence this error was neglected.

(6) Test Bearing Fluid Supply

The fluid supplied was air and was obtained from the 80 psig shop compressed air supply. The air was first fed through a moisture separator, pressure regulator, coarse filter (Fulflo Filter, Model B7-A, Commercial Filters Corp., Melrose, Mass.), and fine filter (Millipore-type AA, 1" diameter, Millipore Filter Corporation, Bedford, Mass.). The fine filter maximum pore size was 0.80 microns. The air was then fed through a flow meter (Sho-Rate 150 Rotameter, Model 1123-1355, Brooks Rotameter Company, Lansdale, Pennsylvania), where the air supply was metered. The accuracy of the flow meter was $\pm$ 2% of the maximum flow of the meter over 10 to 100% of the meter range. After the flow meter the air was fed to the test bearing at the supply pressure, p_s. All fluid pressures were determined by means of Bourdon tube type pressure gages (Marsh Instrument Company, Skokie, Illinois). The accuracy of these gages was $\pm$ 1/2% of the gage reading.

(7) Fixed External Restriction

The fixed external restriction employed in this investigation was a sharp-edged orifice which conformed to the specifications of a VDI

sharp-edged orifice[10]. The orifice was part of a plug which screwed into the feed ports of the bearing. The plug was flat on the end where the orifice hole was located. The plug could be positioned within the feed port by turning the plug and hence the volume of the feed port, V_p, could be varied. The plug was sealed with Duco cement to prevent air leaks when a position for the plug was selected. The feed port diameter, d_p, was relatively large, because the initial plan was to employ a porous plug for the fixed external restriction instead of an orifice. This was unfortunate, because the large d_p meant that the orifice plug had to be located very close to the bearing surface to keep the value of V_p at a minimum. The minimum safe clearance between the end of the plug and the bearing surface was felt to be 0.001". This is the clearance which was employed for each orifice plug in this thesis investigation. The ratio of $V_p/(A_b h_o)$ has been calculated for this clearance and is 2.55. From Figure 23, it is seen that this value places a strict stability requirement on this bearing. The most stable bearing is achieved for $z > 0.8$ and $q > 0.7$. The requirement of $q > 0.7$ corresponds to $p_s < 6.3$ psig, which is a relatively low supply pressure.

The value of the orifice diameter, d_o, necessary to yield a specific z for a given q can be calculated by equating equation (64) to equation (72) and solving for d_o. This relation for d_o was used to help visualize the stability trend for a given d_c. An orifice of $d_o = 0.011$" will yield a value of $z \approx 0.8$ for $q = 0.42$, a value of $z \approx 0.9$ for $q = 0.55$ and a value of $z \approx 0.95$ for $q = 0.60$. For $q = 0.42$, the bearing is definitely unstable. As q is increased, the bearing tends to be more stable. At $q = 0.55$, the bearing operation is approximately on the stable-unstable boundary line. At $q = 0.60$, the bearing operation is below this boundary line and hence the bearing is stable. The q values of 0.42, 0.55 and 0.60 correspond to p_s values of 20, 12 and 9.8 psig respectively. Hence it is seen that the bearing will not be stable for p_s values greater than about 12 psig. An orifice of $d_o = 0.011$" was employed as the fixed external restriction in this thesis investigation.

c. Experimental Results

(1) Bearing Stability

The stability of the above described four sector axial exhaust groove bearing with fixed external orifice restriction was experimentally

investigated with regard to supply pressure, p_s. The orifice employed was d_o = 0.011" and it was located to give $V_p/(A_b h_o) = 2.55$. This bearing remained stable for supply pressures up to p_s = 25 psig; thereafter the journal exhibited vibration. The amplitude of vibration was small initially, but increased with increase in supply pressure. At p_s = 27 psig, the vibration became audible. Further increases in supply pressure led to total vibration amplitudes equal to the bearing diametral clearance. It was not the goal of this investigation to obtain dynamic information about this bearing, but only to provide a stable bearing for further testing. Thus, detailed dynamic information is not presented herein. From this investigation it was seen that this bearing could be stably operated at supply pressures below p_s = 25 psig. This bearing arrangement was accepted as a satisfactory one for further testing. To insure stable operation a bearing orifice supply pressure of 20 psig was selected as a standard for further testing. This standardization of p_s for this bearing arrangement also serves to fix the bearing static stiffness at a constant value. The weight rate flow of air through one bearing sector was 20×10^{-6} lb/sec. or Q_T was 80×10^{-6} lb/sec. for p_s = 20 psig.

A comparison of the experimentally determined upper p_s limit for stable operation with the theoretical upper limit predicted in the above section of this thesis, shows that this bearing actually remains stable up to a supply pressure which is about double the predicted value. The theoretical upper p_s limit was 12 psig. The reason for this discrepancy is the small clearance between the fixed external orifice restriction and the bearing journal. For the concentric journal position, this clearance is only 0.0015". This gives rise to an inherent orifice, which is formed between the edge of the fixed orifice hole and the bearing journal, besides the fixed orifice already discussed. This additional orifice will increase the overall flow resistance of the external restriction which now includes the inherent orifice and hence will decrease the value of z. Rightmire[16] indicates that this inherent orifice tends to improve the stability of the bearing, but it does so at the expense of the bearing static stiffness. These trends occur because the area of the inherent orifice changes in the direction opposite to that required for improving the bearing static stiffness. This is what is referred to as "negative feedback" which will always tend to improve vibration stability.

The bearing was also tested without an external restriction. For this arrangement, the bearing exhibited lockup for all supply pressures, that is, the journal would move to the bearing surface and be held there by the bearing internal pressure. The bearing would only be stable when it was locked up against the bearing surface. The lockup would always occur in the direction of one of the four feed ports.

(2) Flow Characteristics

(a) Fixed External Orifice Restriction

The fixed external orifice restriction of $d_o = 0.011"$ was calibrated by means of the flowmeter of the air supply. Since the supply pressure to this fixed orifice was standardized at 20 psig for the test bearing, the calibration was carried out by holding p_s constant at 20 psig and varying the back pressure of the orifice by means of a needle valve in the exhaust line of the calibration unit. The calibration results are shown in Figure 28a. This calibration curve is plotted in gage pressure units. When $p_s = 20$ psig, the non-choked operation of this orifice occurs for $p_{bo} = 20$ to 3.6 psig. The choked operation occurs for p_{bo} less than 3.6 psig.

Theoretical orifice weight rate flows can be obtained from equation (64) and Table II. For this calculation $d_o = 0.011"$, $P_s = 34.7$ psia and C can be taken as 0.675. These calculations have been made for z = .6, .7, .8, .9, .95 and 1.0 and the results are shown plotted on Figure 28a as open circles. Hence it is seen that fairly good agreement exists between the experimental and theoretical orifice weight rate flow for the assumed C = 0.675.

(b) Fixed External Orifice Restriction plus Inherent Orifice Restrictions

The fixed external orifice restriction plus the inherent (fixed orifice-journal)orifice restriction could not readily be calibrated. However, the total flow characteristics of the combination can be estimated. Figure 28b illustrates the fixed orifice and the inherent (fixed orifice-journal) orifice. Also shown is another minor inherent orifice, that is, the orifice formed between the feed port edge and the journal. The restriction of this inherent orifice is small because of the large value of d_p. The total flow resistance of these combined external restrictions is the sum of the individual flow resistances, that is

$$R_t = R_o + R_{oj} + R_{pj} \qquad (82)$$

where R_t = total flow resistance of external restriction, sec/in^2.

R_o = flow resistance of fixed orifice restriction, sec/in^2.

R_{oj} = flow resistance of inherent (fixed orifice-journal) orifice restriction, sec/in^2.

R_{pj} = flow resistance of inherent (feed port-journal) orifice restriction, sec/in^2.

For a rough approximation, the flow resistance can be taken as inversely proportional to the orifice area. Hence

$$\frac{R_{oj}}{R_o} = \frac{A_o}{A_{oj}} \quad \text{and} \quad \frac{R_{pj}}{R_o} = \frac{A_o}{A_{pj}} \qquad (83), (84)$$

where the A_o = the fixed orifice area $= \frac{\pi d_o^2}{4}$, in^2.

A_{oj} = the inherent (fixed orifice-journal) orifice area $= \pi d_o h_p$, in^2.

A_{pj} = the inherent (feed port-journal) orifice area $= \pi d_p h_o$, in^2.

and h_p = the fixed orifice-journal clearance, inch.

Hence

$$\frac{R_{oj}}{R_o} = \frac{d_o}{4h_p} \quad \text{and} \quad \frac{R_{pj}}{R_o} = \frac{d_o^2}{4d_p h_o} \qquad (85), (86)$$

Equation (82) can be rewritten in the following form

$$\frac{R_o}{R_t} = \frac{1}{\left(1 + \frac{R_{oj}}{R_o} + \frac{R_{pj}}{R_o}\right)} \qquad (87)$$

For the bearing under investigation, $d_o = 0.011"$, $h_o = 0.0005"$, $d_p = 0.213"$ and $h_p = .0015"$. For these values $(R_o/R_t) = 1/3.11$. This ratio indicates that only about a third of the total flow resistance of the external restriction is due to the original fixed orifice restriction and the remaining two-thirds is due to the inherent orifice restrictions. Most of this remaining two-thirds of the total flow resistance is due to the inherent orifice formed between the edge of the fixed orifice hole and the journal. This calculation plus the fact that this bearing exhibited greater stability than expected for a fixed external orifice restriction bearing is substantial proof that the inherent orifices were present in this bearing arrangement.

The ratio of pressure drop for the fixed orifice restriction by itself to the pressure drop for the fixed orifice restriction plus the inherent orifice restrictions can then be approximated as

$$\frac{(P_s - P_{bo})_o}{(P_s - P_{bo})_t} = \frac{R_o}{R_t} \tag{88}$$

for the same weight rate flow through each. Hence for the bearing under investigation, this ratio is 1/3.11. The flow curve of Figure 28a for the fixed orifice restriction by itself can be corrected approximately to the actual case by multiplying the $(p_s - p_{bo})$ values at given W_{in} values by 3.11 and replotting the new $(p_s - p_{bo})$ values at the same W_{in} values. The results of this procedure are also plotted in Figure 28a. Thus it is seen that for $W_{in} = 20 \times 10^{-6}$ lb/sec and $p_s = 20$ psig, the inherent orifice restrictions can reduce the bearing pressure p_{bo} from about 18 psig to about 14 psig, which corresponds to a reduction of z from 0.94 to 0.83.

(c) Bearing Flow Characteristics

The weight rate flow characteristics for the bearing under investigation can be determined from equations (72) and (74) and the internal dimensions of the bearing. From the bearing dimensions given in the above section of this thesis concerned with the experimental apparatus, the following can be calculated:

$B_A = 0.526$ inch.
$B_B = 1.000$ inch.
$L_1 = 0.107$ inch.
$L_2 = 0.500$ inch.
$L_3 = 0.263$ inch.

For these values, when the fluid is air and the ambient temperature is 70 F, equations (72) and (74) become

$$W_{out} = 12.35 \times 10^{-6} \left[\left(\frac{P_{bo}}{P_a} \right)^2 - 1 \right] \tag{89}$$

This is the theoretical weight rate flow relation for the bearing and it is plotted in Figure 29a. Here W_{out} is plotted against $(P_{bo}/P_a)^2$ and hence the relationship is merely a straight line. The auxiliary plot of Figure 29b converts the ratio $(P_{bo}/P_a)^2$ to P_{bo} or p_{bo}.

It was not possible to calibrate the bearing flow for a number of reasons. The calibrated fixed orifice restriction could not be employed to determine bearing feed port pressures because of the presence of the non-calibrated inherent orifices. The bearing feed port pressure could not be measured directly because the pressure tap would increase the feed port volume and hence might cause instability. The bearing could not be calibrated without the fixed orifice restrictions present because this would have led to journal lockup and error in the bearing flow calibration. The journal must be concentrically located and must be stable during the flow calibration. Two possible methods which might have allowed bearing flow calibration are: clamping the journal in the central position with the aid of gage blocks to prevent lockup and calibrating without external restrictions or relocating the fixed external orifice restrictions so that the inherent orifices would be negligible and calibrating by means of the calibrated fixed external orifice restriction. This latter method might not have been possible because the feed port volume was already quite large compared to the bearing internal volume. Further increases in feed port volume most likely would have led to an unstable bearing.

Although the bearing was not calibrated with regard to flow characteristics, it was felt that the bearing feed port pressure, p_{bo}, could be determined from Figure 29 within an accuracy of $\pm$ 10%. Later a similar theoretical flow determination will be presented where experimental confirmation is available. This will substantiate this statement. Hence the value of p_{bo} for the standardized p_s of 20 psig supplied to the bearing arrangement under investigation can be determined from Figure 29. For this condition W_{in} was experimentally determined as 20×10^{-6} lb/sec. For steady-state flow W_{out} will be equal to W_{in}, hence $W_{out} = 20 \times 10^{-6}$ lb/sec. for this condition also. For this value of W_{out}, Figure 29 indicates that $p_{bo} \approx 10$ psig. This value of p_{bo} is less than that which was estimated from Figure 28. However it is felt again that the determination here is the more accurate of the two since that value

found in Figure 28 was based on a rough approximation of the flow resistance of the inherent orifice restrictions. It is seen now that this rough approximation estimated the flow resistance of the inherent orifice restrictions too low.

(d) Summary of Flow Characteristics

The flow characteristics of the fixed external orifice restriction bearing under consideration here with $d_o = 0.011$ inch requires a 1/4 bearing flow of 20×10^{-6} lb/sec. or Q_T of 80×10^{-6} lb/sec. for a standardized supply pressure of 20 psig. This gives rise to a bearing feed port pressure of 10 psig. This corresponds to z and q values of 0.712 and 0.424 respectively. Here it is seen that the inherent orifice restrictions reduce z from 0.94 to 0.712. In terms of β_3 this bearing arrangement provides $\beta_3 = 2.0$. This bearing arrangement will be hereafter referred to as the standardized test bearing.

The exact value of the bearing feed port pressure, p_{bo}, is not really essential in this investigation because it was held constant in all remaining experimentation by holding W_{in} constant. Hence an error in p_{bo} will only change all values of z or β_3 by the same proportion. This error if present is expected to be small.

(3) Bearing Static Stiffness

(a) Non-Rotating Journal

Journal load-displacement data was obtained for the standardized test bearing for the non-rotating bearing case. These data are plotted in Figure 30a. From this figure it is seen that the load-displacement curve is fairly linear up to $\epsilon/h_o \approx 0.4$ and within this linear region the bearing non-dimensional static stiffness, S, is 0.75. The predicted S for $z = .712$ and $q = .42$ from Figure 24 is approximately 2.0. Hence the effect of the inherent orifice restrictions on the bearing static stiffness is seen to reduce S in accordance with Rightmire's[16] prediction. The value of $S = 0.75$ for the standardized test bearing corresponds to $K = 4770$ lb/in.

(b) Rotating Journal

Journal load-displacement data was obtained for the standardized test bearing for journal rotational speeds of 500, 1000, 2000, 3000, 4000, 5000 and 6000 rpm. The journal was loaded only up to loads which caused a

maximum $\epsilon/h_o \approx 0.2$. These results are shown in Figure 30b along with the results for the non-rotating journal. Here it is seen that the effect of the rotating journal is to increase the bearing static stiffness as Raimondi and Boyd[8] predicted. The value of S increases with N and at 6000 rpm the value of S is increased by about 10% compared to the value of S at N = 0 rpm.

During these rotational tests there was a noticeable journal whirl present. The whirl total amplitude for the no-load case varied from $\epsilon/h_o \approx 0.1$ at N = 500 rpm to $\epsilon/h_o \approx 0.4$ at N = 2000 to 3000 rpm and then reduced gradually again to $\epsilon/h_o \approx 0.1$ at N = 6000 rpm. These amplitudes were decreased somewhat as the journal was loaded. The rotational speeds employed were low compared to the mechanical critical speed of 61,500 rpm, the inversion point critical speed of 9,460 rpm and the whirl critical speeds of 18,900 to 56,700 rpm for this journal. The journal exhibited a whirl even at a journal speed of $N \approx 0$ rpm and its total amplitude was $\epsilon/h_o \approx 0.1$. It was also noticed for the no-load journal condition that the journal mean position was at $\epsilon/h_o \approx +0.2$ for N = 500 to 6000 rpm, whereas $\epsilon/h_o = 0$ for N = 0 rpm. It is believed that these effects were caused by misalignment between the rear pivot ball bearing and the front test bearing and perhaps misalignment between the jack shaft and the journal. The presence of the whirl at journal speeds of a few rpm seems to substantiate this belief. Furthermore, the whirling speed of the journal was identical with the journal rotating speed. Thus it seems reasonable to assume that these effects were caused by the testing apparatus and not caused by the test bearing.

In these rotational tests the journal mean position was observed as the journal with a constant rotating speed was loaded. The change of the journal mean position with load from the journal mean position for the journal no-load condition was obtained from these data. These changes in journal mean position from the no-load mean position expressed in terms of eccentricity ratios are the ϵ/h_o values plotted in Figure 30b for the rotational tests. This is legitimate, because the bearing static stiffness is linear for ϵ/h_o up to at least 0.4.

3. Design Procedure

A completely reliable design procedure cannot be presented because extensive testing was not carried out to verify the theoretical results. However, the following design steps may be helpful as a guide for the design of an externally pressurized air bearing with fixed external orifice restrictions.

a. Employ a bearing of the four sector axial exhaust groove type with one central feed port in each sector. With this type bearing little circumferential flow should occur between bearing sectors because of the axial exhaust grooves. This should provide a bearing with maximum stiffness.

b. Select D and L_b so that $D/L_b = 0.75$.

c. Select h_o so that $D/h_o = 750$ to 1500.

d. Select $w_g = C_g = 100\ h_o$.

e. Calculate $w_b = D/\sqrt{2}$.

f. Select d_p from $d_p \approx L_b/8$.

g. Calculate A_b from equation (80).

h. Calculate $A_b h_o$.

i. Select a clearance between the fixed external orifice restriction and the bearing surface so that $V_p/(A_b h_o) \approx 0$. To achieve this it may also be necessary to reselect values of d_p and h_o and to change the feed port configuration from a cylindrical port to a conical port. When selecting this clearance and the feed port configuration, insure that the flow resistance of the inherent orifices will be negligible by making the ratios of A_o/A_{oj} and A_o/A_{pj} as small as possible. This is the same as requiring that the ratios of $d_o/(4\ h_p)$ and $d_o^2/(4\ d_p h_o)$ be as small as possible. (See equations (83), (84), (85), (86) and (87).)

j. Select a practical supply pressure and calculate $q = P_a/P_s$ for this pressure.

k. Select a value of z from Figure 24 which will provide a high bearing static stiffness for the selected q value. It is recommended that z be selected so that the fixed external orifice restriction will be operating in the non-choked condition.

l. Check to see if this choice of q and z will be a stable condition for the $V_p/(A_b h_o)$ ratio of the bearing from Figure 23. If it is an unstable condition, reselect z so as to provide a stable bearing.

m. Calculate the orifice diameter, d_o, of the fixed external orifice restriction which is necessary to provide the selected value of z from the following expression:

$$d_o = \left\{ \frac{\frac{50.5 n_o^3}{C} \left(\frac{B_A}{L_2 \ln\left(\frac{L_2}{L_1}\right)} + \frac{B_B}{L_3 \ln\left(\frac{L_3}{L_1}\right)} \right) q \left(\left(\frac{z}{q}\right)^2 - 1 \right)}{z^{.715} \left(1 - z^{.286}\right)^{\frac{1}{2}}} \right\}^{\frac{1}{2}} \qquad (90)$$

where an average value for $C \approx 0.675$. Equation (90) assumes that the supply air is at a temperature of 70 F and was derived from equations (64) and (72). The orifice employed should conform to the specifications of the sharp-edged VDI orifice.[10] (See Appendix G for derivation of equation 90).

n. Calculate the air flow required to achieve the selected values of z and q from equation (64) or equation (72).

o. Calculate K from the already selected S as follows:

$$K = S \frac{A_b P_s}{h_o} \qquad (91)$$

This design should produce a bearing which is stable and which is relatively stiff. The value of S should lie between 0.5 and 2.0. It should be kept in mind that Figures 23 and 24 assumed a parallel surface bearing and isentropic expansion of the air in the bearing. These assumptions are questionable, since the bearing is a round bearing and it is customary to assume isothermal expansion in the bearing. However, as long as there are four bearing sectors, the round bearing should approximate a parallel surface bearing fairly well. Also the isentropic expansion assumption should not greatly affect the trends of S and T_a/T_b with respect to z and q compared to those for the assumption of isothermal expansion. However, the magnitudes S and T_a/T_b may be affected to some extent.

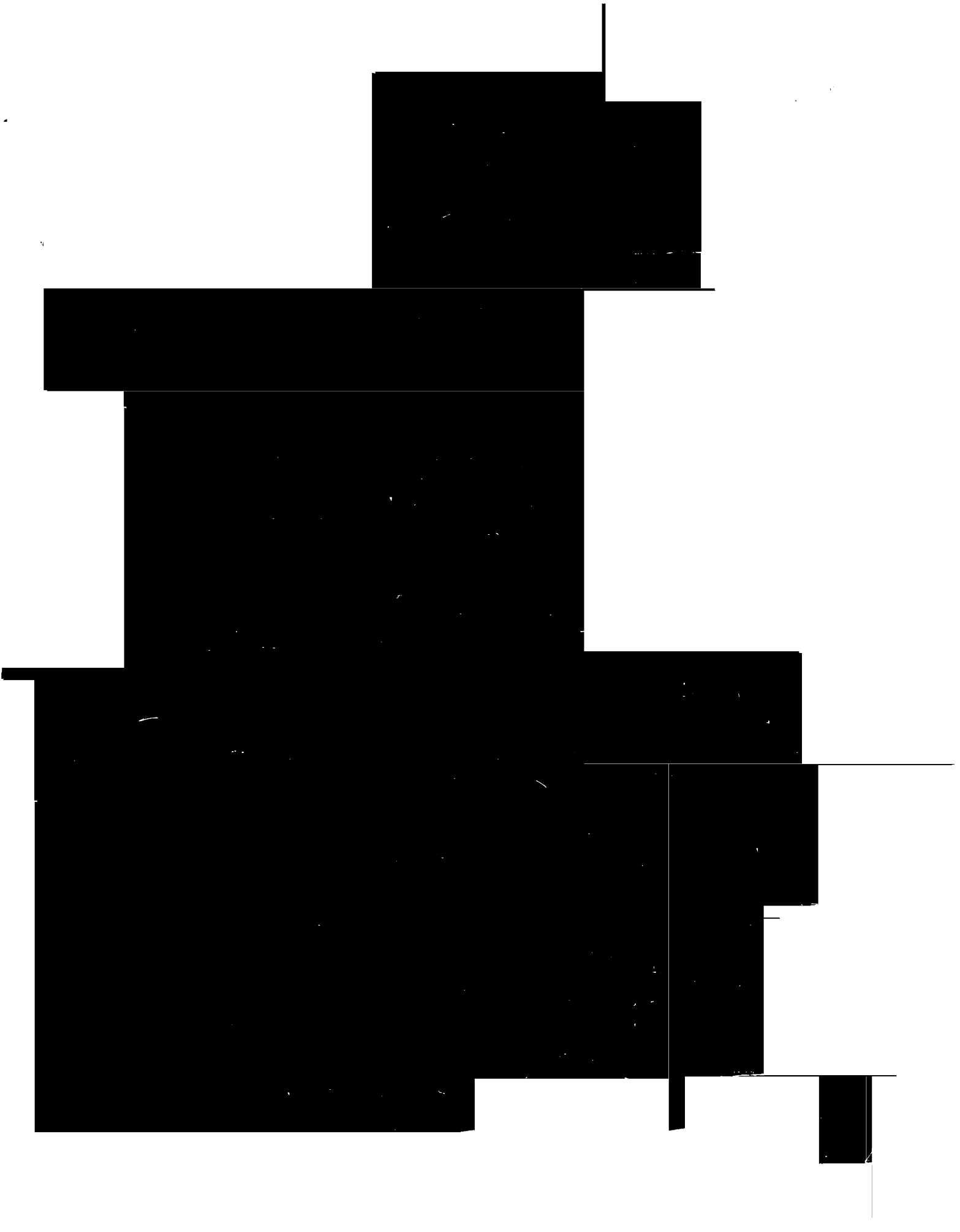

B. EXTERNALLY PRESSURIZED BEARING WITH VARIABLE EXTERNAL RESTRICTION (LOAD SENSING)

1. Theoretical Considerations

a. Bearing Stability for Variable External Restriction

The type of variable external restriction which was investigated here is the same type that was proven successful for the incompressible fluid case. It is the variable external spool valve restriction (spool valve controller) and it was illustrated by Fig. 15. This controller requires relatively long feed passages between the controller and a pair of bearing sectors that are located directly opposite from each other. This requires that the feed port volume, V_p, be very large. From the above stability investigation for the case of the fixed external restriction, it is seen that the direct connection of the controller to the bearing sectors would necessarily lead to an unstable bearing. This type of controller cannot be placed close to one bearing sector without being located far from the opposite sector. The need for making V_p small was essential. This required that a fixed external orifice restriction be placed in the feed passage from the controller very close to the bearing surface as it was in the case of the fixed external orifice restriction bearing. Here the flow from the controller must pass through the orifice restriction before passing through the bearing. The controller spool valve can not be positioned by the bearing pressure as in Fig. 10 because this again would lead to a large

V_p. Hence, the controller spool valve must be positioned by the pressure before the orifice restriction. This should decrease the effectiveness of the controller with regard to bearing stiffness.

Hence, it is seen that the controller cannot be connected directly to the bearing, but instead a fixed orifice restriction must be employed to isolate the controller volume from the bearing feed port volume in order to stabilize the bearing. The fixed orifice is expected to establish and maintain a stable bearing and the controller is expected to improve the static stiffness of the bearing. Furthermore, it was hoped that the controlling action of the controller would not effect the bearing stability. This bearing arrangement is illustrated in Fig. 31 and it might be thought of as a bearing with fixed external restriction which has variable supply pressure to each fixed external restriction. This bearing arrangement is different from that employed in Fig. 15 and will only approach this previous arrangement when the flow resistance of the fixed orifice restriction is small compared to the flow resistance of the bearing. The bearing arrangement of Fig. 31 is not expected to greatly improve the dynamic bearing stiffness because of the controller's isolation from the bearing feed port pressure.

b. Bearing Static Stiffness for Variable External Restriction

The method which was employed in Chapter II to obtain an expression for the journal static load-displacement relationship for the case of the spool valve controller can also be utilized for the bearing arrangement of Fig. 31. Here for simplicity

the fluid is assumed to be incompressible. It was seen in Part A of this chapter that the compressibility did not greatly effect the value of S_{max} nor the optimum value of β_3 which is necessary to produce the S_{max} value compared to the incompressible results. Hence a theoretical expression for the journal static load-displacement relationship based on an incompressible fluid supply should not be too greatly in error from the result based on a compressible fluid supply. This expression based on an incompressible fluid supply, a linearized stabilizing fixed orifice restriction, and the assumption of no circumferential flow between bearing sectors can be written as follows:

$$\frac{\epsilon}{h_o} = \frac{\left[2C_c(\beta_3-\beta_2)\beta_2 - \beta_3^2\right]\frac{W}{A_b P_s} + \left[C_c(\beta_3-\beta_2)\beta_2\right]^2\left(\frac{W}{A_b P_s}\right)^3}{6C_c(\beta_3-\beta_2)\beta_2\left(\frac{W}{A_b P_s}\right)^2 - 6(\beta_3-1) + 12C_c\beta_2\left[1-\left(\frac{\beta_2+1}{\beta_3}\right)\right]\left[1+C_c(\beta_3-\beta_2)\beta_2\left(\frac{W}{A_b P_s}\right)^2\right]} \qquad (92)$$

(See Appendix H for the derivation of equation (92)). A comparison of this expression with equation (33) for the bearing arrangement of Fig. 15 shows that these expressions have the same exact form except for two differences: the term $C_c\,\beta_2$ is replaced with $C_c(\beta_3 - \beta_2)\,\beta_2$ and there is an additional term in the denominator. The additional term in the denominator will always be positive because $(\beta_2 + 1)/\beta_3$ will never be greater than unity and β_3 will always be greater than β_2, hence the presence of

this term should increase the static stiffness of the bearing, since the value of ϵ / h_o will be less for a given $W/(A_b p_s)$ value. The presence of this additional term and the additional $(\beta_3 - \beta_2)$ factor in the $C_c \beta_2$ term is expected to change the optimum value of C_c and of β_3 which was experimentally determined in Chapter II. These optimum values were $C_c = 4.5$ and $\beta_3 = 1.8$. It should be recalled that equation (33) was in error due to the circumferential flow effect, however, equation (33) did give the important non-dimensional parameters which were eventually optimized by experimental means. Since equations (92) and (33) have a similar form, predictions of the actual optimum values of the non-dimensional parameters might possibly be obtained from equation (92) and the optimum values of C_c and β_3 from Chapter II. From equation (92) it can be seen that if the pressure ratios are held constant and if the additional term in the denominator is negligible compared to the other terms in the denominator, then the optimum value for $C_c(\beta_3 - \beta_2)$ should be equal to the optimum C_c value which was determined in Chapter II, that is

$$C_c(\beta_3 - \beta_2) = 4.5 \tag{93}$$

or

$$(C_c)_{opt} = \frac{4.5}{(\beta_3 - \beta_2)} \tag{94}$$

Furthermore it was shown in Chapter II that the value of β_2 could greatly effect the bearing stiffness for a fixed value of C_c and β_3, hence in order to obtain similar results for the bearing arrangements of Fig. 15 and of Fig. 31 it is necessary

that they have identical β_2 values. In the case of the bearing arrangement of Fig. 15, $\beta_2 = (\beta_3 - 1)$ and in the case of the bearing arrangement of Fig. 31,

$$\beta_2 = \beta_3 - (1 + \beta_4) \tag{95}$$

where

$$\beta_4 = \frac{P_o'''}{P_{bo}} \quad .$$

The pressure ratio β_4 is not an independent parameter because only β_2 and β_3 are necessary to specify all pressures in the bearing arrangement for a given p_s. For the bearing arrangement of Fig. 15, the value of β_2 for the optimum value of β_3 was $\beta_2 = 0.8$, hence for a similar result for the bearing arrangement of Fig. 31 the value of β_2 should be

$$\beta_2 = \beta_3 - (1 + \beta_4) = 0.8 \tag{96}$$

and the optimum value for β_3 should be

$$(\beta_3)_{opt} = 1.8 + \beta_4 \tag{97}$$

The value of β_4 will of course depend on the size of the orifice hole diameter of the stabilizing fixed orifice restriction for a given bearing. Now substitution of equation (95) into equation (94) yields the following expression:

$$(C_c)_{opt} = \frac{4.5}{(1 + \beta_4)} \tag{98}$$

Hence it is seen that the optimum C_c and β_3 values for the variable external spool valve restriction bearing with stabilizing external fixed orifice restriction can be predicted from the optimum C_c and β_3 values for the bearing with spool valve controller directly connected to the bearing. The optimum β_3 value is merely the optimum value for the directly connected controller plus the ratio of the pressure drop across the stabilizing fixed orifice restriction to the pressure drop through the bearing. The optimum C_c value is merely the optimum value for the directly connected controller divided by the sum of unity and the ratio of the pressure drop across the stabilizing fixed orifice restriction to the pressure drop through the bearing.

Equation (92) was not employed to obtain a theoretical plot of $W/(A_b p_s)$ versus ϵ/h_o. Its main purpose was to point out the important non-dimensional parameters which could be used as a guide for experimental investigations. The important non-dimensional parameters are, of course, $W/(A_b p_s)$, ϵ/h_o, C_c, β_2 and β_3. However, it is seen that it was also possible to predict optimum values of the important non-dimensional parameters from this equation.

c. Flow Characteristics of Bearing Components

(1) Stabilizing Fixed Orifice Restriction Flow Characteristics

The flow characteristics of the stabilizing fixed

orifice restriction is given by equations (49) and (63) except that P_s should be replaced by P'_{so} and z by z'. And for the case where the fluid is air the flow characteristics are given by equation (64) where the same P_s and z replacements are also to be made. Hence, for air, the weight rate flow expression is

$$W_{in} = .0703\, C\, d_0^2\, P'_{so}\, (z')^{.715} \left[1 - (z')^{.286} \right]^{\frac{1}{2}} \qquad (99)$$

where P'_{so} = the back pressure of the controller for the concentric, no-load journal condition, psia.

$z' = P_{bo}/P'_{so}$.

(2) Bearing Flow Characteristics

The expression for rate of flow through one bearing sector of the axial exhaust groove bearing for the concentric, no-load journal condition is exactly as given by equations (72) and (74).

(3) Variable External Spool Valve Restriction Flow Characteristics

The mass flow rate through one side of the spool valve to a stabilizing fixed orifice restriction for the central spool valve position can be determined from the flow expression for flow through parallel surfaces which assumes laminar sub-sonic flow,

$$\dot{m}_c = \frac{h_c^3 B_c}{12 \mu} \rho \frac{\partial P}{\partial x_c} \qquad (100)$$

which can be obtained from equation (65). In Equation (100), the new symbols are

B_c = width of controller flow path = πd_c, inches

x_c = distance along the controller flow path, inches.

If an isothermal expansion is assumed through the spool valve restriction, then

$$\rho = \frac{\rho_a}{P_a} P \tag{101}$$

and equation (100) becomes

$$m_c = \frac{\pi h_c^3 d_c}{12 \mu} \frac{\rho_a}{P_a} P \frac{\partial P}{\partial x_c} \tag{102}$$

An expression for m_c in terms of the controller dimensions can be obtained by integrating equation (102) as follows:

$$m_c \int_0^{\ell} dx_c = \frac{\pi h_c^3 d_c}{12 \mu} \frac{\rho_a}{P_a} \int_{P'_{s0}}^{P_s} P \, dP$$

$$m_c \ell = \frac{\pi h_c^3 d_c}{12 \mu} \frac{\rho_a}{P_a} \left(\frac{P_s^2 - (P'_{s0})^2}{2} \right)$$

or

$$m_c = \frac{\pi h_c^3 d_c}{24 \mu \ell} \rho_a P_a \left(\frac{P'_{s0}}{P_a} \right)^2 \left[\left(\frac{P_s}{P'_{s0}} \right)^2 - 1 \right] \tag{103}$$

When the fluid is air, equation (103) becomes

$$m_c = 82 \frac{d_c h_c^3}{\ell} \left(\frac{P'_{so}}{P_a}\right)^2 \left[\left(\frac{P_s}{P'_{so}}\right)^2 - 1\right] \qquad (104)$$

or

$$m_c = 82 \frac{d_c h_c^3}{\ell} \left(q'\right)^{-2} \left[\left(\frac{q'}{q}\right)^2 - 1\right] \qquad (105)$$

where $q' = \frac{P_a}{P_{so}}$.

For the four sector exhaust groove bearing, the total bearing flow for the concentric, no-load journal case is four times the flow through one side of the controller, hence

$$m_T = 4\, m_c \qquad (106)$$

Equations (103), (104), and (105) can be expressed in terms of weight rate of flow as follows:

$$W_c = m_c\, g \qquad (107)$$

and equation (106) as

$$W_T = 4\, W_c \qquad (108)$$

2. Experimental Investigations

a. Goal of Experimental Investigations

The goal of the experimental investigations of this part of the thesis was fourfold: to determine if the spool valve controller exhibits controlling action with compressible fluids, to determine if the spool valve controller will cause instability in a stabilized test bearing, to determine if the spool valve controller can be optimized for a standardized test bearing, and to determine the effect of journal rotation on the bearing static stiffness. Hence, it is seen that the goal was not to obtain a bearing arrangement of the highest possible static stiffness, but instead to achieve maximum static stiffness for a given standardized test bearing. The term "standardized test bearing" refers to a bearing of given internal composition which is stabilized by means of a given fixed external orifice restriction.

b. Experimental Apparatus

The experimental apparatus that was employed here was exactly the same as that of Part A of this chapter with regard to the test bearing fixture, journal loading and counter-balancing device, journal rotational drive mechanism, journal displacement measuring device, and test bearing fluid supply. The test bearing employed was the standardized test bearing also of Part A of this chapter and a detailed discussion of it can be found therein. In brief summary, the standardized test bearing had a stabilizing fixed orifice restriction of $d_o = 0.011$ inches which was located in the bearing feed port such that it gave rise to inherent

orifice restrictions, a $V_p/(A_b h_o)$ ratio of 2.55 and $z' = 0.712$, $\beta_2 = 0$, $\beta_3 = 2.0$, and $\beta_4 = 1.0$ all for $q' = 0.424$. The 1/4 bearing flow rate, W_{in}, necessary to achieve these standarized conditions was 20×10^{-6} lb./sec.

As was already pointed out, the test bearing was integral with the test bearing fixture. The fixture was so designed that spool valve controllers could be mounted directly on the fixture. The flow passages connecting the controller to the proper bearing feed ports were made within the test bearing fixture and the controller housing. At the junction between the controller housing and test bearing fixture, O-ring seals were employed to prevent the escape of fluid from the flow passages.

The controller's internal composition is illustrated in Fig. 31. The controller housing material was mild steel and the spool valve material was aluminum. The spool valve compression springs fit into holes, which are not shown in Fig. 31, in the ends of the spool valve. The reason for these holes and the use of aluminum as the spool valve material was to keep the inertia effects of the spool valve mass to a minimum. For the supply pressures anticipated in this investigation the pressure force on the spool valve is relatively small, hence, a spool valve of large mass would lead to time delays in the control system which might cause instability of the bearing. The weight of the spool valve was approximately 0.0013 lb. The pertinent controller internal dimensions are as follows:

d_c = 0.250 inch

ℓ = 0.102 inch

w_{gc} = 0.125 inch

$L_c = (2\ell + w_{gc})$ = 0.329 inch

$A_c = (\pi d_c^2)/4$ = 0.049 in^2.

h_c = varied.

K_c = varied

and the ratio of the controller internal volume including connecting flow passages to the bearing internal volume, $V_c/(A_b h_o)$, was approximately 220. For this investigation, the pressure ratio, β_3, was varied by changing h_c. Here β_3 was varied from 2.1 to 4.1 as h_c was changed from 0.00056 to 0.00028 inches. The flow rate through the bearing was maintained constant by proper adjustment of the overall supply pressure, p_s. The 1/4 bearing flow rate was maintained at 20×10^{-6} lb./sec. This meant that p_s changed with changes of h_c and hence changes of β_3; however, it insured a constant value of p_{so} = 20 psig which provided the standardized testing bearing always with the same $z' = 0.712$, $q' = 0.424$ and $\beta_4 = 1.0$ values. The value of p_s varied from 21 to 41 psig as β_3 was varied from 2.1 to 4.1. The value of the controller constant, C_c, was varied for a fixed value of p_s by changing the spool valve spring constant, K_c. The controller would accommodate compression coil springs of 1/8" maximum O.D. and of 1/2" to 1 1/2" in length. Provisions were made to prevent buckling of the springs. The springs which were employed were standard "Wickwire" compression coil springs and were obtained

from the Hardware Products Company, Boston, Massachusetts. The springs employed had spring constants which varied from 3.3 to 16.6 lb./in. In some cases only one spring was employed in the controller to achieve a lower effective spring constant. The other side of the spool valve in this case was positioned for the concentric, no-load journal condition by a spool valve stop. This arrangement was only employed for the non-rotational journal tests since this controller arrangement only had controlling action for journal loads in one direction. Also an infinite spring constant was achieved by positioning the spool valve in the central position by means of a spool valve stop on each side of the spool valve. These methods provided an effective K_c range of from 1.65 lb./in. to infinity. The range of C_c will also vary with p_s. For example C_c varied from 3.64 to 0 and from 3.06 to 0 for p_s = 25 psig (β_3 = 2.5) and 21 psig (β_3 = 2.1) respectively for the same effective K_c range of 1.65 lb./in. to infinity. For all tests, the controller was provided with additional spool valve stops which prevented the trailing edge of the spool valve from entering the fluid inlet annulus. This prevented accidental negative journal loading by the controller as already discussed in detail in Chapter II.

c. Experimental Results

(1) Bearing Stability

During this investigation the spool valve controller did not cause the standardized test bearing to become unstable. This was found to be true for both the non-rotational and

rotational tests. The rotational test was the most severe of these two tests with regard to stability. As was pointed out in Part A of this chapter, the rotational drive mechanism caused the rotating journal to whirl; but even though this was present the spool valve controller did not excite the bearing into instability. Also when the journal was given sudden loadings during the non-rotational tests, the bearing stability was maintained.

Instability could be made to occur if the flow rate to the controlled bearing was increased just as it could be made to occur for the standardized test bearing without the controller. In Part A of this chapter it was stated that the standardized test bearing became unstable if the supply pressure to it was increased above 25 psig. This supply pressure requires a 1/4 bearing flow rate of 27.5×10^{-6} lb./sec. for this bearing. For the case of the standardized test bearing with the spool valve controller, the bearing became unstable when the 1/4 bearing flow rate was increased above 28×10^{-6} lb./sec. Hence, it is seen that the controller does not effect the stability condition for the standardized test bearing. This means that the stabilizing orifice restriction is rather effective in isolating the controller internal volume from the bearing feed port volume and that the only volume which is important relative to the bearing internal volume with regard to stability is the bearing feed port volume.

For one special test the controller was connected directly to the bearing feed ports without the stabilizing orifice

restrictions in place. This bearing arrangement led to instability immediately upon being pressurized. As the overall supply pressure was increased the amplitude of vibration of the journal increased and for overall supply pressures above 20 psig the total amplitude of vibration was equal to the diametral clearance of the bearing. The frequency of vibration was about 30 cps. Thus, the necessity for employing the stabilizing orifice restrictions is quite obvious.

(2) Flow Characteristics

The experimental flow characteristics of the test bearing and stabilizing fixed orifice restriction have been considered in Part A of this chapter and need not be presented here. The new experimental flow characteristics which are to be presented here are for the variable external spool valve restriction, that is for the spool valve controller. However, before the experimental results are presented, a theoretical controller weight flow rate plot can be obtained from equations (104) and (107). Since in this investigation d_c, ℓ and P'_{so} were held constant at 0.250 inch, 0.102 inch, and 34.7 psia respectively, then equation (107) becomes

$$W_c = 432 \times 10^3 \, h_c^3 \left[\left(\frac{P_s}{P'_{so}} \right)^2 - 1 \right] . \qquad (109)$$

The values of h_c for the spool valves employed in this investigation were 0.00028, 0.00042 and 0.00056 inches. The relationship between W_c and $(P_s/P'_{so})^2$ has been calculated for these

values of h_c and the results are shown on Fig. 32a. For h_c constant, this relationship is linear and the straight lines in this figure are the theoretical results. Figure 32b is an auxiliary plot for converting $(P_s/P'_{so})^2$ values to p_s values and is only valid for p'_{so} = 20 psig.

The experimental weight flow rate through the spool valve controller for the three spool valve sizes was determined by varying the supply pressure to the controller and maintaining the controller back pressure at 20 psig. The flow was measured by means of the flow meter of the test bearing pressure supply unit. The experimental data points are plotted on Fig. 32a. It is seen that fairly good agreement does exist between the theoretical and experimental results, especially for the lower flow rates. The weight flow rate through one side of the controller, W_c, is equal to the weight flow rate through 1/4 of the bearing, W_{in} or W_{out}, hence $W_c = 20 \times 10^{-6}$ lb./sec. since W_{in} has been standardized at this value. Thus for the flow rates of this investigation good agreement exists between the theoretical and experimental flow rate results for the controller. Hence, good agreement can be expected to exist between theoretical and experimental flow rate results for the test bearing for the flow rates of this investigation because both theoretical analyses were similar. In Part A of this chapter it was pointed out that the test bearing could not be readily calibrated, but it is seen now that the use of the theoretical result should be sufficiently accurate.

Special tests were performed to see if the flow characteristics of the spool valve controller is independent of the orientation of the spool valve axis with respect to the gravitational direction. It was found that the flow characteristics were identical for the spool valve controller when it was tested horizontally and vertically. Hence, gravity seems to have a negligible effect on the flow characteristics of the spool valve controller.

(3) Bearing Static Stiffness

(a) Non-Rotating Journal

Journal load-displacement data was obtained for the variable external spool valve restriction bearing for the non-rotating journal case where the test bearing was the standardized test bearing of Part A of this chapter. In these tests the initial flow through the standardized test bearing for the concentric, no-load journal condition was always maintained identical to the condition of Part A, that is the initial 1/4 bearing flow was 20×10^{-6} lb./sec. or the initial total bearing flow was 80×10^{-6} lb./sec. This, of course, means that for the investigation now being reported the test bearing always had values of $z' = 0.712$, $q' = 0.424$ and $\beta_4 = 1.0$ and hence always had a basic bearing static stiffness of $S = 0.75$ as was determined in Part A of this chapter. Therefore, any improvement of the bearing static stiffness compared to $S = 0.75$ must be entirely due to the action of the spool valve controller.

Journal load-displacement data was obtained for three different spool valve clearances which gave rise to β_3 values

of 2.1, 2.5 and 4.1. The results of these investigations are shown in Figs. 33, 34, and 35 respectively. In each of these investigations for β_3 held constant, the value of C_c was varied by changing the value of K_c. It can be seen from these figures that the spool valve controller does exhibit controlling action for the compressible fluid supply case. The load-displacement curves are seen to be linear up to $\epsilon/h_o \approx 0.3$ to 0.4. The bearing static stiffness is improved by the controller and it is seen to be a function of both C_c and β_3 just as it was for the incompressible fluid supply case in Chapter II. Also shown on these figures is the journal load-displacement curve for the standardized test bearing without the controller which was originally plotted in Fig. 30a. Of the data shown in Figs. 33, 34 and 35 it is seen that $C_c = 1.82$ for $\beta_3 = 2.5$ yields the highest bearing static stiffness which is $S = 1.68$. This is an improvement of 2.24 times the value of S for the standardized test bearing without the controller. The value of $S = 1.68$ here corresponds to $K = 13{,}400$ lb./in. Values of β_2 have not been included here because for this case β_2 is a function of β_3 and hence is not an independent variable. Here $\beta_4 = 1.0$, thus from equation (95) it is seen that

$$\beta_2 = \beta_3 - (1 + \beta_4) = (\beta_3 - 2) \quad . \tag{110}$$

Figures 33, 34, and 35 indicate that the spool valve controller can be optimized with regard to bearing static stiffness

with respect to C_c and β_3. For the fixed β_3 values of each of these figures, C_c was varied over a range wide enough to see than an optimum C_c value does exist for each of these β_3 values. In order to determine the optimum values of C_c and β_3 for the bearing arrangement here under consideration, Fig. 36 was plotted from Figs. 33, 34 and 35. Here Fig. 36a is a plot of the bearing load capacity, $W/(A_b p_s)$, for a fixed value of ϵ/h_o of 0.2 versus C_c with β_3 as the parameter for the family of curves. From this figure it is seen that the optimum value of $C_c \approx 1.9$. Fig. 36b is a plot of the bearing load capacity, $W/(A_b p_s)$, for a fixed value of ϵ/h_o of 0.2 versus β_3 with C_c as the parameter for the family of curves. From this figure it is seen that the optimum value of $\beta_3 \approx 2.8$. Also from Fig. 36b the value of S for optimum $C_c \approx 1.9$ and $\beta_3 \approx 2.8$ can be estimated as 1.74 which here corresponds to K = 15,500 lb./in. These values of S and K are approximately the same as the values for the condition of $C_c = 1.8$ and $\beta_3 = 2.5$ for which experimental data were obtained.

In the theoretical section above, expressions for optimum β_3 and C_c were presented for the bearing arrangement here under consideration. These expressions were equations (97) and (98) respectively. Since the value of β_4 here was held fixed at 1.0, then equations (97) and (98) yield

$$\left(\beta_3\right)_{opt} = 1.8 + \beta_4 = 2.8 \qquad (97)$$

and $$(C_c)_{opt} = \frac{4.5}{(1 + \beta_4)} = 2.25 \quad (98)$$

respectively. A comparison of these predicted values with the experimentally determined optimum values of $\beta_3 \approx 2.8$ and of $C_c \approx 1.9$ shows very good agreement. Hence it should be possible to predict the optimum values of β_3 and C_c for bearing arrangements where the spool valve controller is applied to a test bearing other than the standardized test bearing here employed.

Thus it can be concluded that the spool valve controller was here optimized with regard to bearing static stiffness for the case when the test bearing was the standardized test bearing. The spool valve controller should be able to provide an even greater improvement in bearing static stiffness if β_4 of the test bearing is decreased.

(b) Rotating Journal

Journal load-displacement data was obtained for the spool valve controller applied to the standardized test bearing for journal rotational speeds of 500, 1000, 2000, 3000, 4000, 5000 and 6000 rpm. The journal was loaded only up to loads which caused a maximum $\epsilon/h_o \approx 0.2$. The spool valve condition was held fixed at $\beta_3 = 2.5$ and $C_c = 1.37$ and p_s was 25 psig. The results of this investigation are shown in Fig. 37 along with the results for the non-rotating journal. Here it is seen that the journal rotation improves the bearing static stiffness much

the same as it did for the standardized test bearing without the controller (See Fig. 30b). Here the bearing static stiffness, S, was again increased by about 10% at N = 6000 rpm compared to the value of S at N = 0 rpm. Hence, this rotational effect seems to be independent of the presence of the spool valve controller.

Journal whirl effects due to apparatus misalignments were present here and they were identical to those which were observed for the rotational tests of the standardized test bearing without the spool valve controller. These effects were discussed in detail and the method of interpreting them with regard to bearing static stiffness is given in Part A of this chapter.

(c) Interaction of Bearing Controllers

Journal load-displacement data were obtained when the spool valve controller was applied to the standardized test bearing only in the direction of loading and also when it was applied in both the direction of loading and perpendicular to the direction of loading. That is to say that the case of one controller and the case of two controllers was investigated. This was carried out for the non-rotational journal condition and it was found that the bearing static stiffness with controller applied to the bearing sectors in the direction of the load was independent of whether or not a controller was applied to the bearing sectors which are located perpendicular to the direction of loading. Thus it is seen that it is not necessary to employ two controllers to obtain bearing static stiffness

information for a particular controller condition. In view of this, only one spool valve controller was employed to obtain the results reported herein.

3. Design Procedure

Design steps are offered here as a guide to the design of a spool valve controller which should provide the maximum bearing static stiffness for a particular stabilized externally pressurized air bearing.

(a) Employ steps (a) through (o) of "Design Procedure" in Part A of this chapter to obtain a stabilized externally pressurized air bearing or employ one which is already available. However, it must have an even number of feed ports.

(b) Determine the value of β_4 of the stabilized bearing at the bearing flow rate, W_T, which is to be employed. The maximum value of W_T will usually be dictated by the stability limit.

(c) Determine the supply pressure to the stabilized bearing, p'_{so}, which is necessary to achieve the bearing flow rate that is to be employed.

(d) Calculate the optimum β_3 for the spool valve controller from

$$(\beta_3)_{opt} = 1.8 + \beta_4 \qquad (97)$$

(e) Calculate the optimum C_c value for the spool valve controller from

$$(C_c)_{opt} = \frac{4.5}{(1 + \beta_4)} \qquad (98)$$

(f) Select a practical spool valve diameter, d_c.

(g) Calculate $A_c = (\pi d_c^2)/4$.

(h) Select a value for the overall spool valve length, L_c, so that $L_c \geq 1.5\ d_c$.

(i) Select a value for the spool valve inlet annulus groove width, w_{gc}, so that the inlet annulus will offer little flow resistance.

(j) Determine the value of ℓ from $\ell = (L_c - w_{gc})/2$.

(k) Calculate the stabilized bearing feed port pressure, p_{bo}, from

$$p_{bo} = \frac{p'_{so}}{(\beta_4 + 1)} \qquad (111)$$

(l) Calculate the overall supply pressure which is necessary to achieve the $(\beta_3)_{opt}$ value from

$$p_s = (\beta_3)_{opt}\ p_{bo} \qquad (112)$$

(m) Convert p_s to P_s and p'_{so} to P'_{so} by adding 14.7 to p_s and p'_{so} respectively.

(n) Calculate q from

$$q = \frac{P_a}{P_s} \tag{113}$$

(o) Calculate q' from

$$q' = \frac{P_a}{P'_{s0}} \tag{114}$$

(p) Determine the controller spool valve radial clearance, h_c, which is necessary to produce $(\beta_3)_{opt}$ for the bearing flow to be employed from the following expression:

$$h_c = 0.0199 \left\{ \frac{W_T \ell}{d_c} \frac{(q')^2}{\left[\left(\frac{q'}{q}\right)^2 - 1\right]} \right\}^{\frac{1}{3}} \tag{115}$$

The value of the ratio ℓ/h_c should be greater than about 350 to insure negligible orifice effects in the controller at the inlet to the spool valve. (Equation (115) can be obtained from equations (105), (107) and (108).

(q) Select a depth for the spool valve inlet annulus groove so that it will be at least ten times the value of h_c.

(r) Determine the spring constant, K_c, of the spool valve compression springs which is necessary to produce $(C_c)_{opt}$ from:

$$K_c = \frac{A_c P_s}{2\ell (C_c)_{opt}} \qquad (116)$$

(s) Use one spool valve controller to feed each set of opposite bearing sectors. In the case of a four sector bearing, two controllers are required. The spool valve controller should be of the design shown in Fig. 31 and it should be connected directly to the bearing stabilizing fixed orifice restrictions as shown in this figure. The spool valve should be provided with a spool valve stop on each side so that the spool valve ends cannot pass into the spool valve inlet annulus. The controller body should be designed so that the spool valve can not close off the flow at the end of its stroke (that is, the only flow restriction within the controller should be that through the diametral clearance of the spool valve).

The resulting design should provide a bearing static stiffness which is the maximum that can be attained with a spool valve controller for the particular stabilized bearing employed. The bearing static stiffness resulting from this design will depend on the static stiffness of the stabilized bearing without the controller and also on the stabilized bearing β_4 value. For a β_4 value of 1.0, the controller should increase the stabilized bearing static stiffness by a factor of about 2.0. If β_4 if less than 1.0, the improvement should become greater because it is known from Chapter II that the optimized controller can increase the bearing static stiffness by a factor of at least 25 when $\beta_4 = 0$.

CHAPTER IV

CONCLUSIONS

The most significant conclusion which can be made from this investigation is the fact that the variable external restriction does offer a means for greatly improving the static stiffness of an externally pressurized fluid bearing. The variable external spool valve restriction improved the non-dimensional bearing static stiffness, S, by a factor of at least 25 for the incompressible fluid supply compared to the S value of 1.0 for the fixed external orifice restriction. This corresponds to a bearing static stiffness of 50×10^6 lb./in. This bearing stiffness is comparable to the bearing stiffness of rolling contact bearings. This achievement should make the externally pressurized fluid bearing with variable external restriction desirable for many applications. When the fluid supply was compressible the variable external spool valve restriction improved the non-dimensional bearing static stiffness by a factor of 2.24 for a particular stabilized bearing. The value of S was improved from 0.75 to 1.68. This corresponds to an improvement of bearing static stiffness from 4,770 to 13,400 lb./in. A greater improvement than this should be possible if proper selection of the stabilized bearing is made. Theoretically a non-dimensional bearing static stiffness as large as that obtained for the incompressible fluid supply should be attainable for the compressible fluid supply.

Another very significant finding was the fact that the variable external spool valve restriction could be optimized with regard to bearing static stiffness for both the incompressible and compressible fluid supplies. The same general trends are exhibited for both of these fluid supplies with respect to the governing non-dimensional parameters and are not altered by the compressibility. The optimum values of the governing non-dimensional parameters, β_3 and C_c, are different for the compressible fluid supply from those for the incompressible fluid supply, but this difference was not directly due to the fluid compressibility. For the incompressible fluid supply these optimum values were $\beta_3 = 1.8$ and $C_c = 4.5$. The compressibility can give rise to bearing instability unless a stabilizing fixed orifice restriction is placed in the bearing feed ports. This added restriction in the feed line between the variable external spool valve restriction and the bearing gives rise to another independent non-dimensional parameter, β_2, and is the reason for the optimum values of the parameters, β_3 and C_c, being different from those for the incompressible fluid supply. The optimum values of the governing non-dimensional parameters for the compressible case can be predicted by theoretical means from those values for the incompressible fluid supply. It was determined that it is essential for β_2 to be equal to the optimum β_2 value for the incompressible fluid supply and for $C_c(\beta_3 - \beta_2)$ to be equal to the optimum C_c value for the incompressible fluid supply in order to achieve maximum bearing stiffness. This requirement placed on β_2 is accomplished

by adjusting β_3, hence the non-dimensional parameter β_2 has a stronger influence than β_3. These requirements for the compressible case can be satisfied if $(\beta_3)_{opt} = (1.8 + \beta_4)$ and $(C_c)_{opt} = 4.5/(1 + \beta_4)$. The β_4 is the ratio of the pressure drop across the stabilizing orifice restriction to the pressure drop through the bearing. In this investigation β_4 was fixed at 1.0 for the compressible case. Hence, the flow resistance of the stabilizing orifice restriction can directly alter the optimum values of the non-dimensional parameters, β_3 and C_c. When the flow resistance of the stabilizing fixed orifice restriction is made very small compared to the flow resistance of the bearing resistance, that is when β_4 approaches zero, the optimum values of the governing non-dimensional parameters approach those values for the incompressible fluid supply. The presence of the stabilizing fixed orifice restriction causes the effectiveness of the variable external restriction to be decreased. If the flow resistance of the stabilizing fixed orifice restriction is reduced, then the total external restriction becomes predominately of the variable restriction type. Hence, the variable external restriction should become more effective and thus the non-dimensional bearing static stiffness should become improved. In the limit, the variable external spool valve restriction for the compressible fluid supply should approach the non-dimensional bearing static stiffness which was obtained for the incompressible fluid supply.

Because the variable external spool valve restriction can be optimized and the optimizing conditions can be predicted for both of the fluid supply types, a design procedure can be specified which will yield optimized variable external spool valve restrictions for other externally pressurized bearing designs. For the pressure pad type bearing for use with incompressible fluid supplies the circumferential flow effect is significant. In order to design an optimized bearing which is to yield a specific bearing static stiffness the bearing factor, F_b, must be identical to that of the bearing on which the design criterion is based or it must be accounted for if they have different bearing factors. For the axial exhaust groove type bearing for use with compressible fluid supplies the circumferential flow between bearing sectors is expected to be less and hence, the circumferential flow effect should be of lesser importance. However, inherent orifice restrictions within the vicinity of the bearing feed port can significantly reduce the bearing static stiffness. The inherent orifice restrictions should be eliminated whenever it is possible to do so. At present it is not possible to predict the bearing static stiffness for the compressible fluid supply. However, the optimum values for the important non-dimensional parameters can be predicted for obtaining the optimum bearing static stiffness for a given stabilized bearing.

The bearing arrangements for the incompressible fluid supply always produced a stable bearing. However, when the fluid supply is incompressible, bearing instability can arise. Proper fixed

orifice restrictions, supply pressure and feed port volumes must be employed to stabilize the bearing for the case of the fixed external restriction. For the case of the variable external spool valve restriction, it is essential to isolate its relatively large internal volume from the bearing feed port volume in order to achieve a stable bearing. Hence, a stabilizing fixed orifice restriction is necessary for this case. The action of the variable external spool valve restriction does not disturb the stability of the stabilized bearing. The effect of the presence of the stabilizing fixed orifice restriction on the bearing static stiffness has already been discussed. Both types of external restrictions were found to retain bearing stability when the journal was rotated for the compressible fluid supply. No rotational information was obtained for the incompressible fluid supply. However, this case is less severe than the compressible case and thus stability is also expected to be maintained during journal rotation.

It was found that of ~~the~~ fixed external restrictions, the orifice restriction offers the greater bearing stiffness. The fixed external orifice restriction with incompressible fluid supply offers a theoretically maximum non-dimensional bearing static stiffness of about 1.8, but the circumferential flow reduces this value to about 1.0 for a bearing factor of $F_b = 0.5$. The values for the fixed external capillary restriction are expected to be somewhat less than these values. The value of β_3 required to achieve the optimum condition is 1.71 for the

fixed external orifice restriction and 2.0 for the fixed extern capillary restriction. It has already been pointed out that th variable external restriction offers a much greater bearing sta stiffness than that attainable with the fixed external restrict For the case of the variable external spool valve restriction, the improvement is by at least a factor of 25. For the case of fixed external restrictions with compressible fluid supply the theoretical maximum non-dimensional bearing static stiffness is almost identical with that for the incompressible fluid supply. However, the actual value can be much lower if inherent orifice are present in the bearing feed port in addition to the fixed external restriction. Also the circumferential flow effect cou tend to reduce the bearing static stiffness but it can not completely account for the large reduction which was observed. For the axial exhaust groove type bearing little circumferentia flow is expected to occur between bearing sectors. For the particular fixed external orifice restriction bearing investiga the bearing non-dimensional static stiffness was 0.75, whereas the theoretical value was about 2.0. The optimum value of β_3 necessary to attain the maximum non-dimensional bearing static stiffness is dependent on the supply pressure, hence there is not one fixed optimum value of β_3 for the compressible fluid supply as there was for the incompressible fluid supply. For the fixed external orifice restriction the range of optimum val of β_3 is 1.56 to 1.82 for most practical supply pressures. Therefore, there really is not an extremely large difference

between the β_3 values for the optimum fixed external restrict for compressible and incompressible fluid supplies. Hence, com pressibility does not greatly influence the maximum bearing sta stiffness, if inherent orifices are not present, nor the value of the governing parameter, β_3, necessary to produce this maxi for the fixed external restriction bearing.

The rotation of the bearing journal improves the bearing static stiffness. It was found that the bearing static stiffne was increased by 10% for a rotational speed of 6000 rpm, compare to the non-rotational condition, for both types of external restrictions with the compressible fluid supply. An even greater improvement is expected for the case of the incompressible flui supply due to the increased viscosity of the fluid, because the improvement in bearing static stiffness is thought to be caused by the pumping action of the rotating journal.

CHAPTER V

FUTURE INVESTIGATIONS

The investigation involving the compressible fluid supply did not produce the stiffest possible air bearing. It was not the goal of that investigation to produce the stiffest possible air bearing, but instead to see if the variable external restriction is feasible with compressible fluids and exhibits the same trends as for the incompressible case and to obtain rotational bearing information. Therefore, a straight forward extension of this work would be to try to obtain the stiffest possible air bearing. This would be done by reselecting stabilizing orifice restrictions so as to decrease the value of β_4 and then optimizing the spool valve controller for this stabilized bearing.

It would also be useful to obtain experimental results for the fixed external orifice restriction with a compressible fluid supply similar to the theoretical results of Figs 23 and 24. This would require an extensive investigation of many different fixed external orifice restrictions. This information would be very useful for design purposes, but care should be taken that the external restriction does not include inherent orifice restrictions. If inherent orifice restrictions are present then the usefulness of the results will be limited.

Information for higher rotational speeds for a compressible fluid supply would be of interest since air bearings are usually

operated at speeds above 6000 rpm. This would probably require going to a turbine drive in order to attain these higher speeds and also to eliminate the mechanical whirl which the present drive system and apparatus imparts to the journal. In regard to rotational tests, it might be of interest to obtain rotational results for the incompressible fluid case to see just how much improvement the journal rotation offers. Of course, this interest is merely of an academic nature for the case of the incompressible fluid because similar trends should be exhibited in this case as has been already determined in this investigation for the compressible fluid case.

The present investigation has been concentrated mainly on the static stiffness of the externally pressurized bearing. It would be of interest to look into the dynamic bearing stiffness and the damping properties of the bearing. In this regard, improvement of the bearing dynamic stiffness might be possible from the knowledge gained in this present investigation:

All of the bearings which were considered in this investigation were of the radial type. However, the knowledge gained here should be directly applicable to the thrust bearing. It would be informative to experimentally verify this possibility.

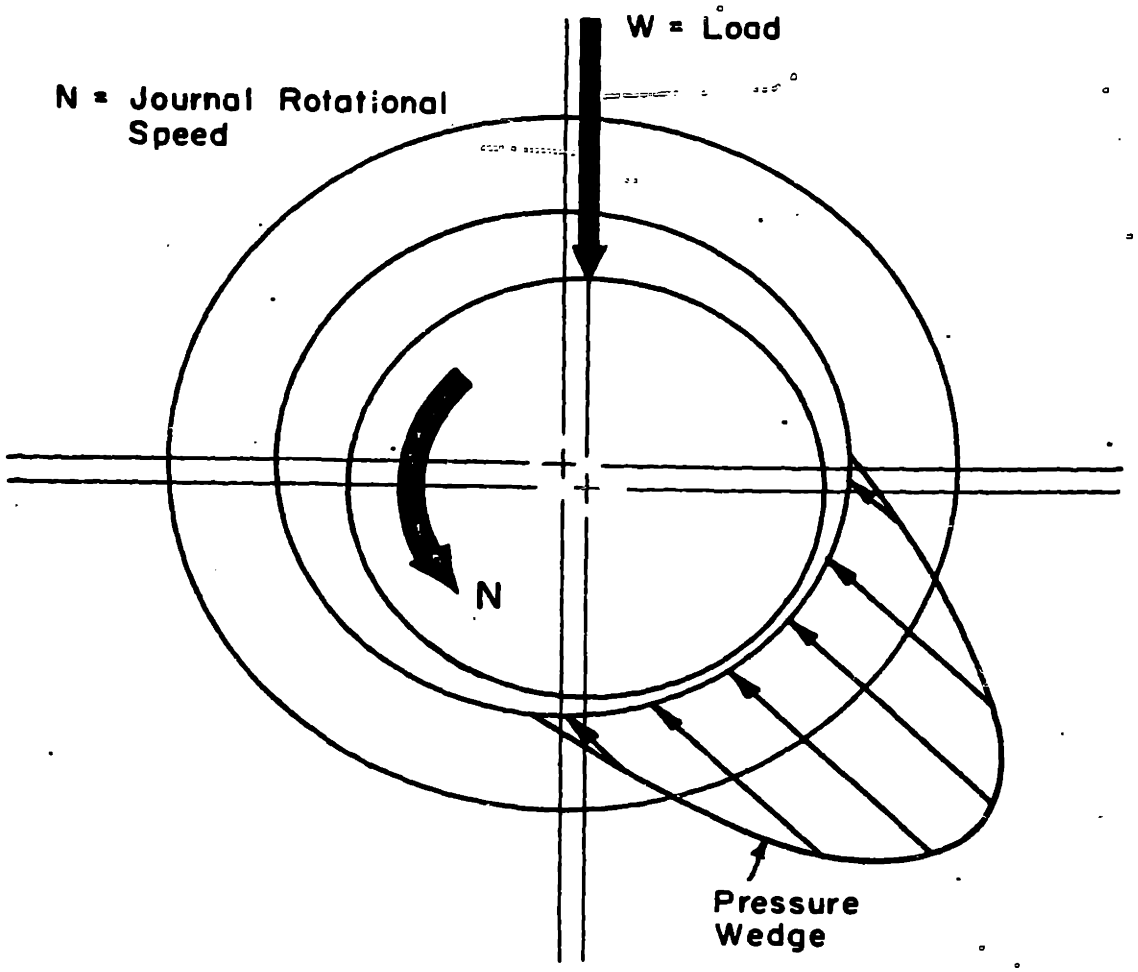

Fig. 1. Self-acting fluid bearing.

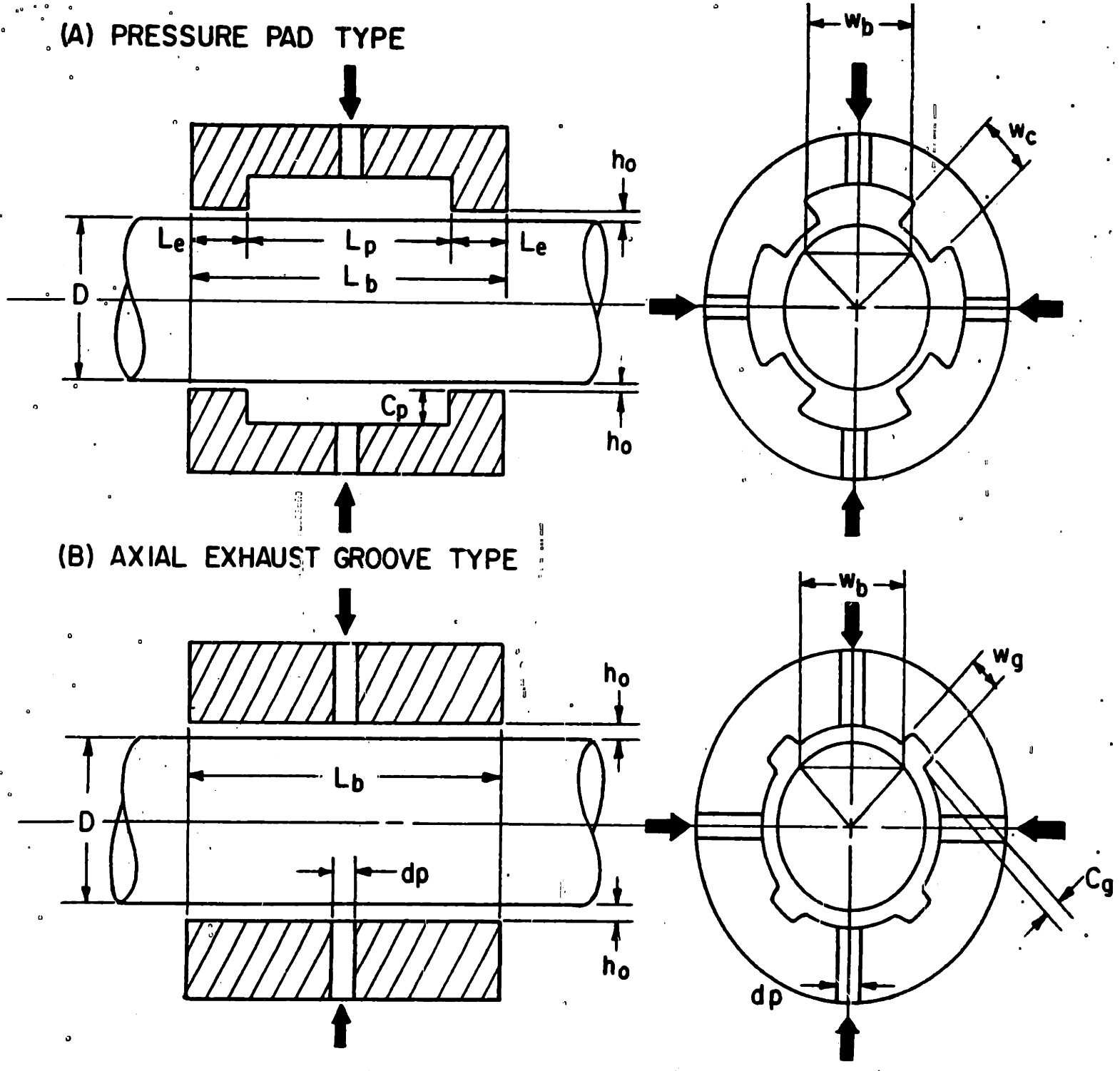

Fig. 2. Internal composition of externally pressurized fluid bearing.

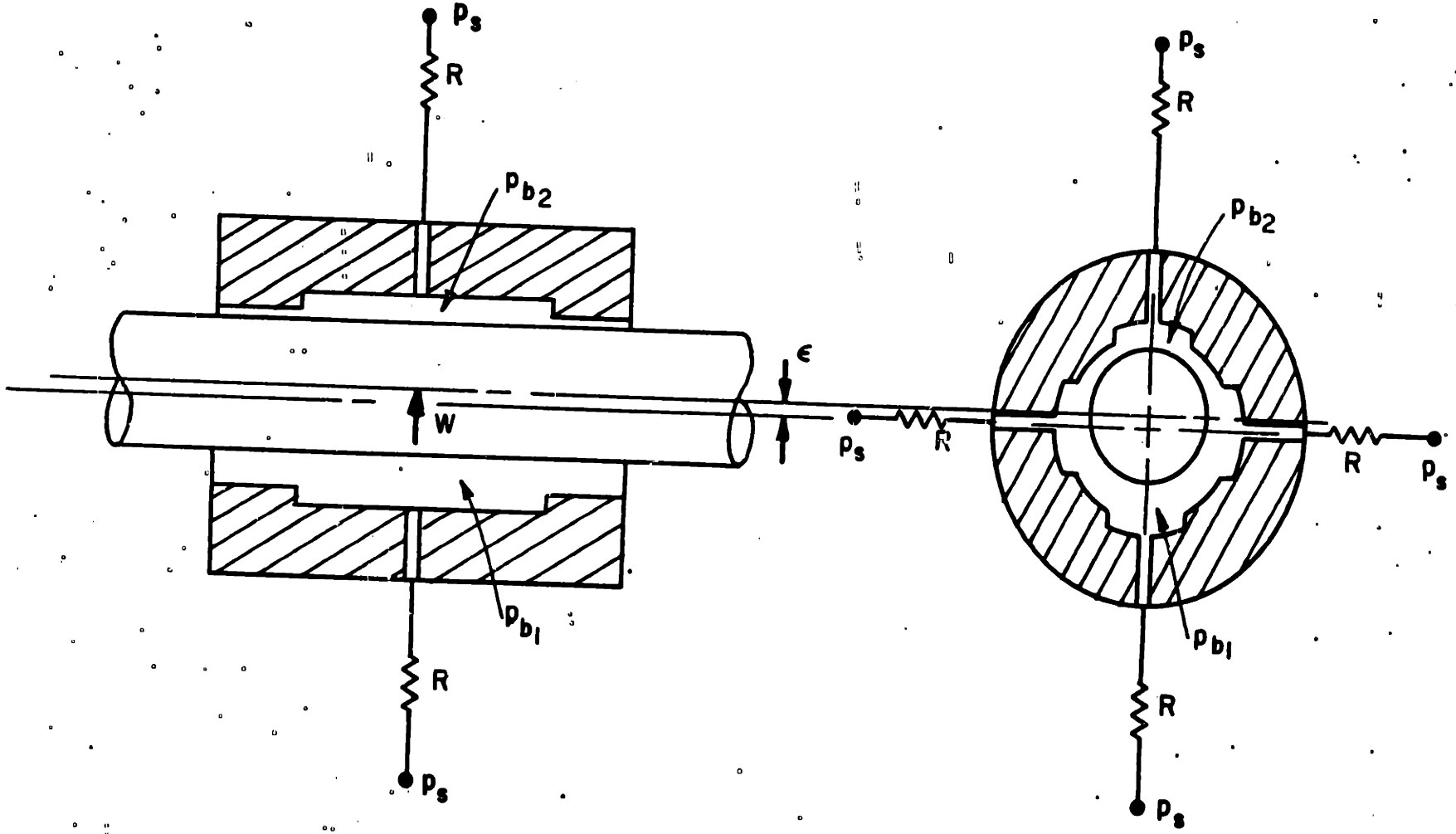

Fig. 3. Arrangement of externally pressurized fluid bearing with external flow restrictions.

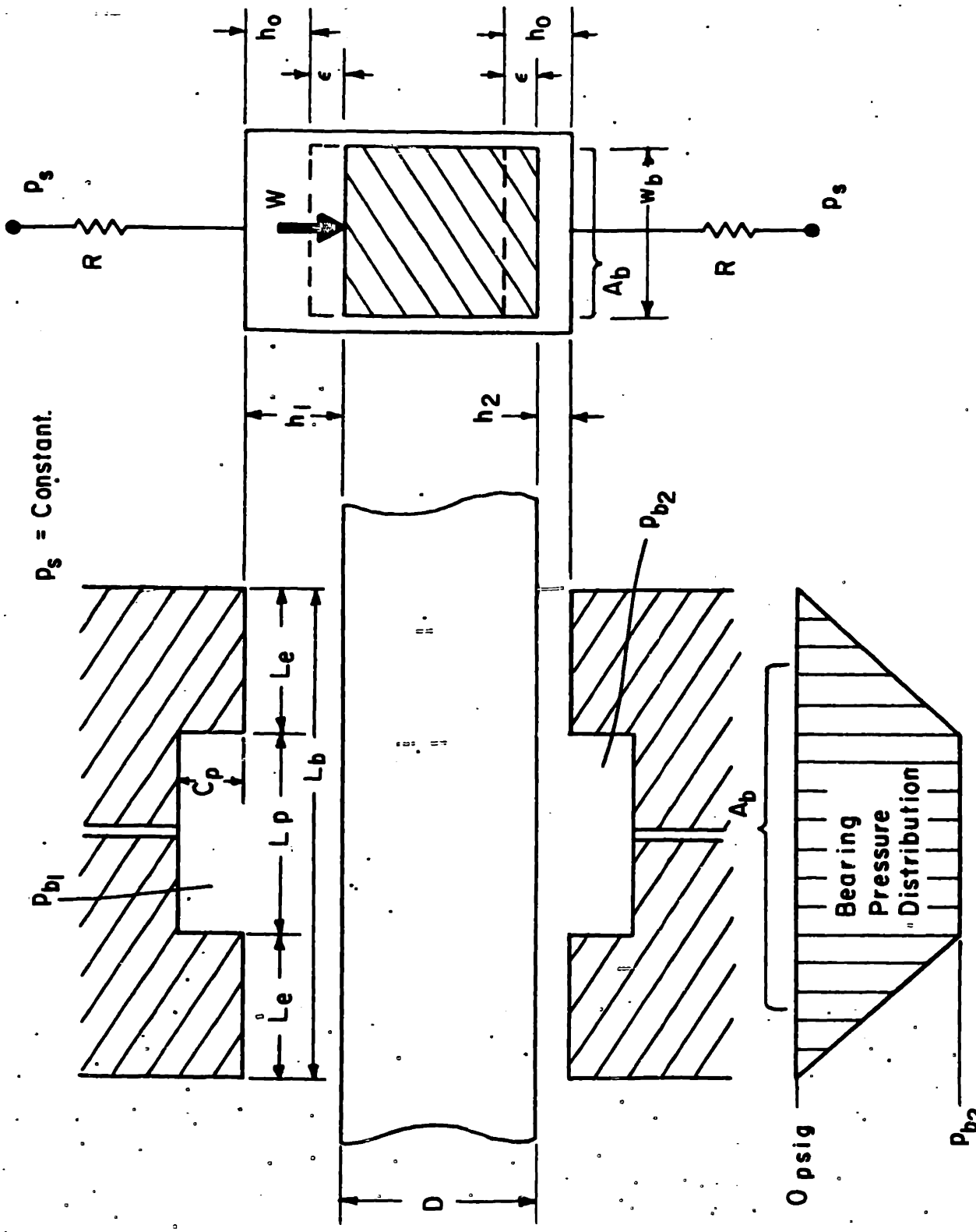

Fig. 4. Analytical model (square bearing) of externally pressurized fluid bearing with external flow restrictions.

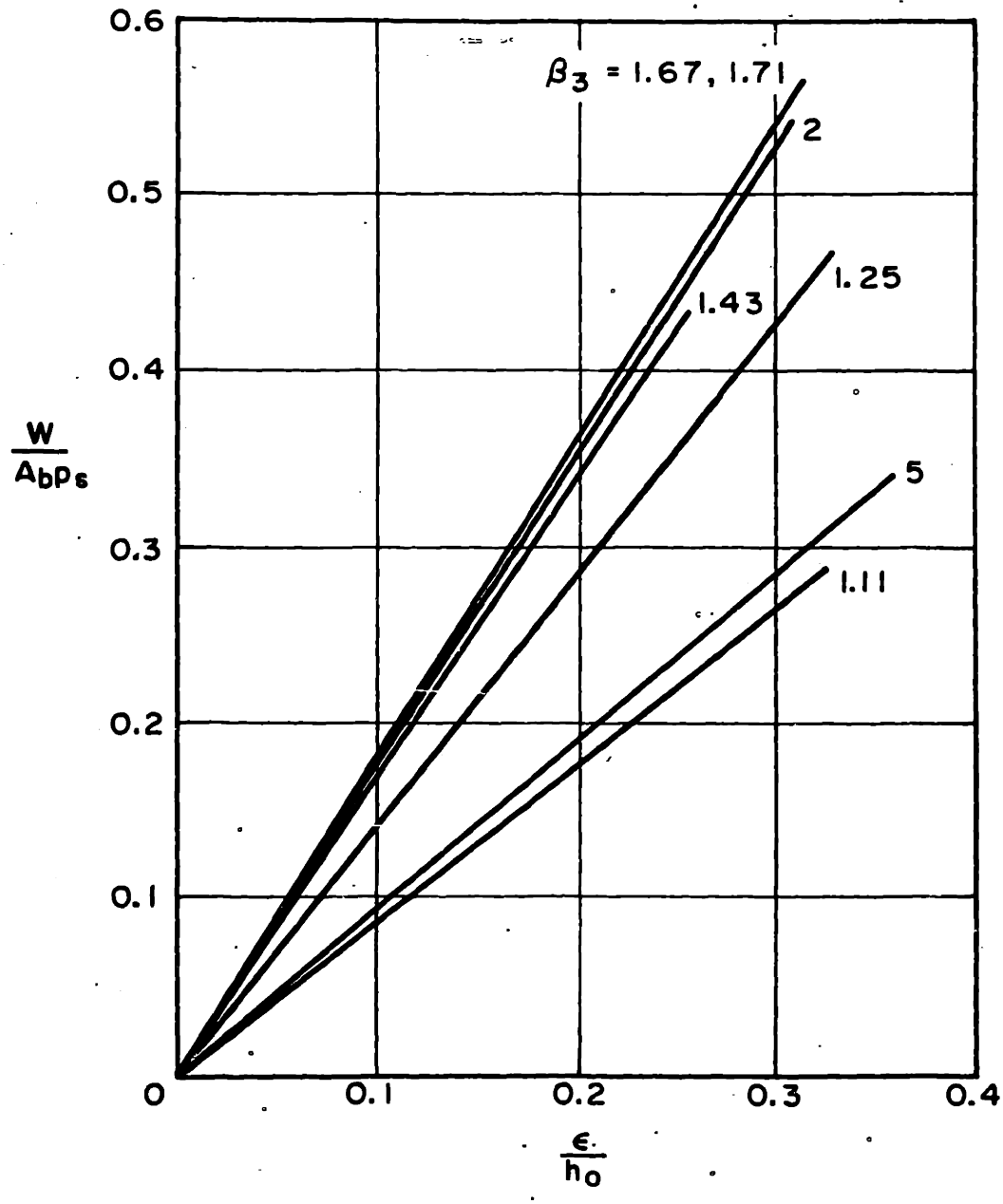

Fig. 5. Theoretical journal load-displacement plot for fixed external orifice (no circumferential flow, non-rotating round bearing, incompressible fluid).

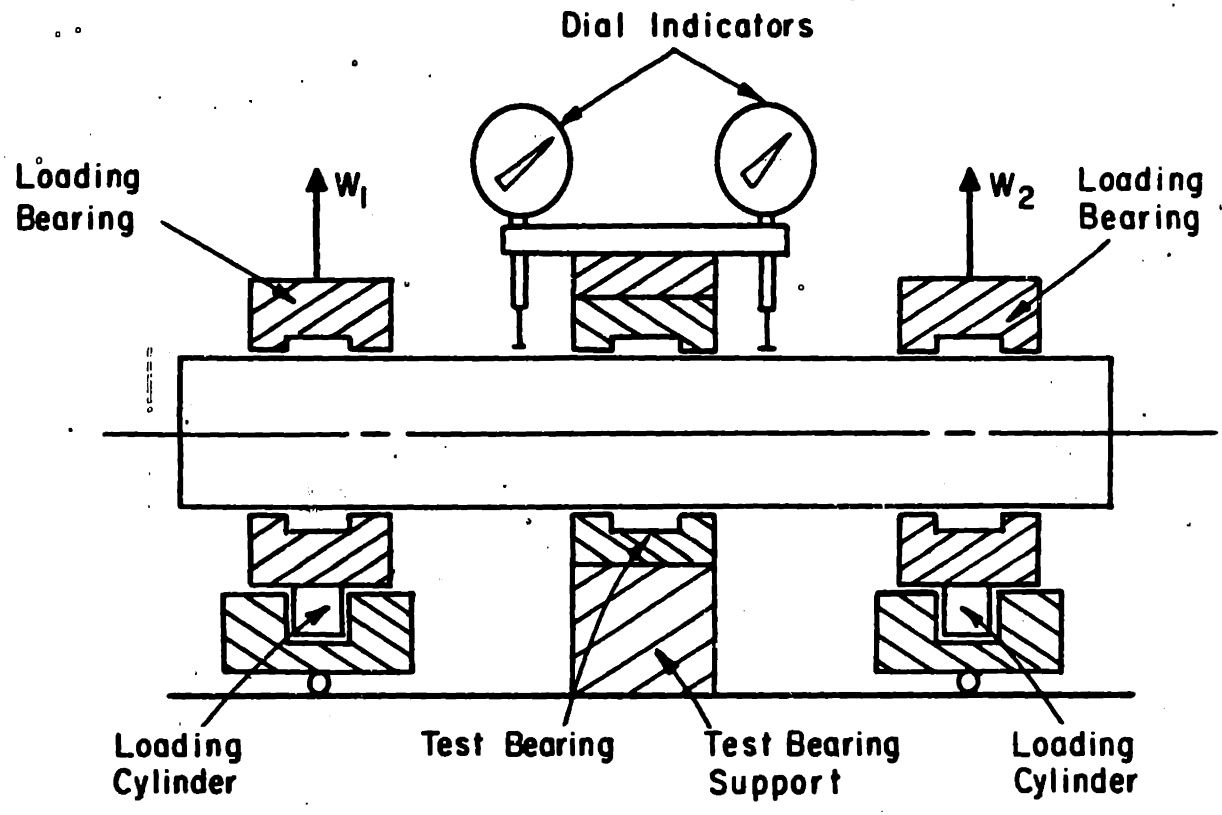

Fig. 6. Test apparatus (single radial bearing, incompressible fluid supply).

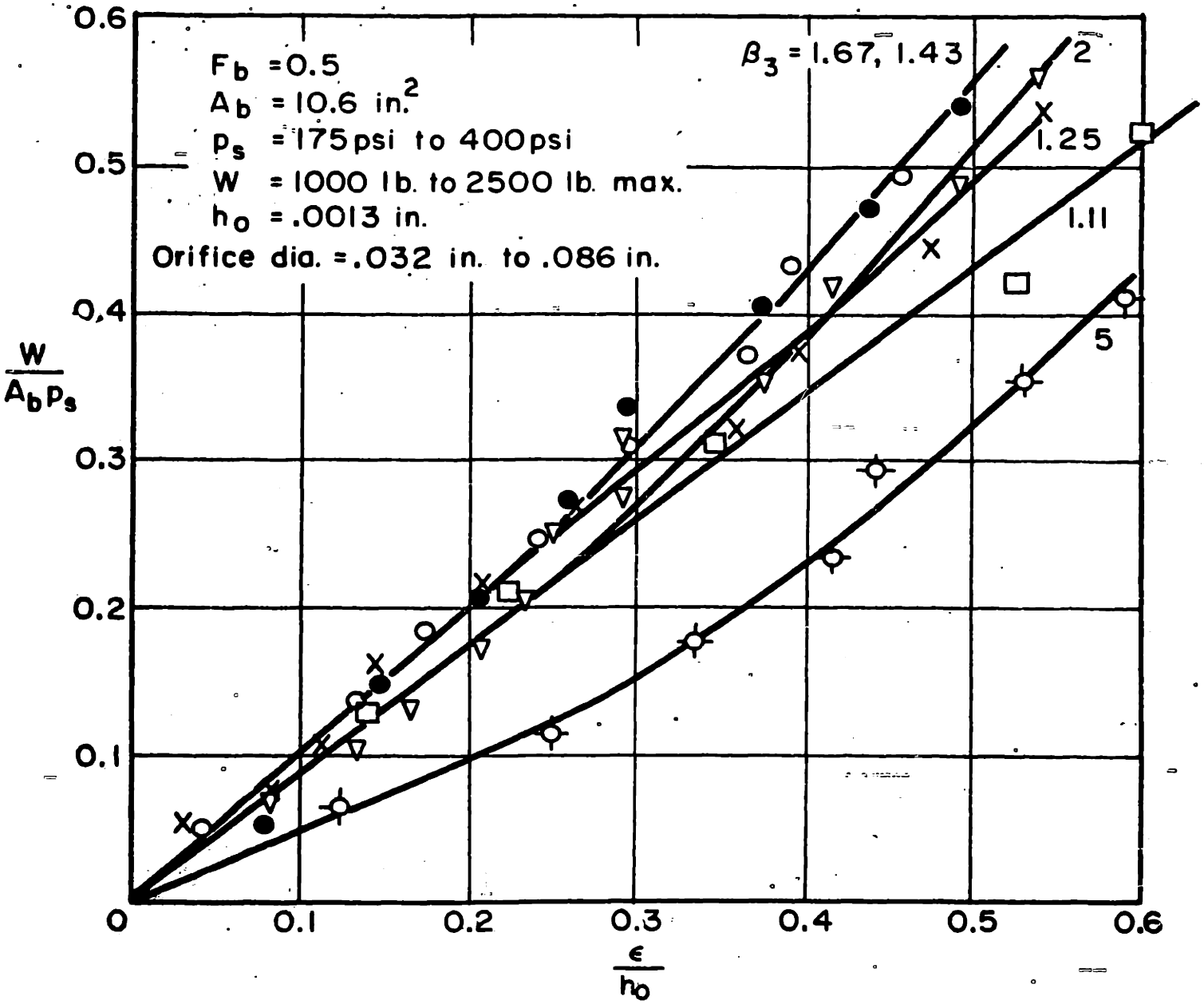

Fig. 7. Experimental journal load-displacement plot for fixed external orifice (non-rotating round bearing, incompressible fluid).

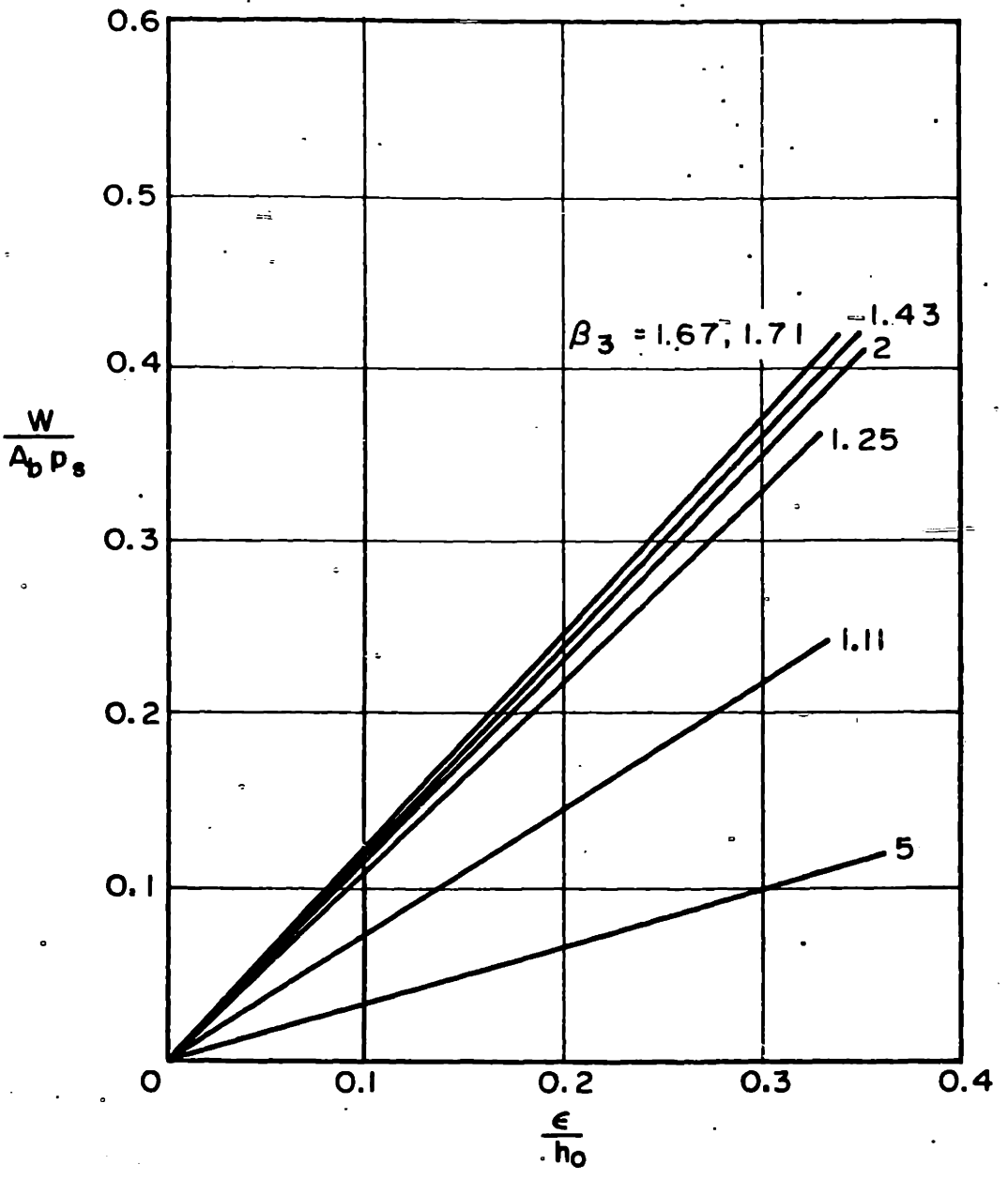

Fig. 8. Theoretical journal load-displacement plot for fixed external orifice (circumferential flow - Raimondi and Boyd Correction, non-rotating round bearing, incompressible fluid).

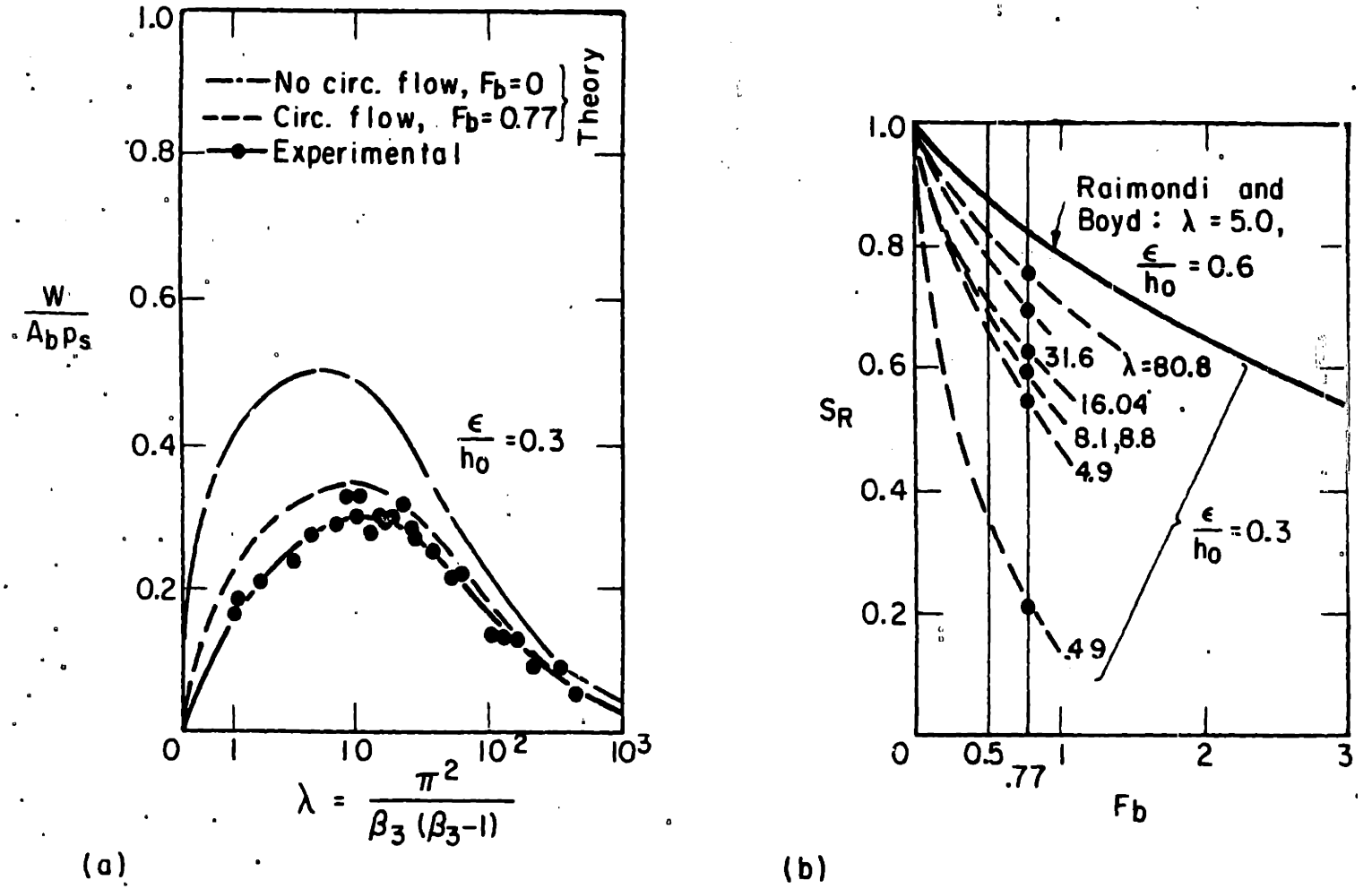

Fig. 9. Raimondi and Boyd bearing stiffness correction for circumferential flow (fixed external orifice restriction, incompressible fluid).

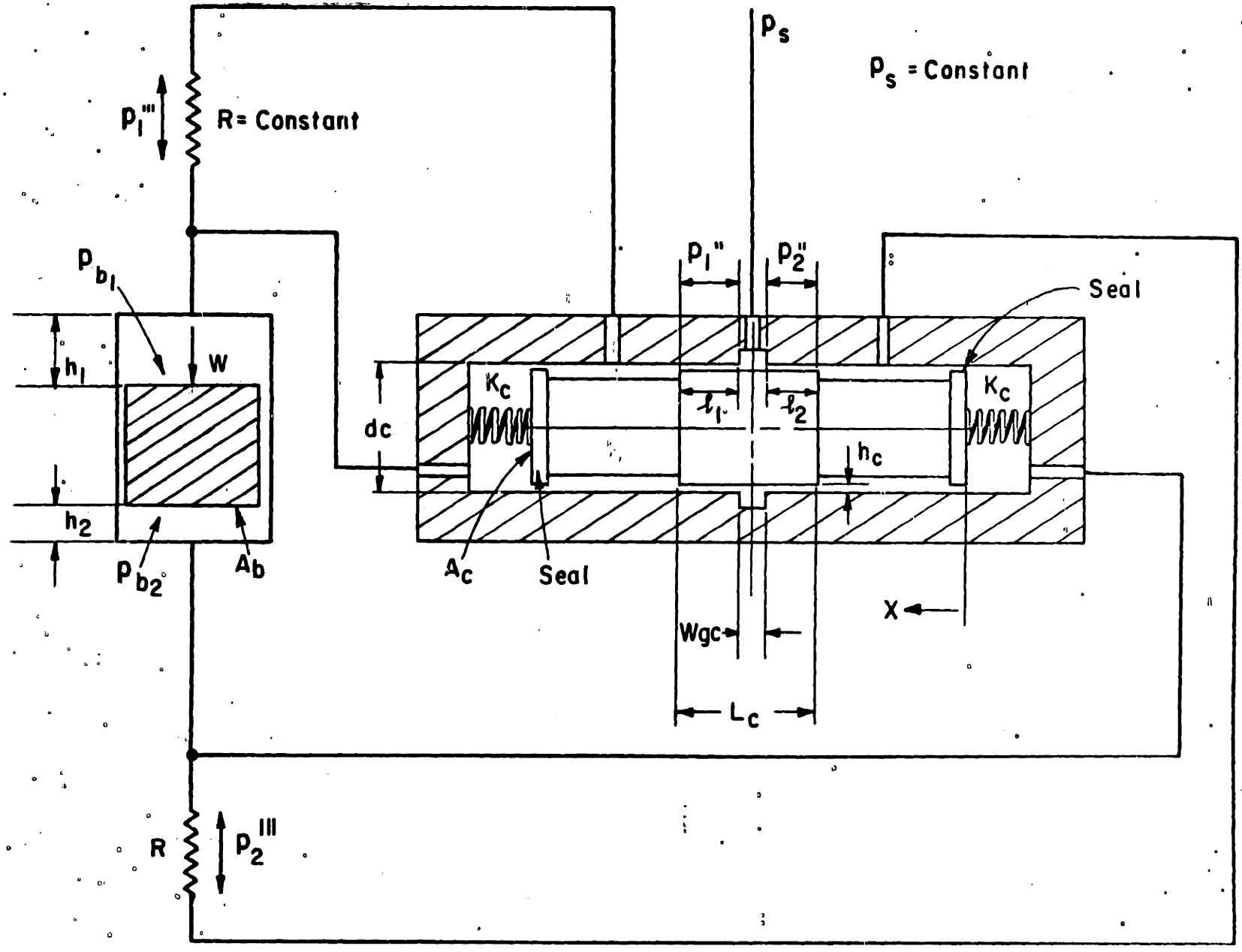

FIGURE 10 VARIABLE EXTERNAL RESTRICTION (LOAD-SENSING) CONCEPT - (GENERAL CASE OF FIXED EXTERNAL RESTRICTION PLUS VARIABLE EXTERNAL RESTRICTION)

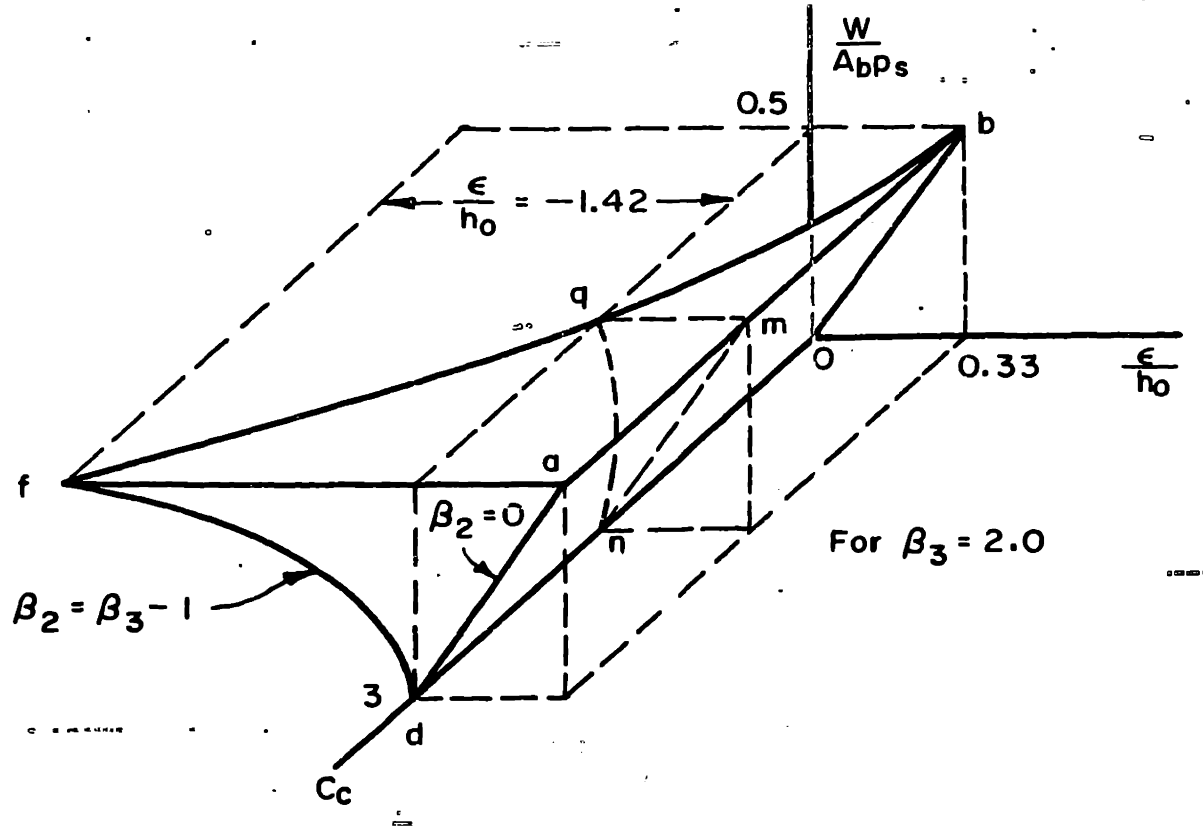

Fig. 11. Theoretical journal load-displacement plot for fixed external linear restriction plus variable external spool valve restriction (constant β_3, non-rotating square bearing, no circumferential flow in bearing, incompressible fluid).

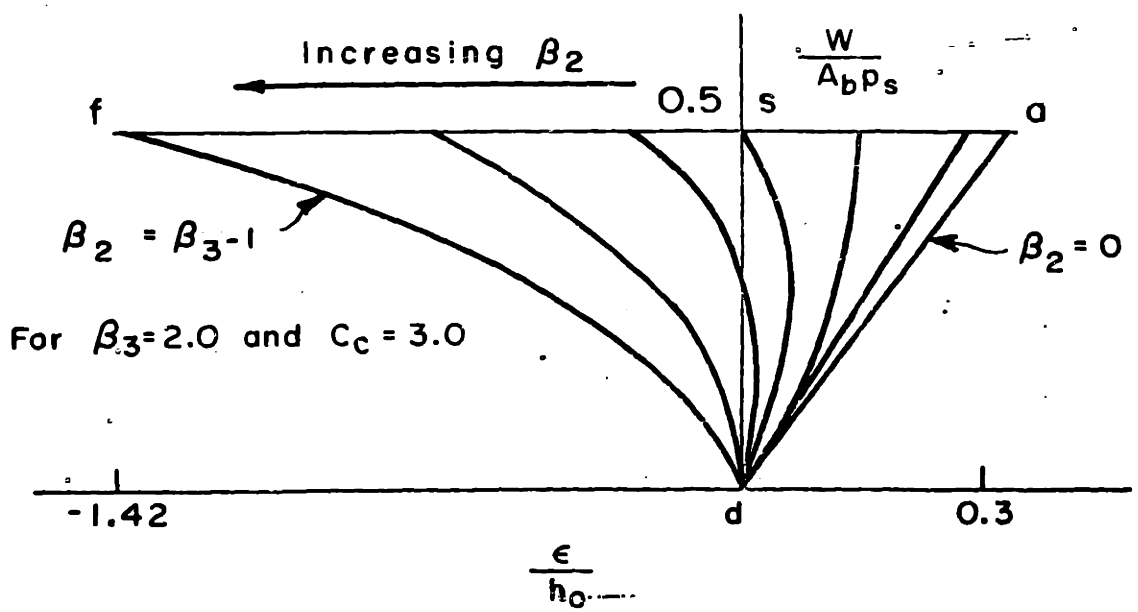

Fig. 12. Effect of β_2 on journal load-displacement plot in Fig. 11 for constant β_3 and C_c.

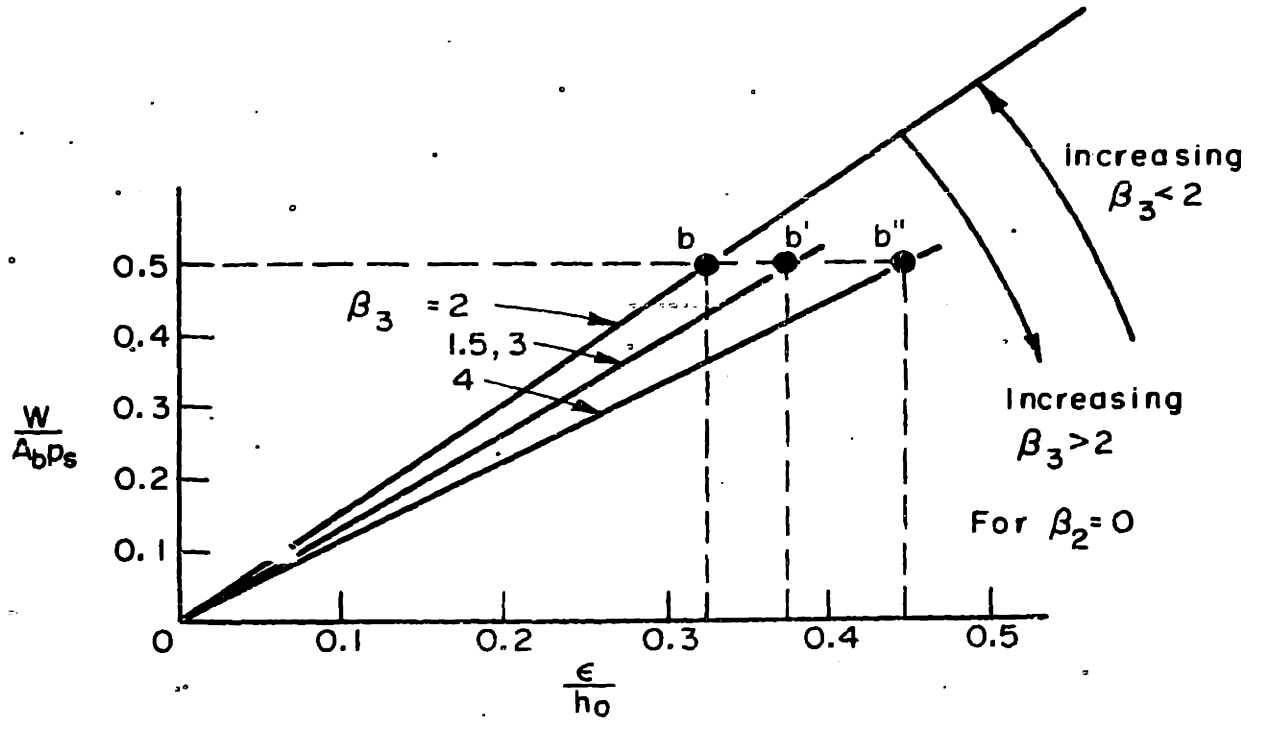

Fig. 13. Effect of β_3 on journal load-displacement plane surface for $\beta_2 = 0$ and variable C_c in Fig. 11 (surface abod).

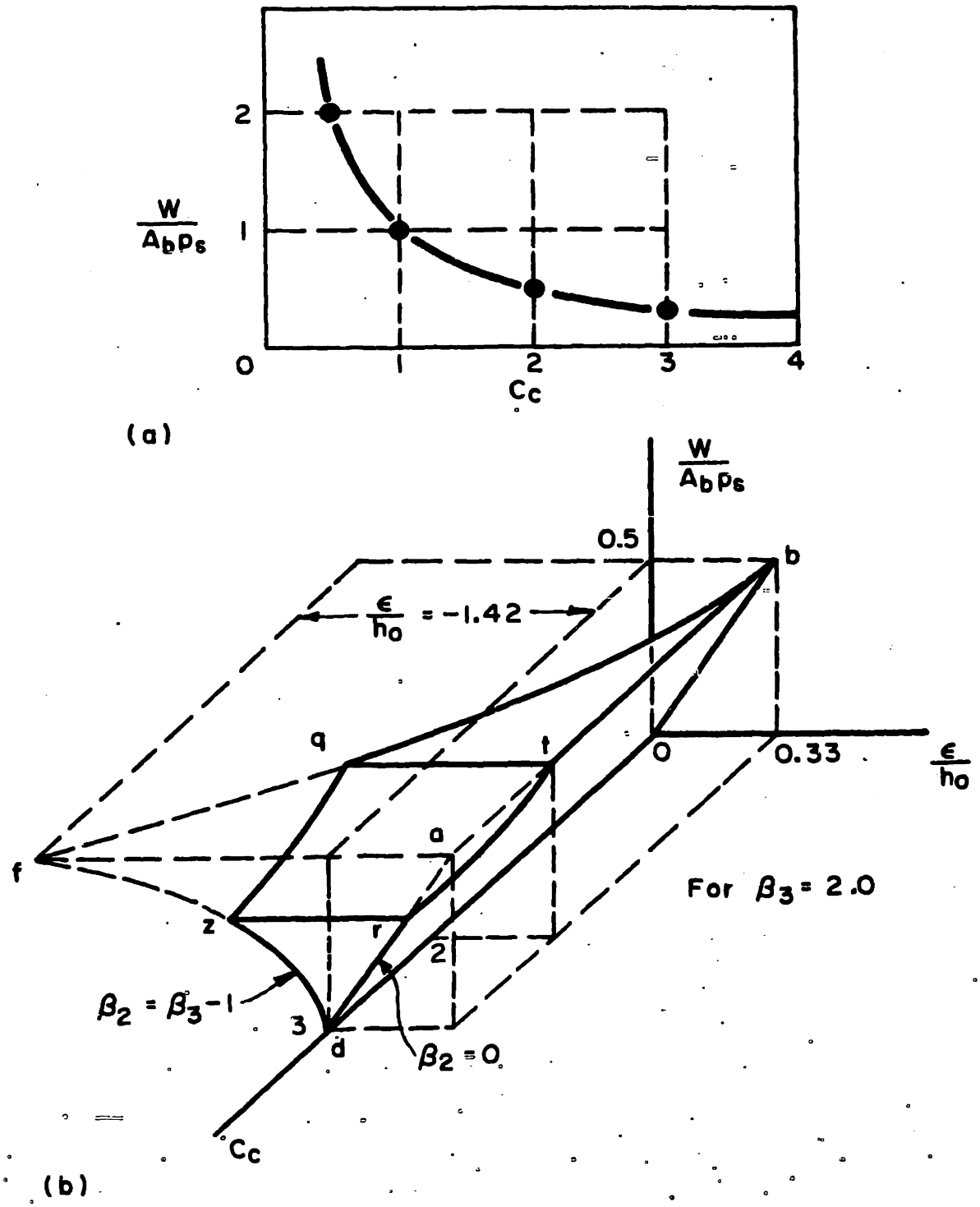

Fig. 14. Controller limitation on journal load-displacement plot in Fig. 11.

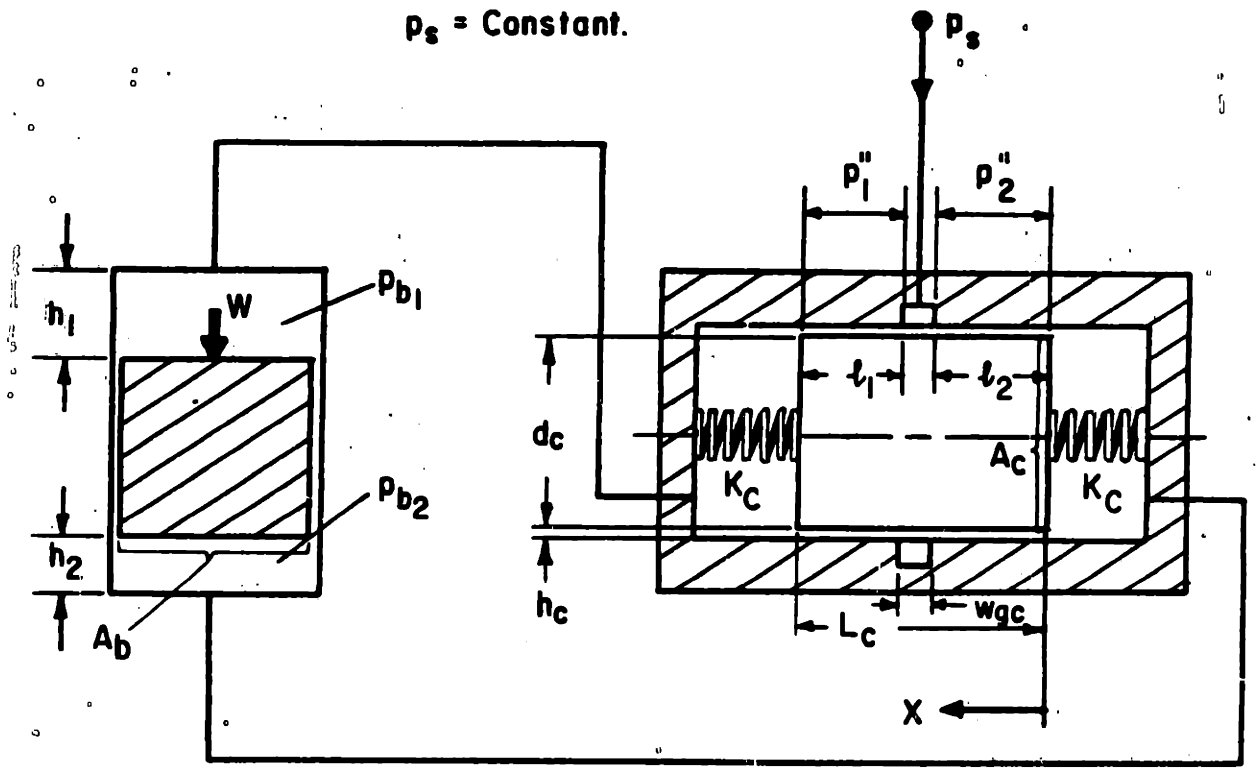

FIGURE 15 VARIABLE EXTERNAL RESTRICTION (LOAD SENSING) CONCEPT-(SPECIAL CASE OF VARIABLE EXTERNAL SPOOL VALVE RESTRICTION WITHOUT FIXED EXTERNAL RESTRICTION).

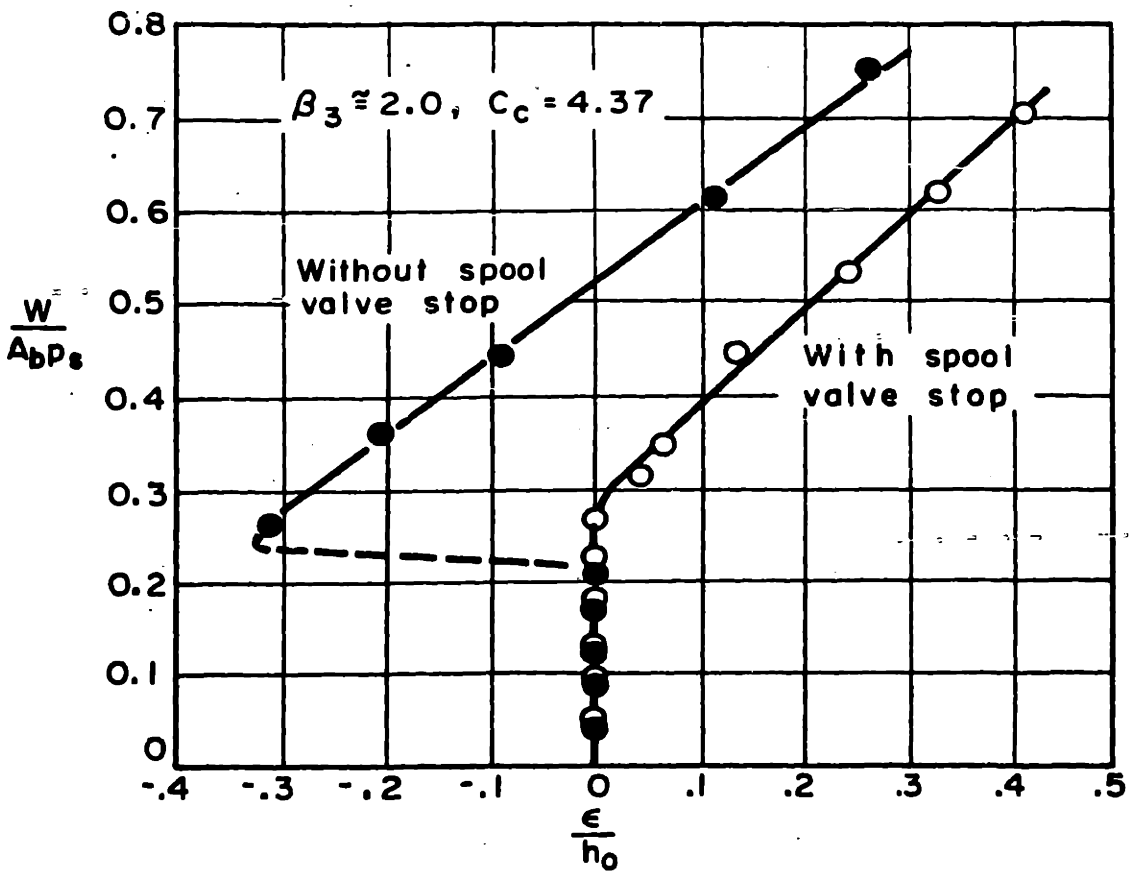

Fig. 16. Experimental journal load-displacement plot for variable external spool valve restriction with and without spool valve stop (non-rotating round bearing, incompressible fluid).

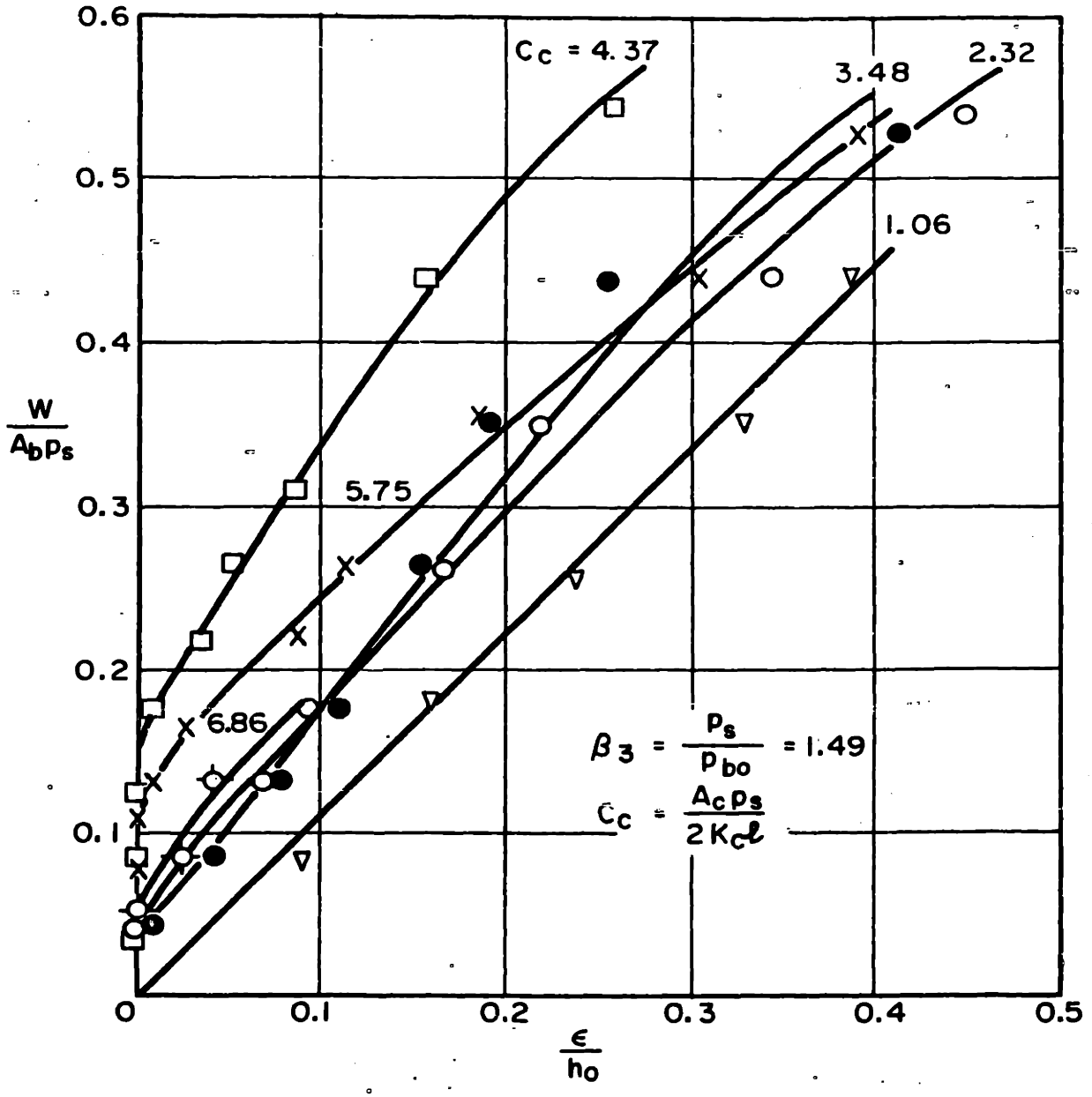

Fig. 17. Experimental journal load-displacement plot for variable external spool valve restriction (β_3 = 1.49, C_c = variable, non-rotating round bearing, incompressible fluid).

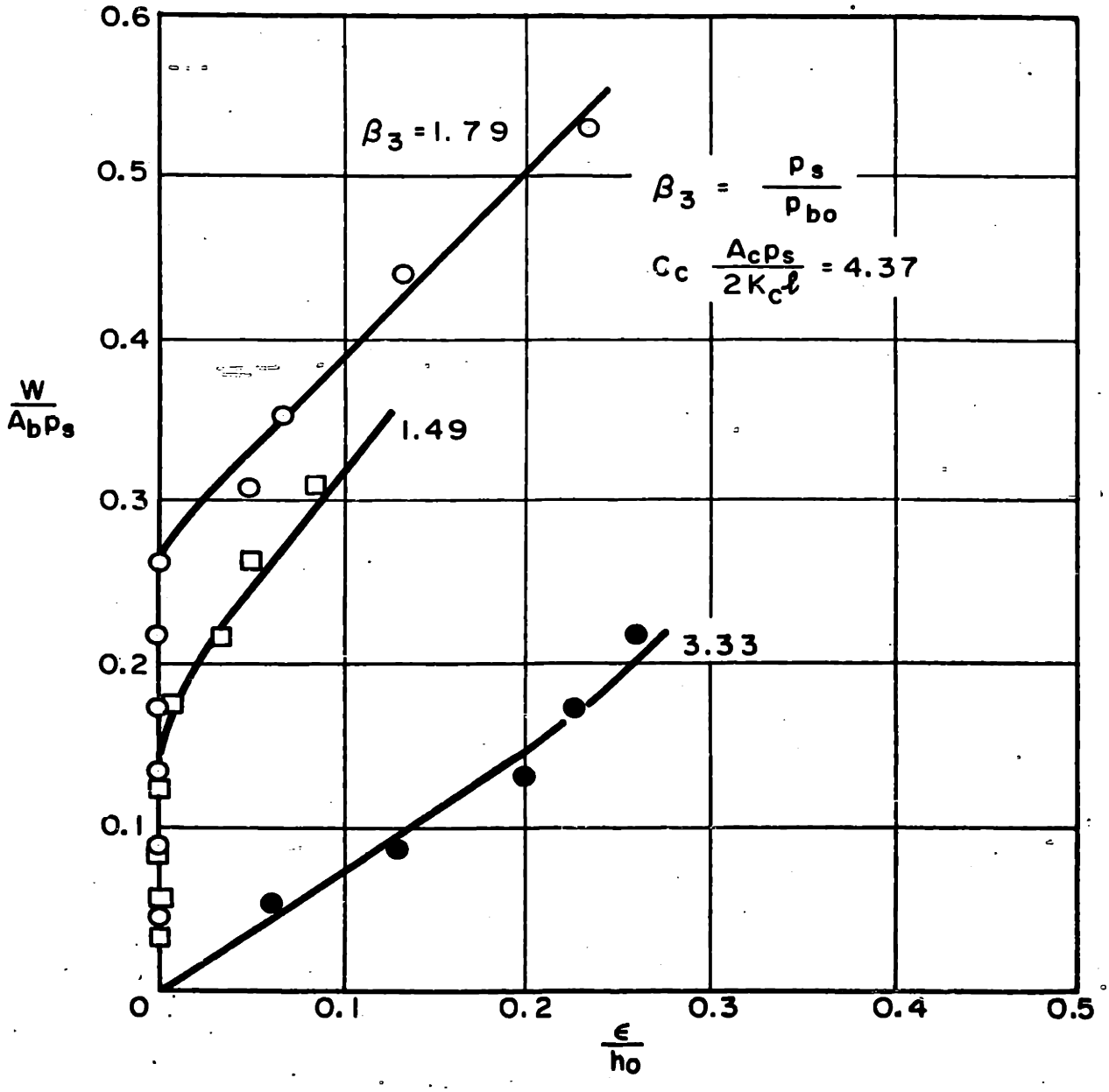

Fig. 18. Experimental journal load-displacement plot for variable external spool valve restriction (β_3 = variable, C_c = 4.37, non-rotating round bearing, incompressible fluid).

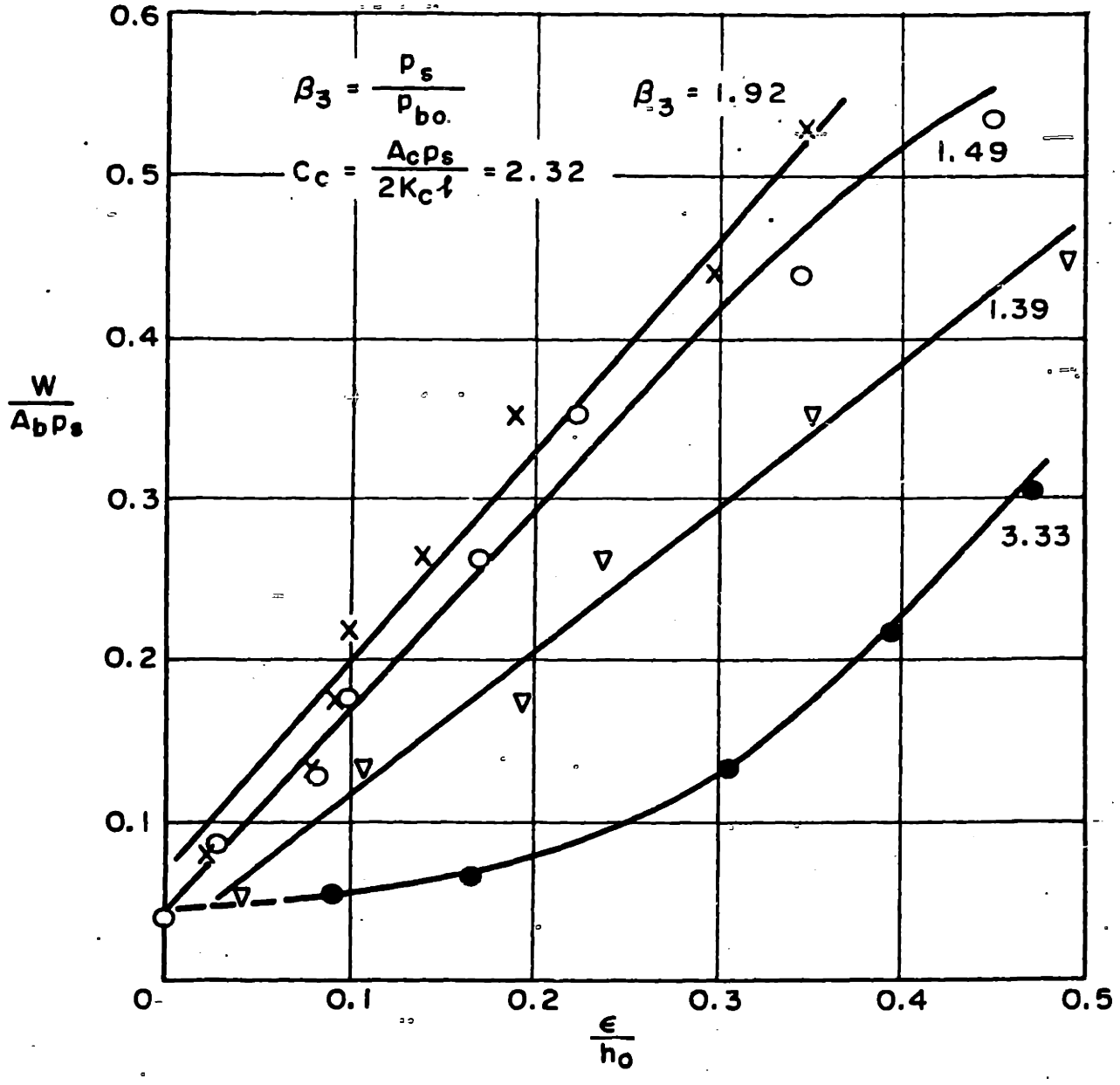

Fig. 19. Experimental journal load-displacement plot for variable external spool valve restriction (β_3 = variable, C_c = 2.32, non-rotating round bearing, incompressible fluid).

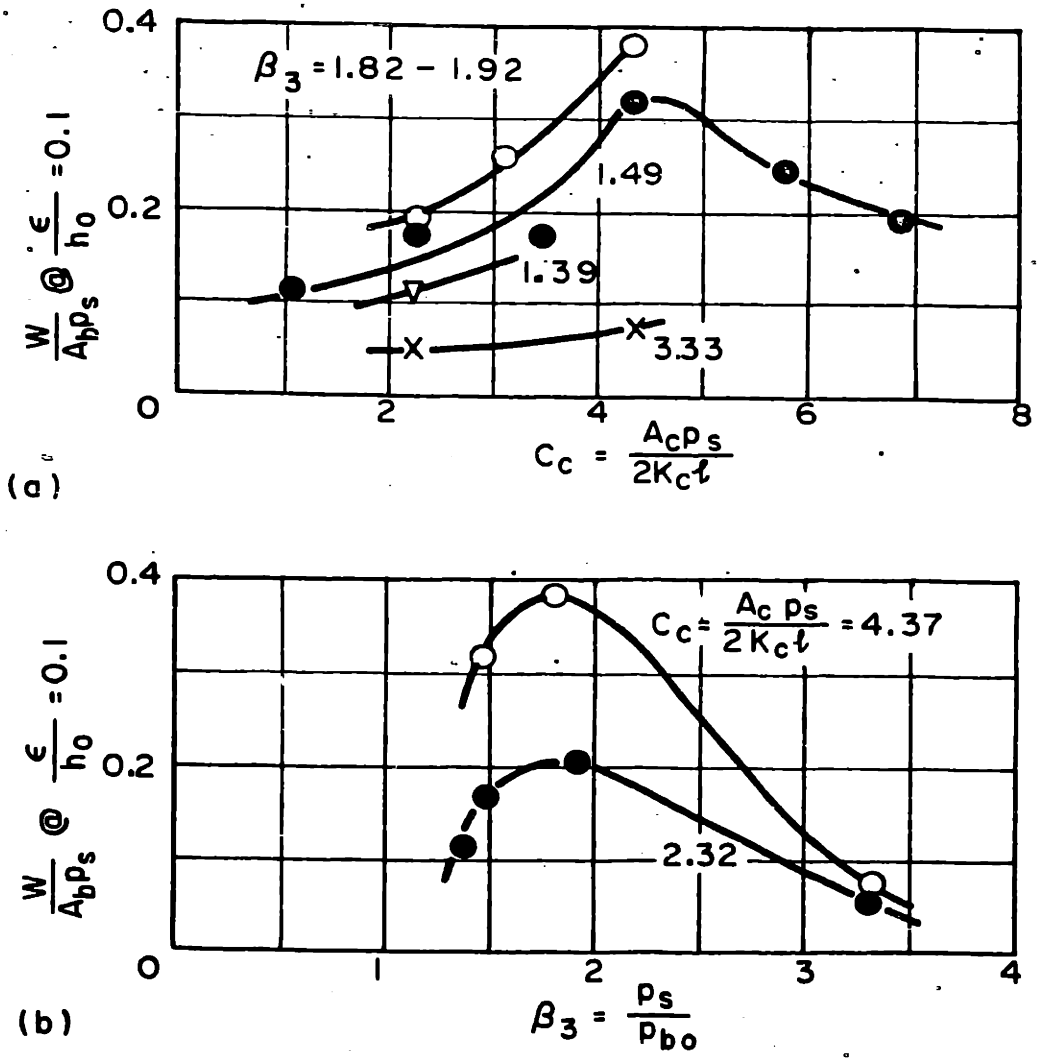

Fig. 20. Experimental load capacity ($\frac{W}{A_b p_s}$) at $\frac{\epsilon}{h_o} = 0.1$ versus C_c and β_3 for variable external spool valve restriction (non-rotating round bearing, incompressible fluid).

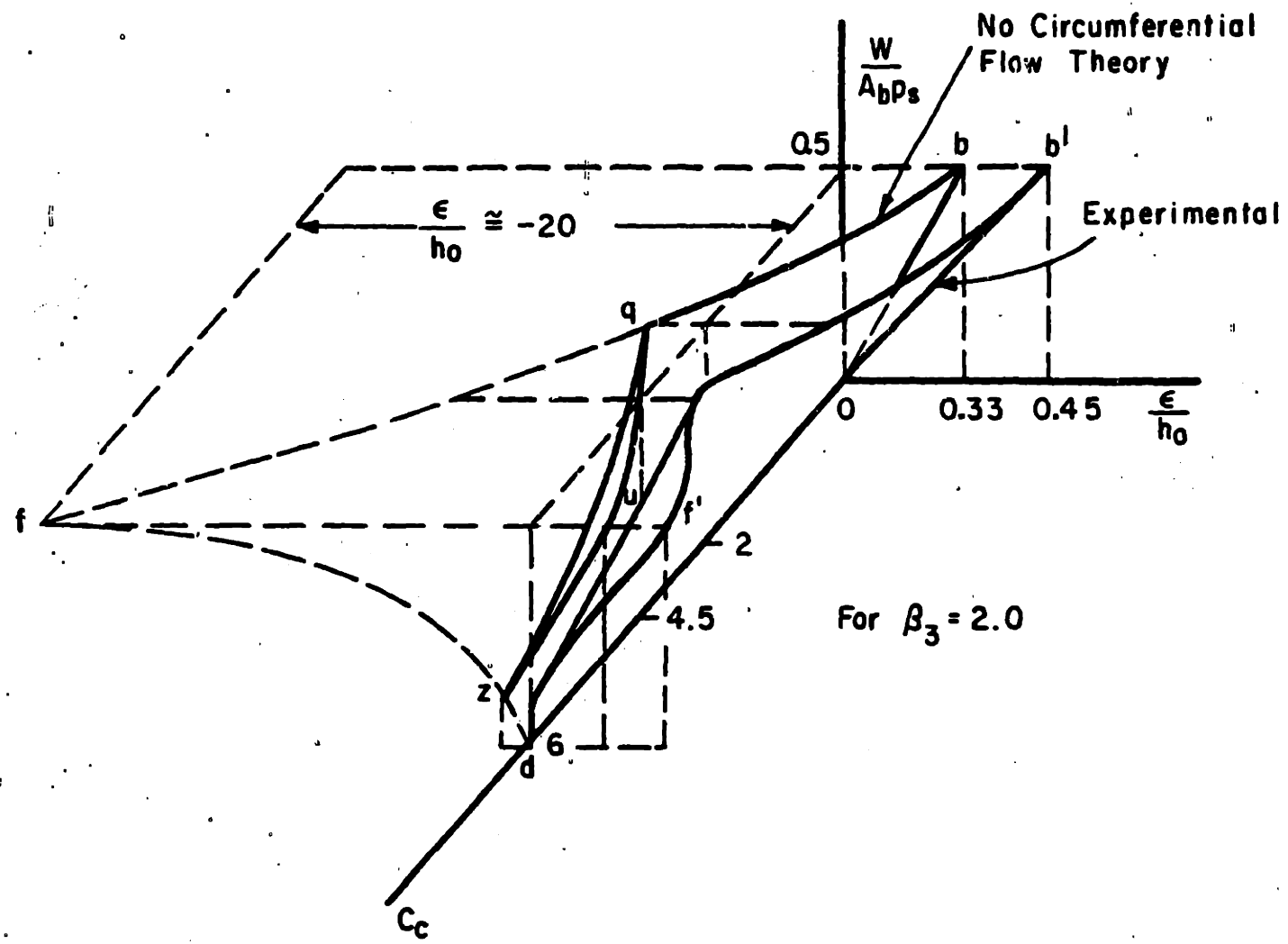

Fig. 21. Effect of circumferential flow on the theoretical non-circumferential flow journal load-displacement plot for variable external spool valve restriction (β_3 = constant, non-rotating bearing, incompressible fluid).

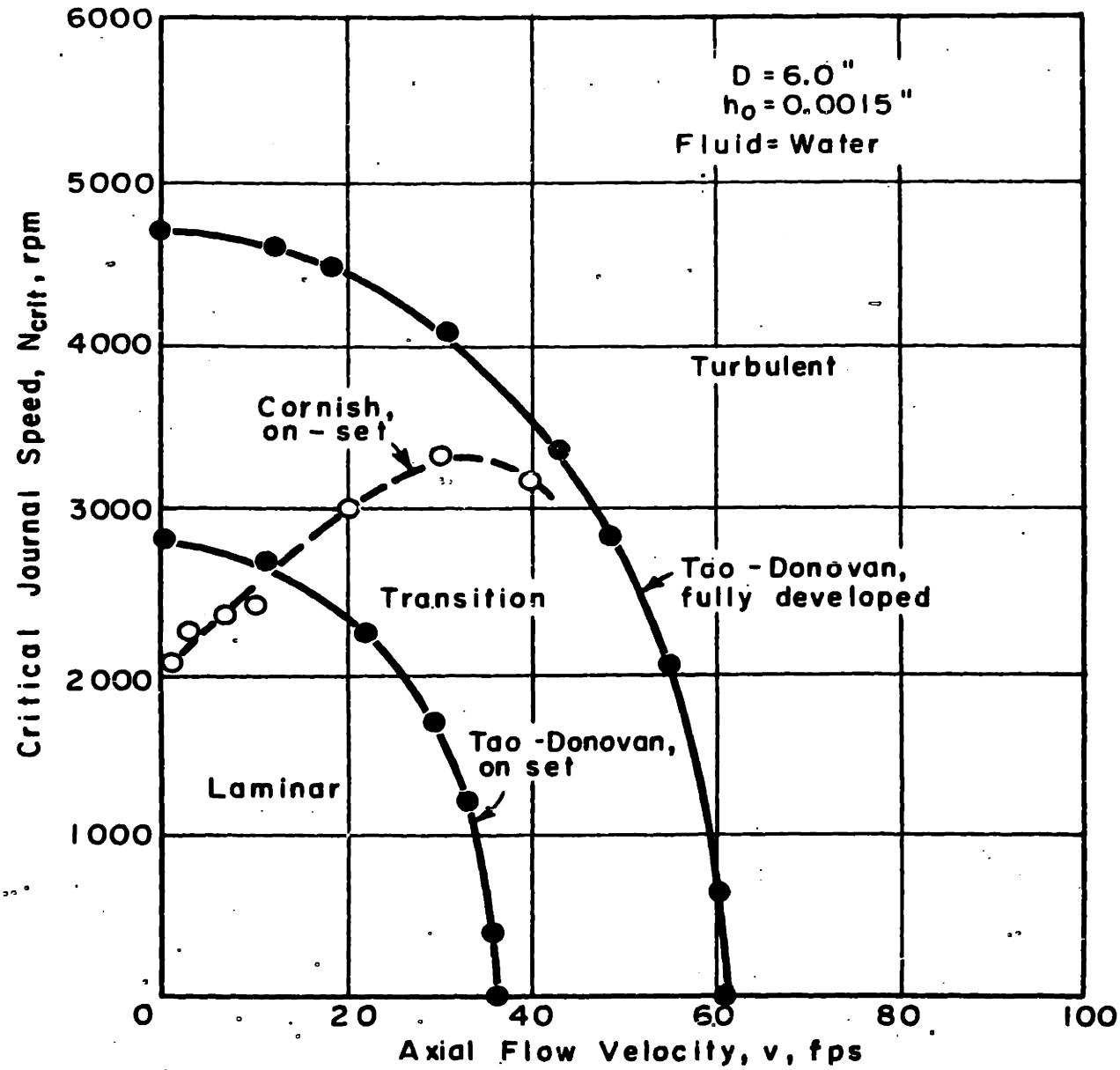

Fig. 22. Transition to turbulent flow for flow through a thin annulus with relative rotation between surfaces (for condition of test bearing, incompressible fluid).

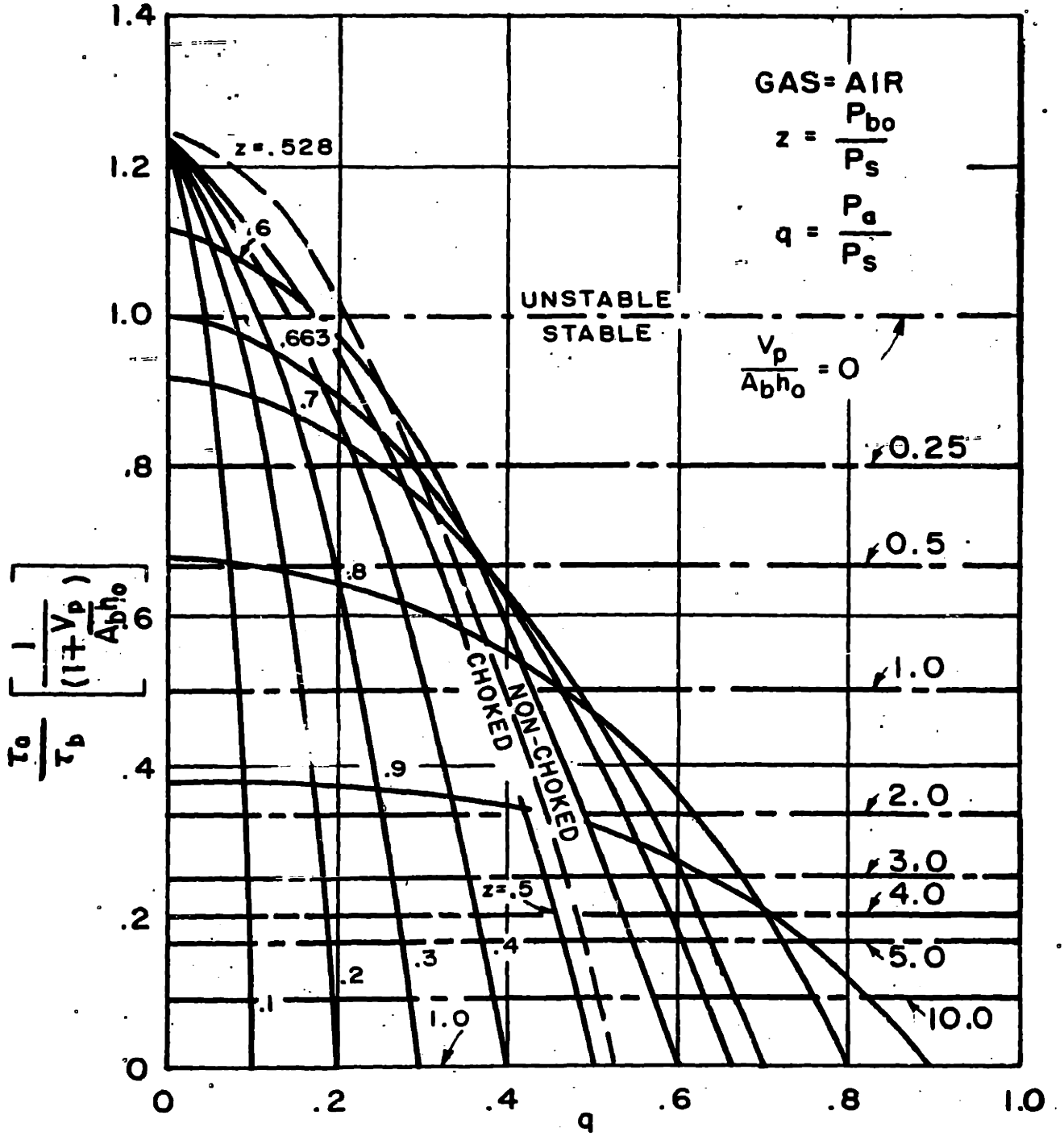

FIGURE 23 STABILITY RATIO FOR A PARALLEL-SURFACE GAS BEARING WITH FIXED ORIFICE EXTERNAL RESISTANCE FOR NON-CHOKED AND CHOKED OPERATION

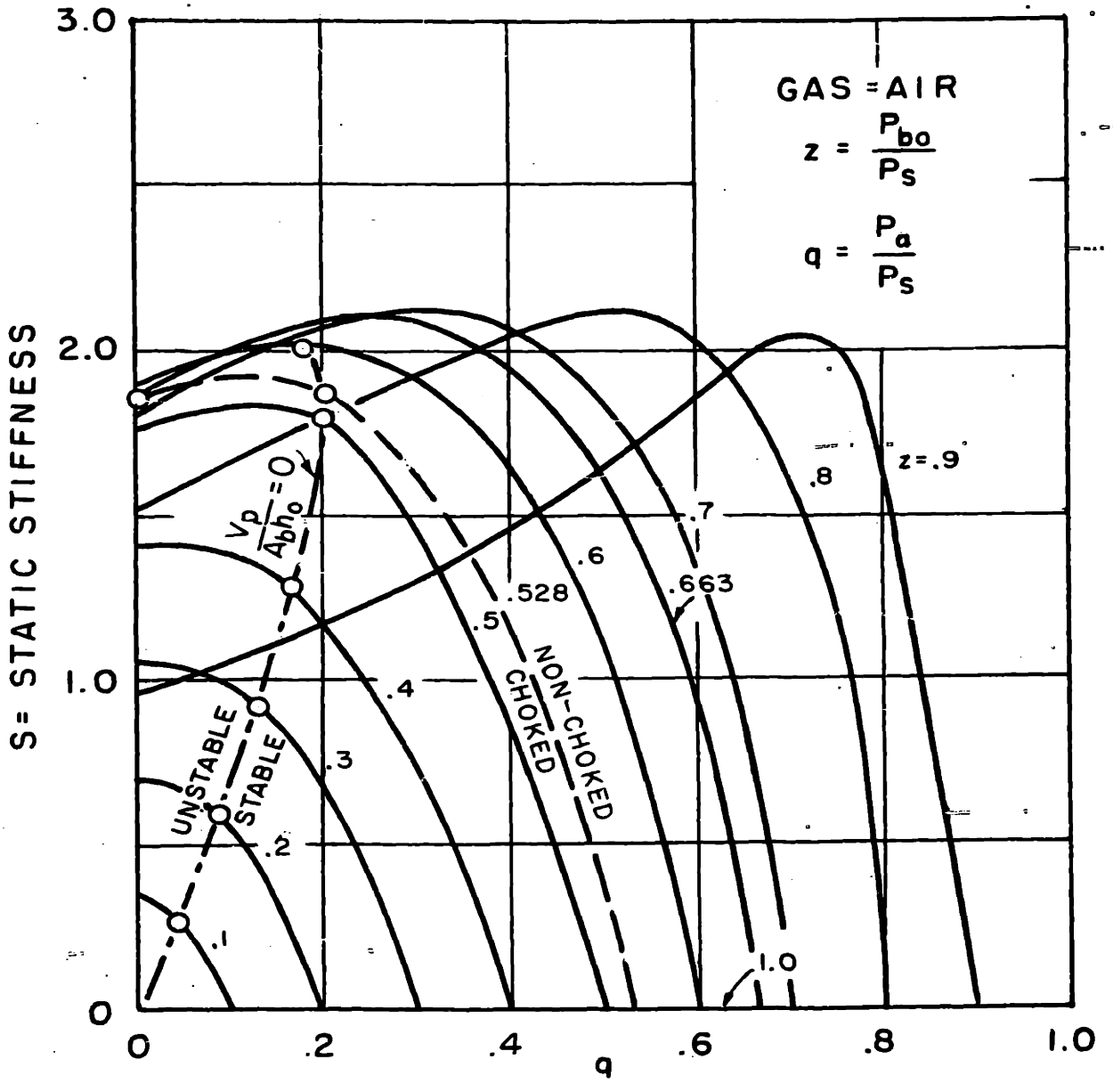

FIGURE 24 STATIC STIFFNESS FOR A PARALLEL-SURFACE GAS BEARING WITH FIXED ORIFICE EXTERNAL RESISTANCE FOR NON-CHOKED AND CHOKED OPERATION

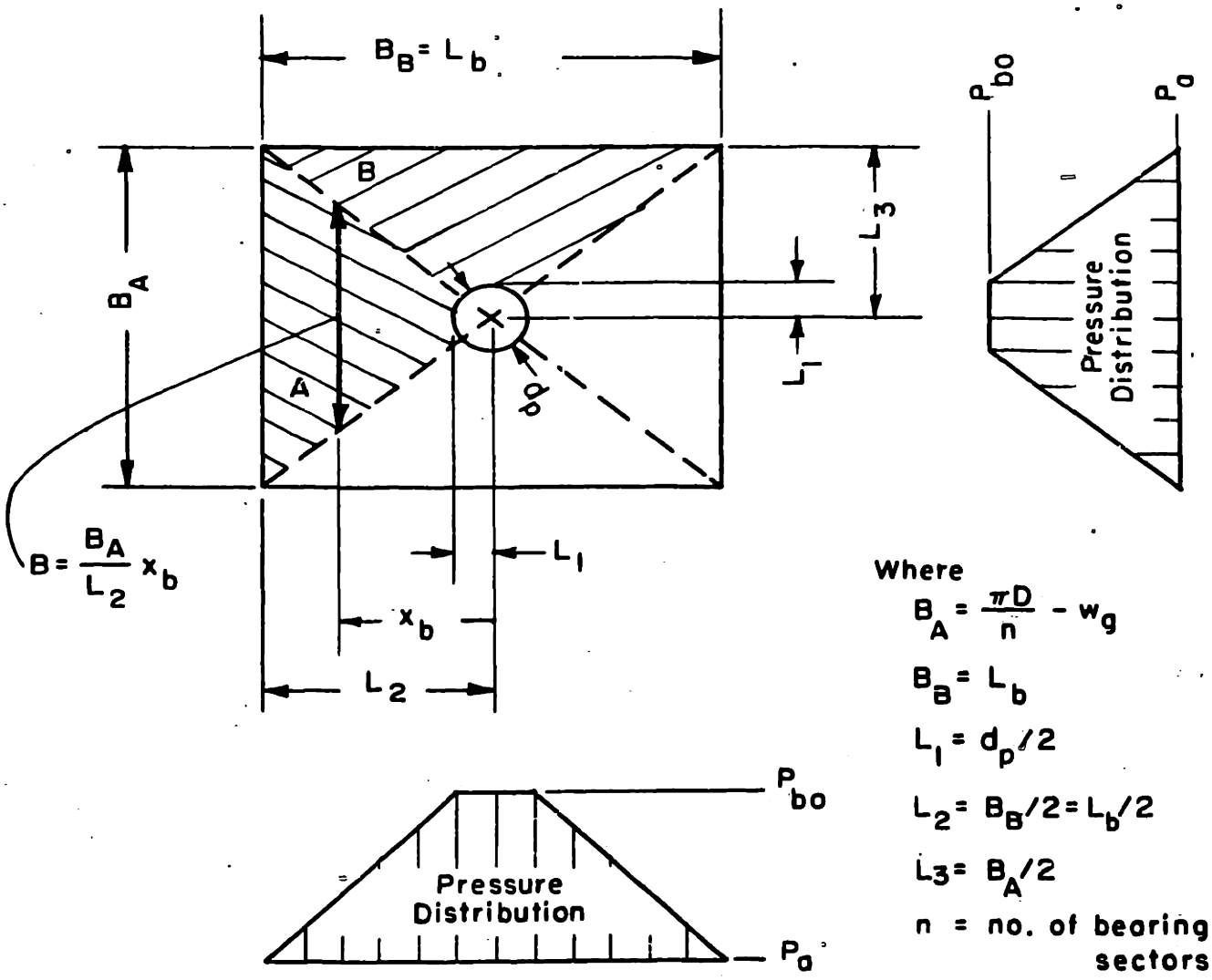

Fig. 25. Developed view of one internal sector of exhaust groove type bearing and pressure distribution through sector.

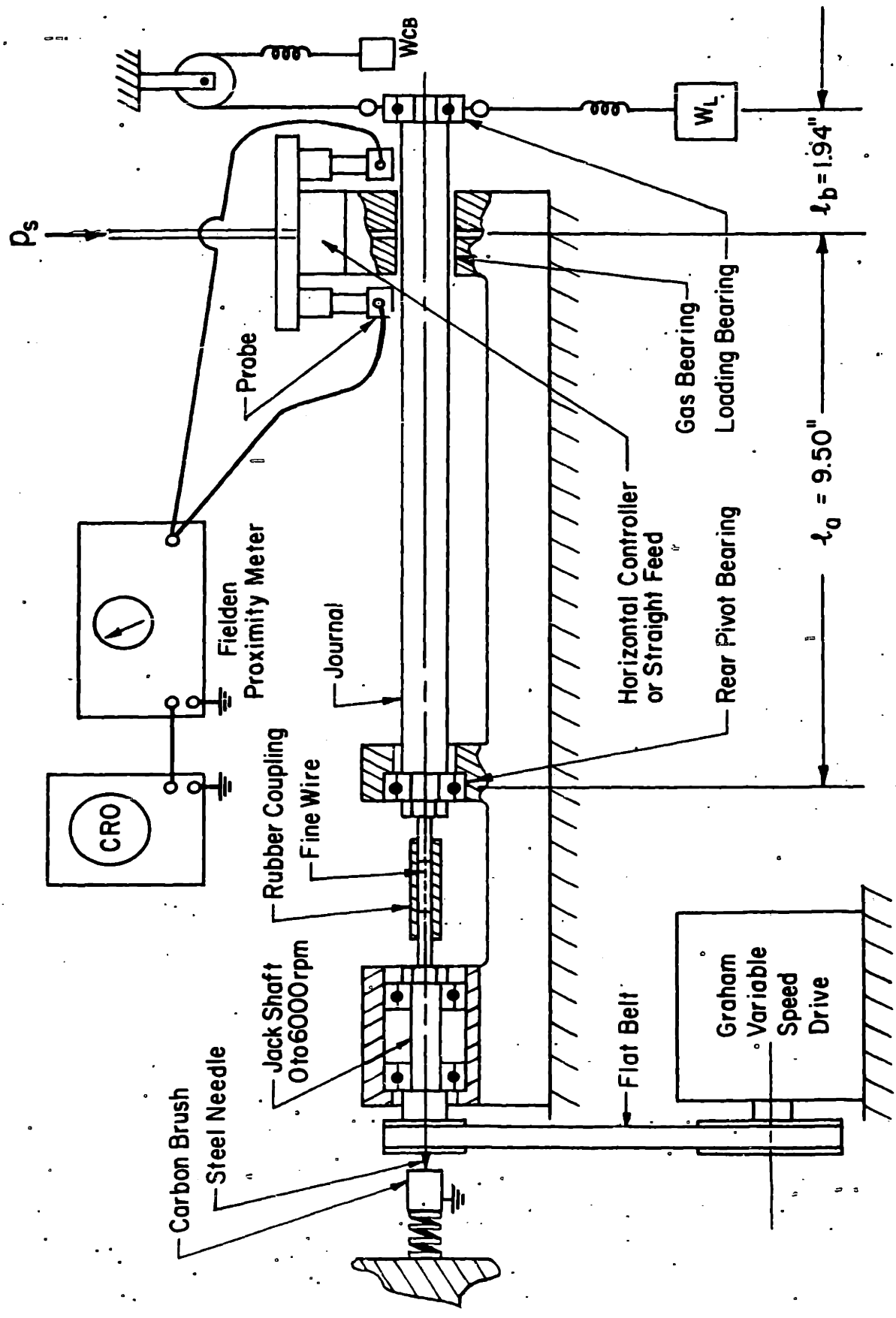

FIGURE 26 - TEST APPARATUS (SINGLE RADIAL BEARING, COMPRESSIBLE FLUID SUPPLY)

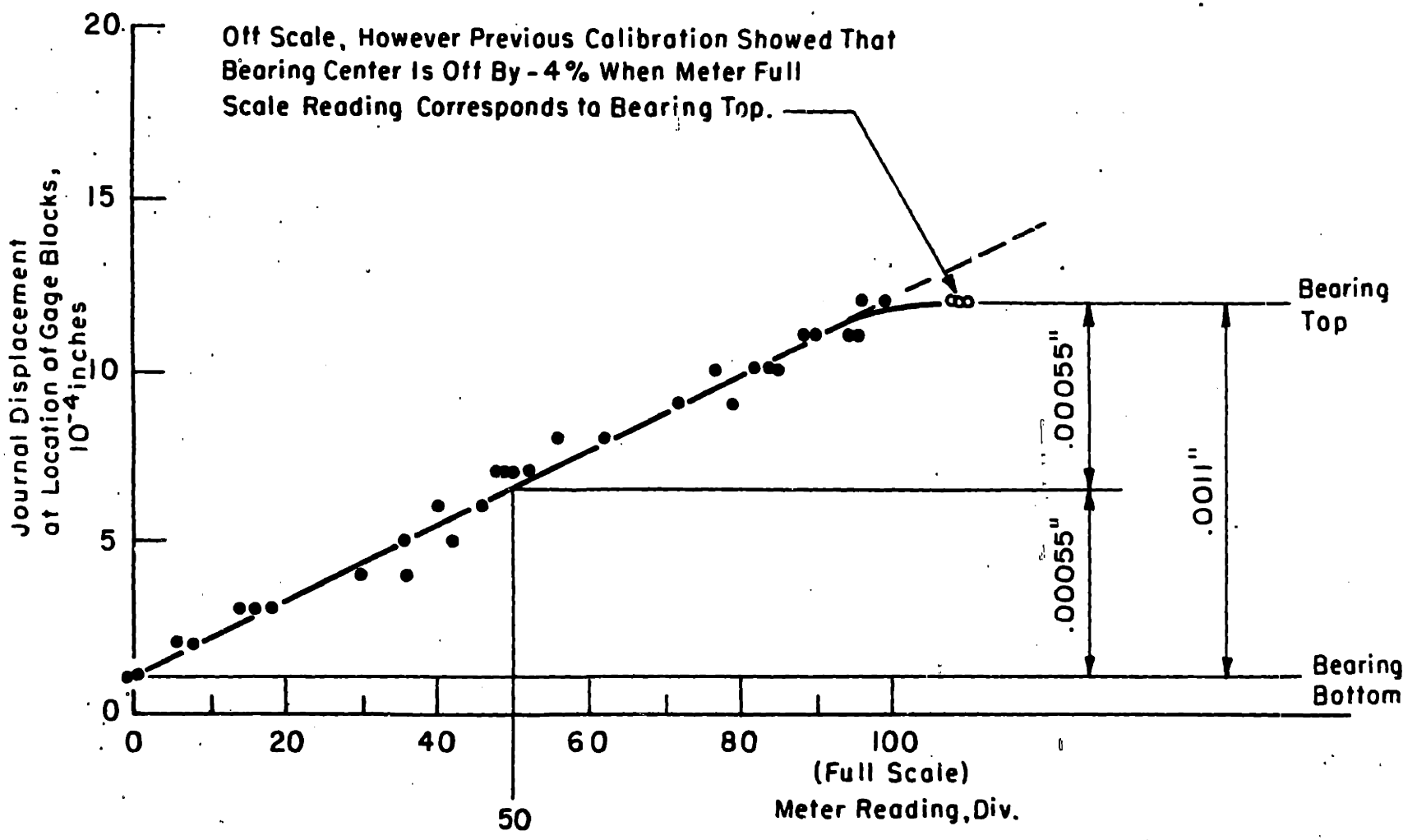

Fig. 27. Proximity meter calibration curve.

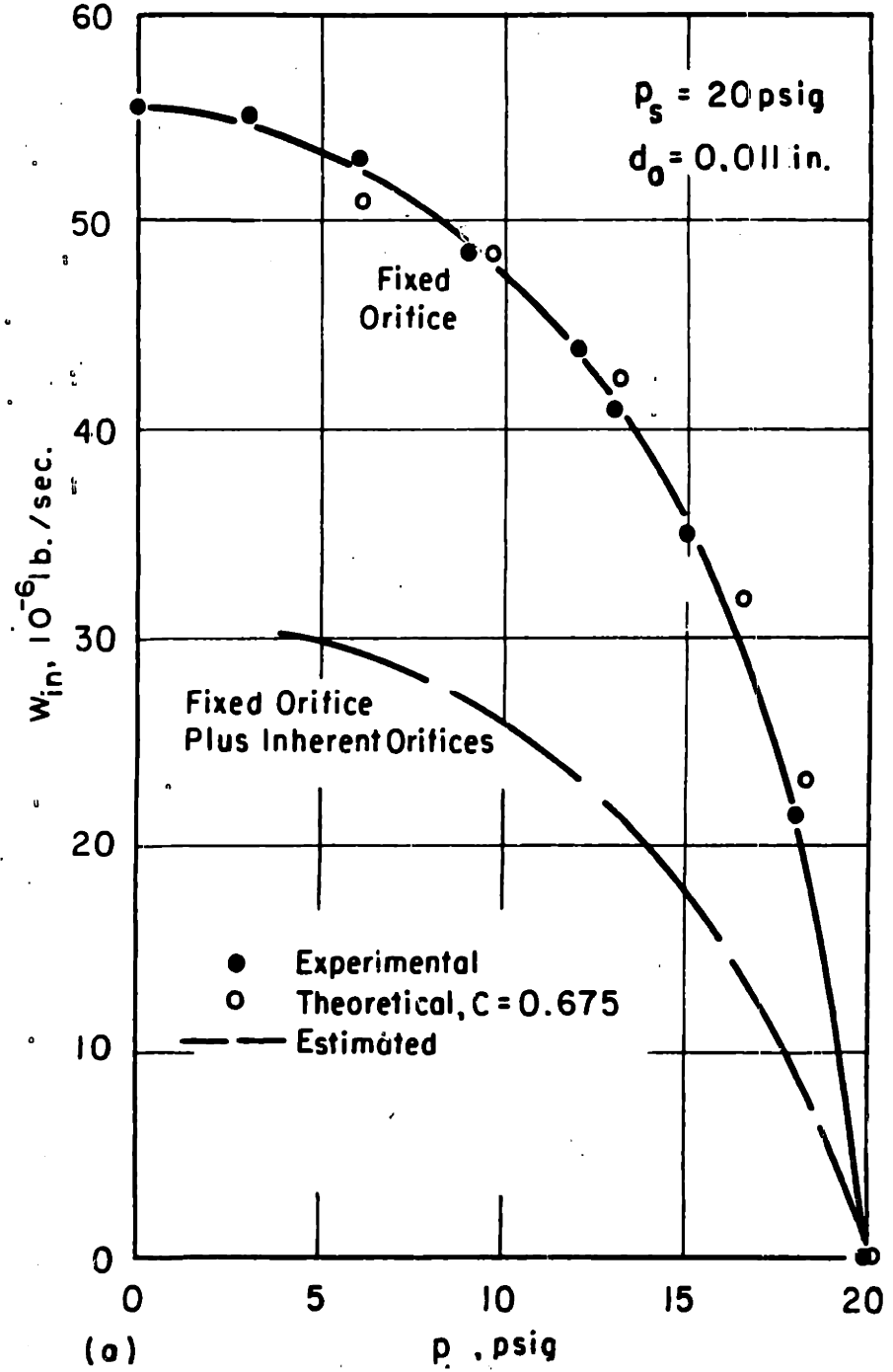

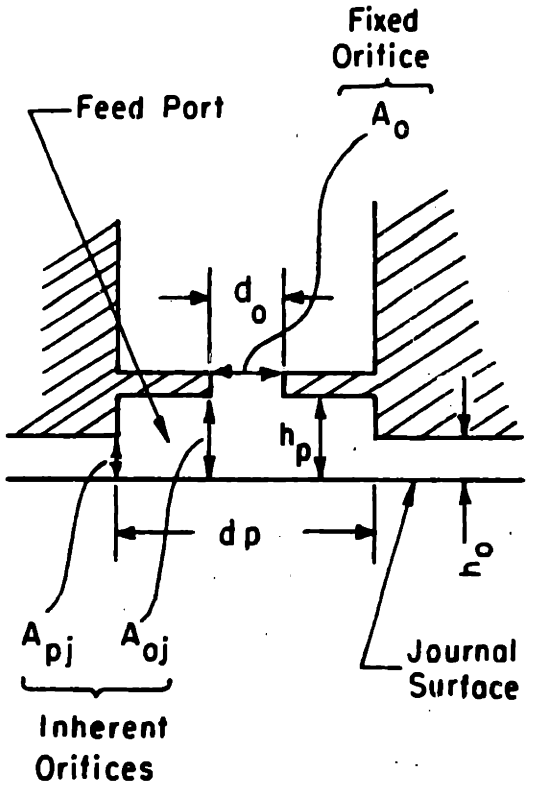

Fig. 28. Fixed external orifice restriction calibration curve.

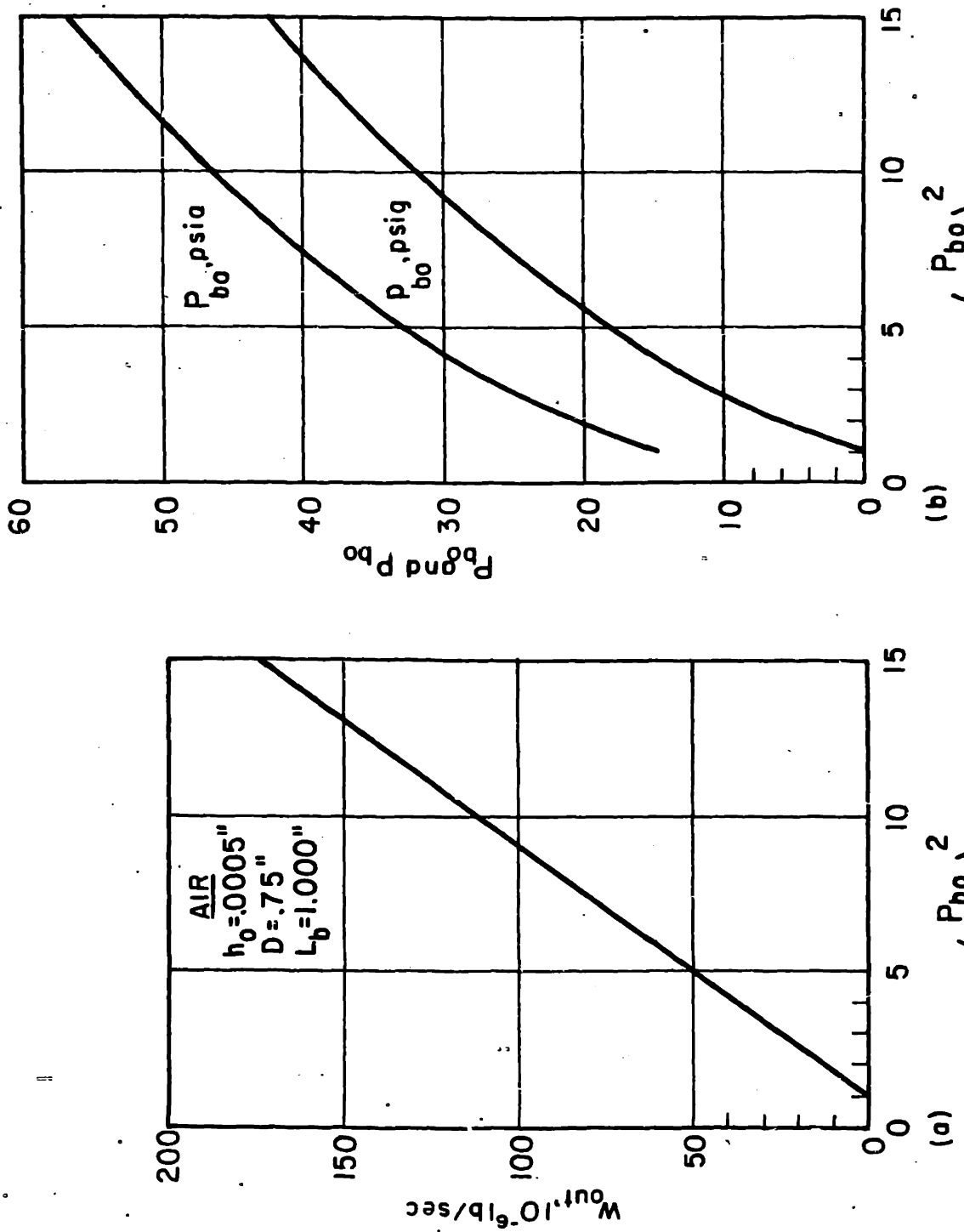

Fig. 29. Theoretical bearing flow through 1/4 bearing (fluid = air).

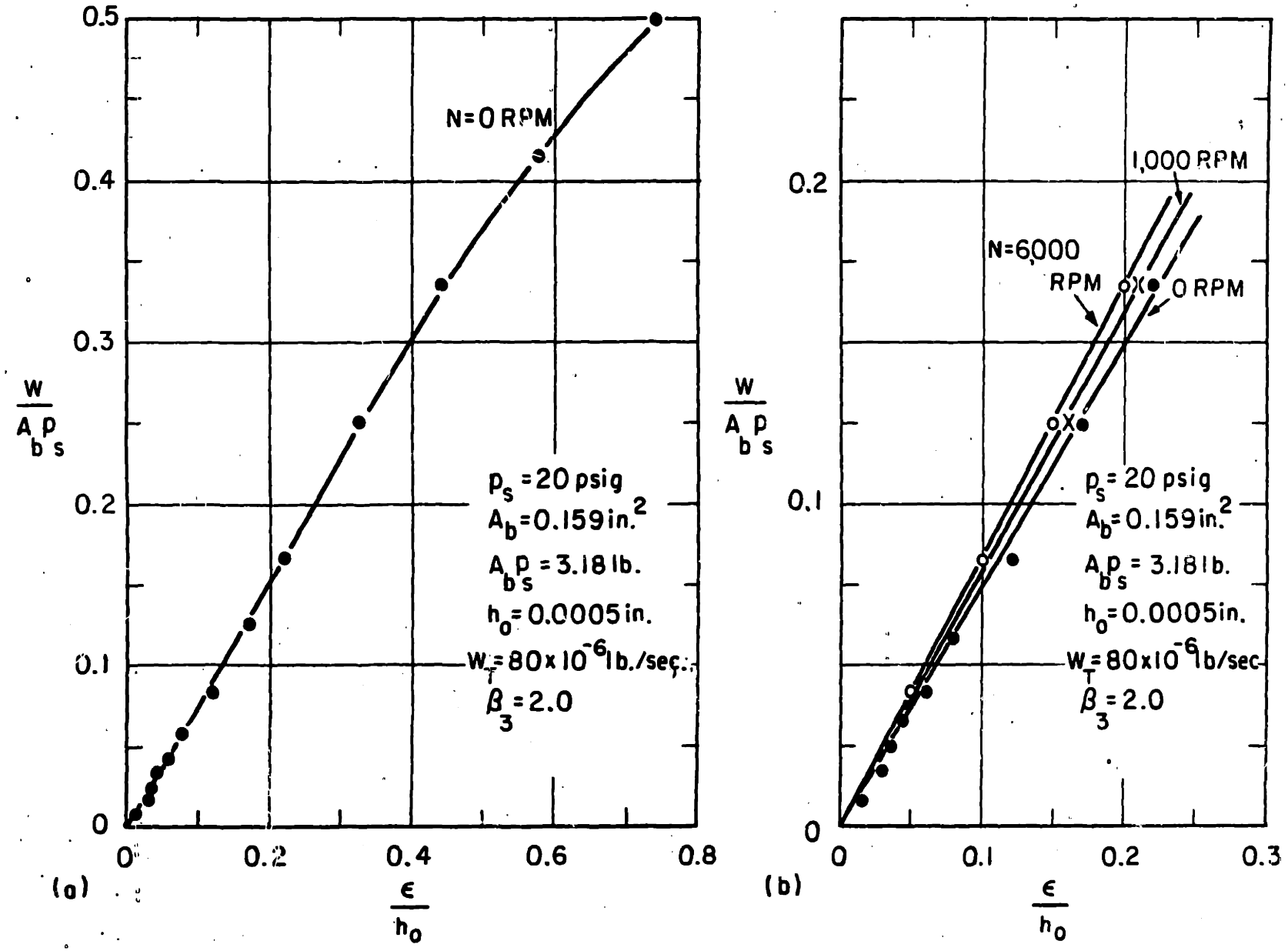

Fig. 30. Experimental journal load-displacement plot for fixed external orifice restriction (p_s = constant, β_3 = constant, fluid = air, non-rotating and rotating bearing).

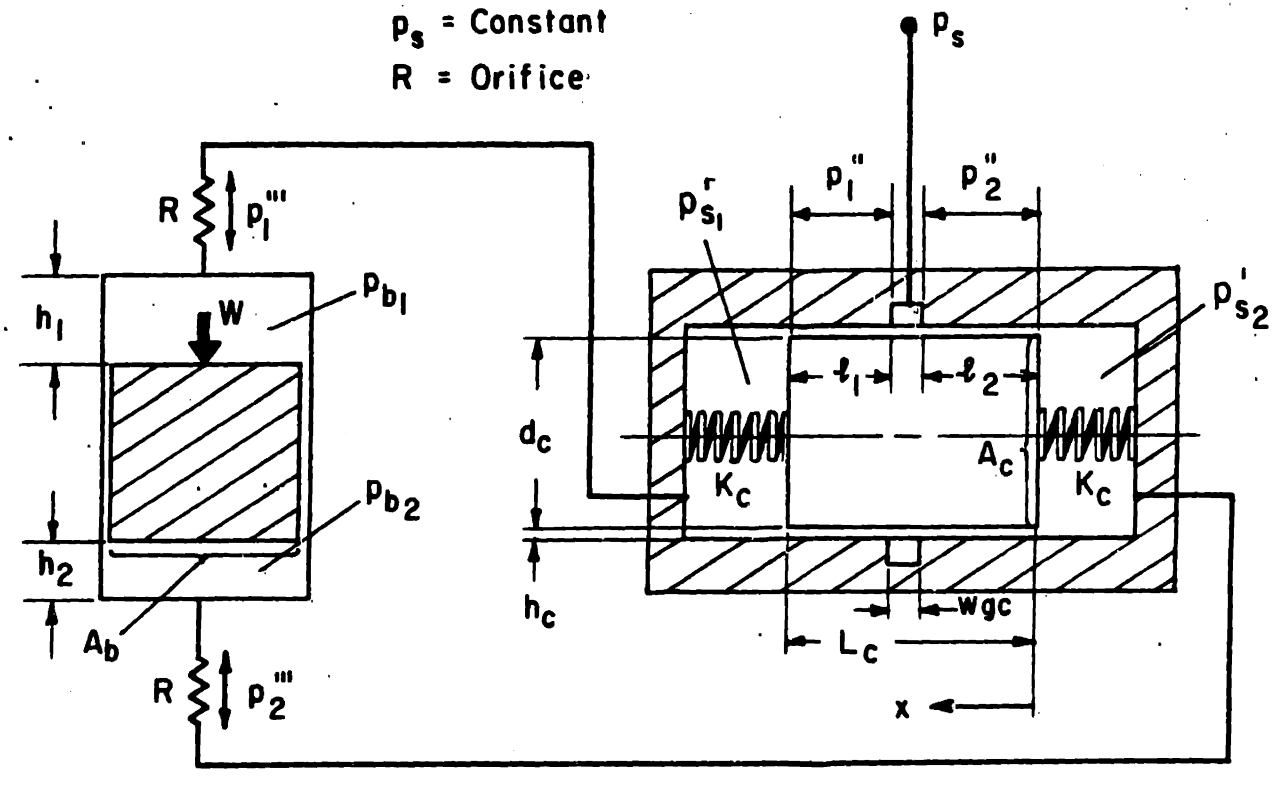

FIGURE 31 VARIABLE EXTERNAL RESTRICTION (LOAD SENSING) CONCEPT - (SPECIAL CASE OF VARIABLE EXTERNAL SPOOL VALVE RESTRICTION WITH STABILIZING FIXED EXTERNAL ORIFICE RESTRICTION FOR COMPRESSIBLE FLUIDS).

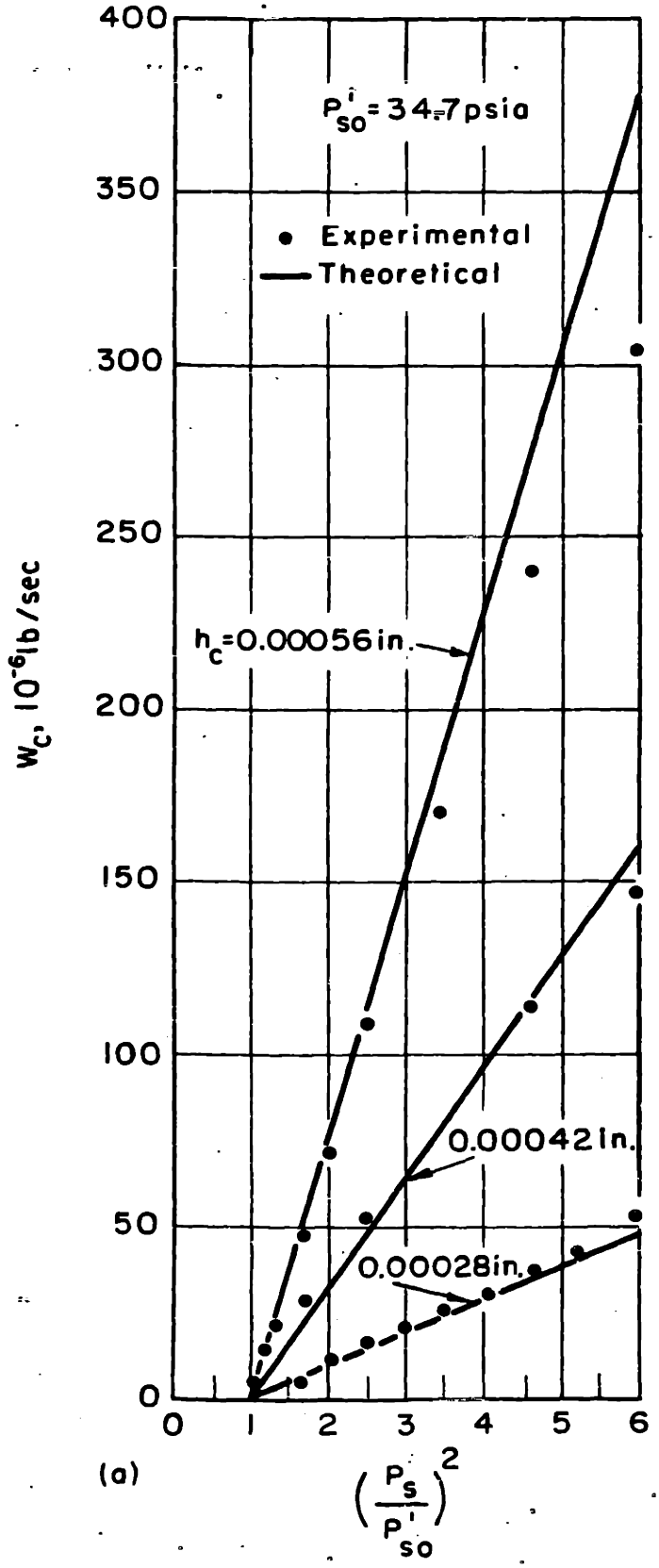

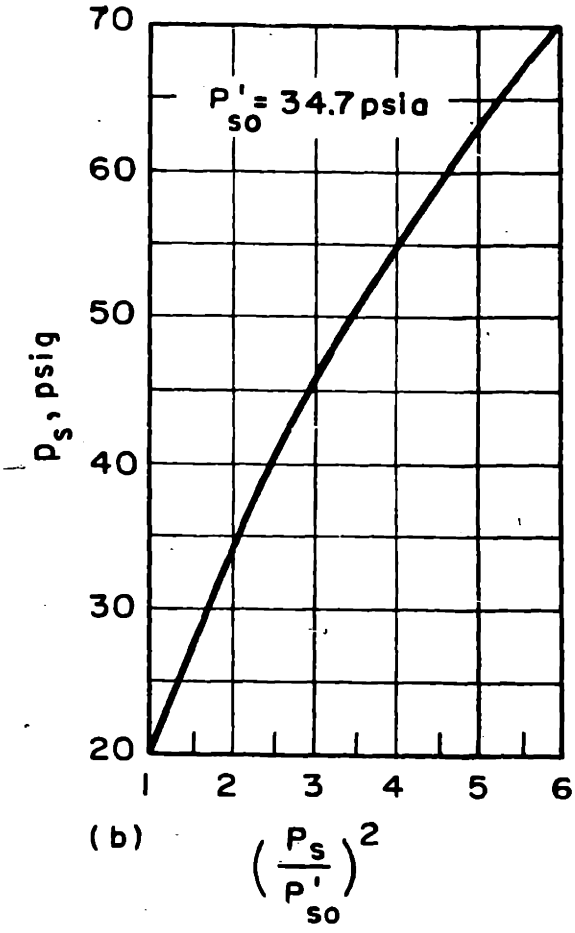

Fig. 32. Variable external spool valve restriction calibration curve.

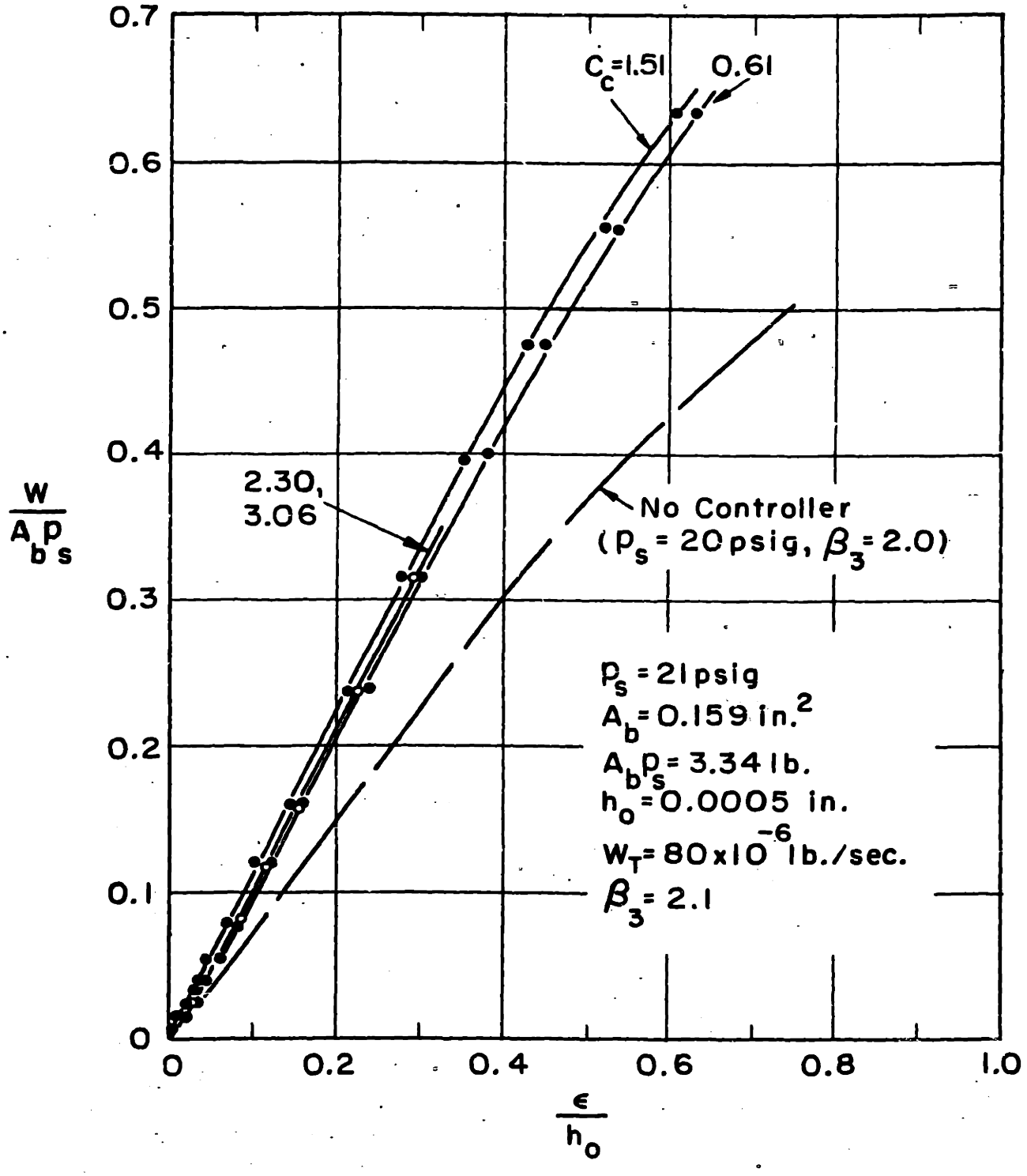

Fig. 33. Experimental journal load-displacement plot for variable external spool valve restriction (β_3 = 2.1, C_c = variable, non-rotating round bearing, fluid = air).

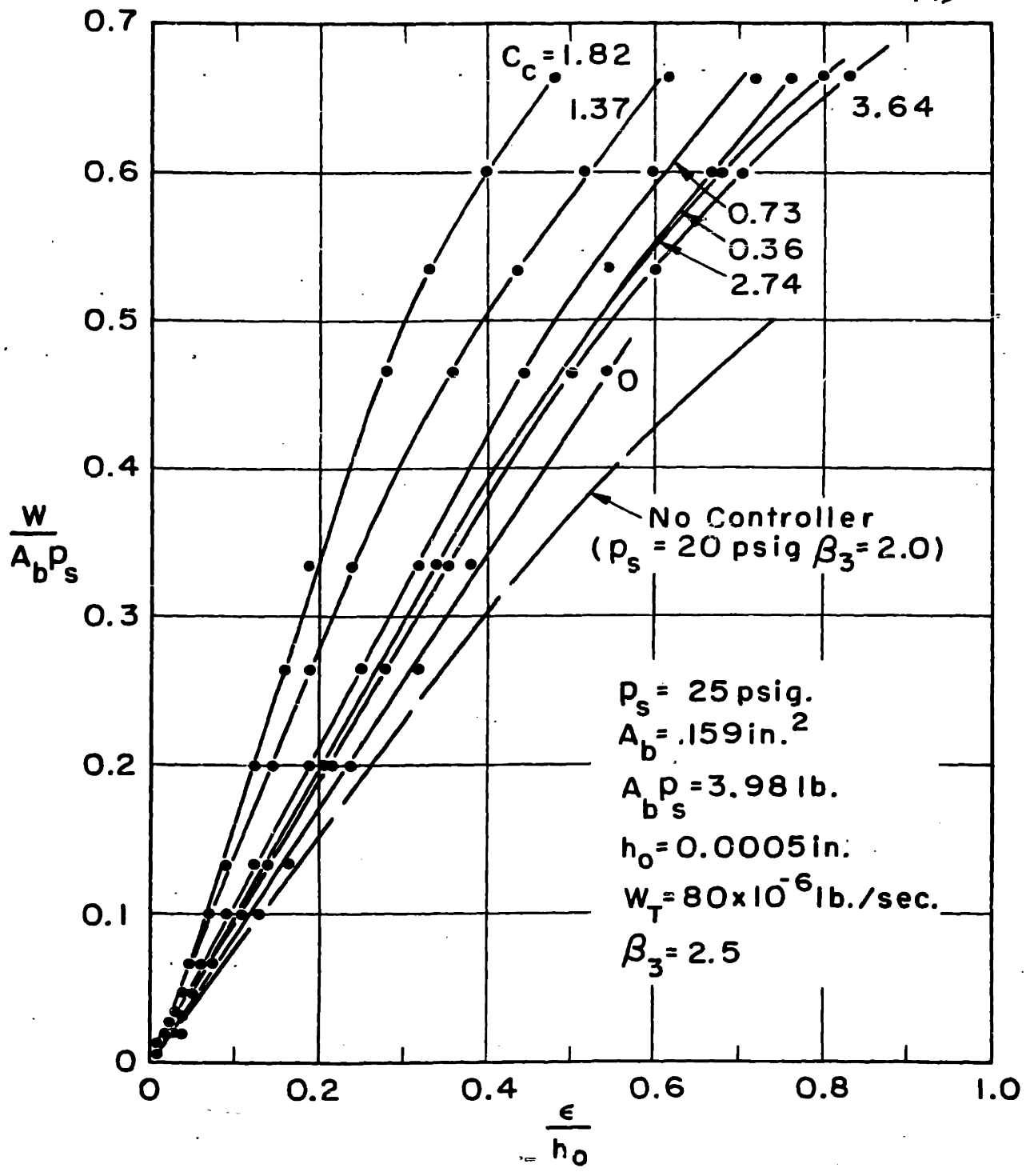

Fig. 34. Experimental journal load-displacement plot for variable external spool valve restriction (β_3 = 2.5, C_c = variable, non-rotating round bearing, fluid = air).

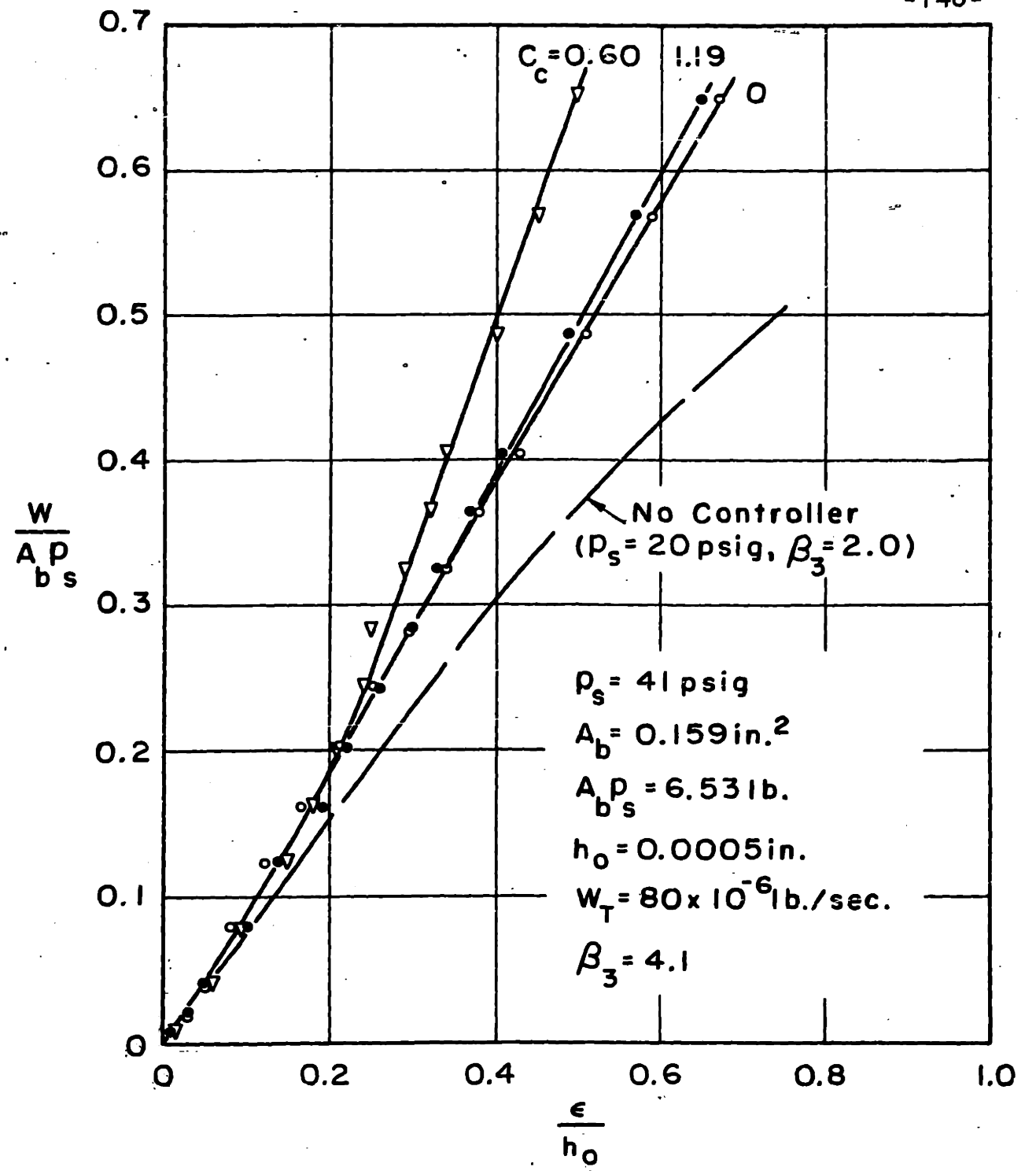

Fig. 35. Experimental journal load-displacement plot for variable external spool valve restriction (β_3 = 4.1, C_c = variable, non-rotating round bearing, fluid = air).

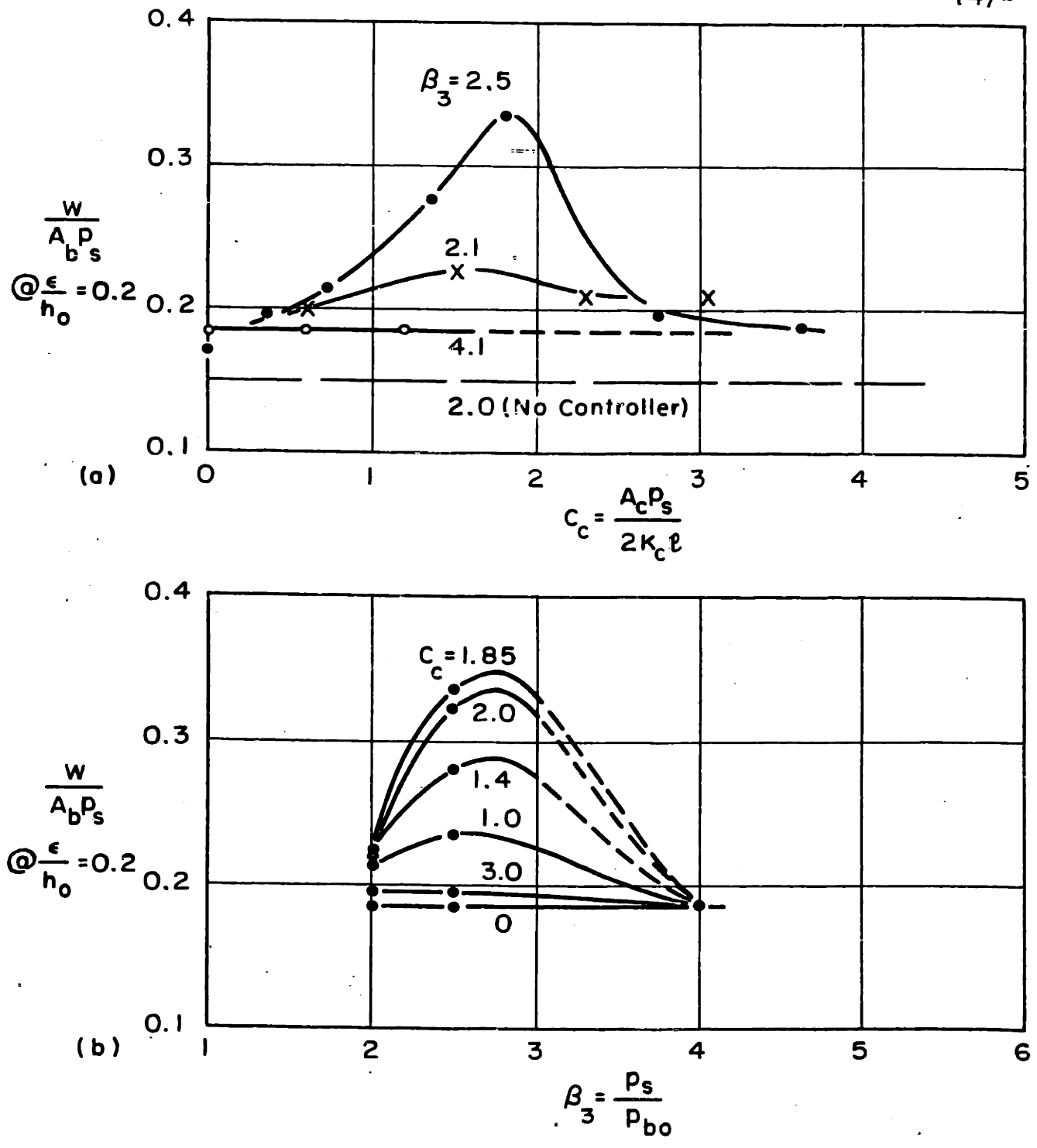

Fig. 36. Experimental load capacity ($\frac{W}{A_b P_s}$) at $\epsilon/h_o = 0.2$ versus C_c and β_3 for variable external spool valve restriction (non-rotating round bearing, fluid = air).

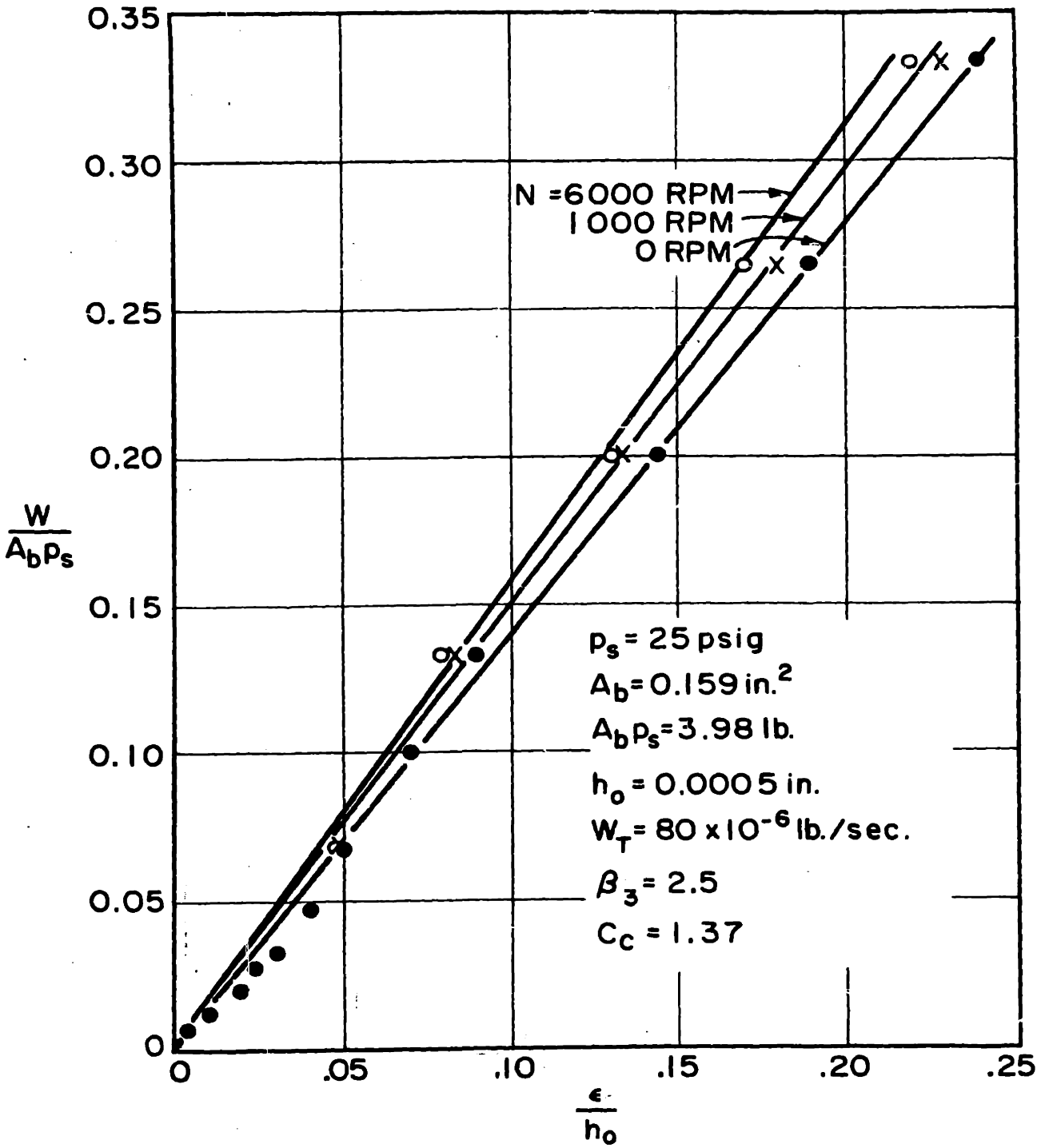

Fig. 37. Experimental journal load-displacement plot for variable external spool valve restriction (p_s = constant, C_c = constant, β_3 = constant, fluid = air, non-rotating and rotating bearing).

APPENDIX A

THEORETICAL BEARING STATIC STIFFNESS FOR EXTERNALLY PRESSURIZED SQUARE BEARING WITH FIXED ORIFICE EXTERNAL RESTRICTION

For this case it is easier to find an expression for K directly instead of finding an expression for W and then differentiating it with respect to ϵ. The procedure is to intially differentiate equation (1) to obtain

$$K = \frac{\partial W}{\partial \epsilon} = A_b \left(\frac{\partial P_{b2}}{\partial \epsilon} - \frac{\partial P_{b1}}{\partial \epsilon} \right) . \tag{117}$$

The pressure drop across the external orifice can be expressed as

$$P_s - P_b = Q_b^2 \frac{P_s - P_{bo}}{Q_{bo}^2} \tag{118}$$

Differentiating this with respect to ϵ, the following is obtained:

$$\frac{\partial P_b}{\partial \epsilon} = -2Q_b \frac{\partial Q_b}{\partial \epsilon} \frac{P_s - P_{bo}}{Q_{bo}^2} \tag{119}$$

Now since $$Q_b = Q_{bo} \frac{P_b}{P_{bo}} \left(\frac{h}{h_o} \right)^3 , \tag{120}$$

then $$\frac{\partial Q_b}{\partial \epsilon} = \frac{Q_{bo}}{P_{bo}} \left(\frac{h}{h_o} \right)^3 \frac{\partial P_b}{\partial \epsilon} + 3 \frac{Q_{bo}}{h_o^3} \frac{P_b}{P_{bo}} h^2 \frac{\partial h}{\partial \epsilon} \tag{121}$$

Substitution of equation (121) into equation (119) and rearrangement of terms yields the following expression for $\partial p_b / \partial \epsilon$:

$$\frac{\partial P_b}{\partial \epsilon} = \frac{-6\left(\frac{h^2}{h_o^3}\right)\left(\frac{Q_b}{Q_{bo}}\right)\left(\frac{P_b}{P_{bo}}\right)\left(P_s - P_{bo}\right)\frac{\partial h}{\partial \epsilon}}{\left[\,1 \;+\; 2\left(\frac{Q_b}{Q_{bo}}\right)\left(\frac{h}{h_o}\right)^3 \frac{\left(P_s - P_{bo}\right)}{P_{bo}}\right]} \qquad (122)$$

If this expression is linearized about $\epsilon = 0$, then $p_b = p_{bo}$, $Q_b = Q_{bo}$ and $h = h_o$, hence

$$\frac{\partial P_b}{\partial \epsilon} = \frac{-6\left(\frac{P_s}{h_o}\right)\left(1 - \frac{1}{\beta_3}\right)\frac{\partial h}{\partial \epsilon}}{\left(2\beta_3 - 1\right)} \qquad (123)$$

Now from equations (6) and (7) it is seen that

$$\frac{\partial h_2}{\partial \epsilon} = -1 \qquad (124)$$

and

$$\frac{\partial h_1}{\partial \epsilon} = +1 \quad , \qquad (125)$$

hence

$$\frac{\partial W}{\partial \epsilon} = A_b\left(\frac{\partial P_2}{\partial \epsilon} - \frac{\partial P_1}{\partial \epsilon}\right) = 12\,\frac{A_b P_s}{h_o}\,\frac{\left(1 - \frac{1}{\beta_3}\right)}{\left(2\beta_3 - 1\right)} \qquad (15)$$

APPENDIX B

BEARING STATIC STIFFNESS CORRECTION FOR ROUND BEARING

In the analyses for the square bearing the following expressions involving the bearing exit path height were employed for $\epsilon \ll h_o$:

$$\left(\frac{h_2}{h_o}\right)^3 = 1 - 3\frac{\epsilon}{h_o} \quad \text{and} \quad \left(\frac{h_1}{h_o}\right)^3 = 1 + 3\frac{\epsilon}{h_o} \qquad (8),(9)$$

From Shaw and Macks[7] it can be seen for a round bearing that for $\epsilon \ll h_o$

$$\left(\frac{h_2}{h_o}\right)^3 = 1 - 2.7\frac{\epsilon}{h_o} \quad \text{and} \quad \left(\frac{h_1}{h_o}\right)^3 = 1 + 2.7\frac{\epsilon}{h_o} \qquad (126),(127)$$

This introduces an error in the calculated value of W and in the calculated value of K or S. The error is of such nature that it is constant and only causes any constant coefficient of the term ϵ/h_o to be increased by 13%. This means that the bearing stiffness should be divided by 1.13 in order to change the calculated square bearing stiffness to round bearing stiffness. The optimum value of the pressure ratio β_3 remains unchanged by this correction.

APPENDIX C

RAIMONDI AND BOYD[8] BEARING STIFFNESS CORRECTION FOR CIRCUMFERENTIAL FLOW

Raimondi and Boyd show a plot of $W/A_b p_s$ for $\epsilon/h_o = 0.3$ and $F_b = 0.77$ versus a design parameter λ for fixed external orifice restrictions. The $\lambda = \pi^2 / [\beta_3 (\beta_3 - 1)]$. This plot has been reproduced and is shown in Fig.9a. They also show a plot of the ratio of the load capacity (Circ. Flow Theory) to the load capacity (No Circ. Flow Theory) for $\epsilon/h_o = 0.6$ and $\lambda = 5$ versus the bearing factor F_b. This plot is reproduced as Fig. 9b. From Fig. 9a, values of $W/A_b p_s$ (No Circ. Flow) and $W/A_b p_s$ (Experimental) for $\epsilon/h_o = 0.3$ and $F_b = 0.77$ were obtained for specific values of λ. The λ values chosen were those calculated for specific β_3 values. Hence, S_R = Load Capacity (exp.)/Load Capacity (No Circ. Flow) could be computed for the various values of β_3 for $\epsilon/h_o = 0.3$ and $F_b = 0.77$. These S_R values were then plotted on Fig. 9b for $F_b = 0.77$. Then curves conforming to the shape of the curve given by Raimondi and Boyd for $\epsilon/h_o = 0.6$ and $\lambda = 5$ were drawn from the point $S_R = 1.0$ at $F_b = 0$ through the above plotted S_R points. From these curves S_R values could be estimated for $F_b = 0.5$, the bearing factor of the bearing employed in Fig. 7. The S_R values thus determined were employed to calculate $W/A_b p_s$ (Circ. Flow) values at $\epsilon/h_o = 0.3$ from the $W/A_b p_s$ (No Circ. Flow) values at

ϵ/h_o = 0.3 which were presented in Fig. 5. This was done and the result is shown in Fig. 8. The computations for this procedure are given in the table below:

Table III

Computation of Raimondi and Boyd Bearing Stiffness Correction for Circumferential Flow

		(For ϵ/h_o = 0.3, F_b = 0.77)			(For ϵ/h_o = 0.3, F_b = 0.5)		
β_3	$\lambda = \frac{\pi^2}{\beta_3(\beta_3-1)}$	$\frac{W}{A_b P_s}$* (No Circ)	$\frac{W}{A_b P_s}$* (Circ)	S_R*	S_R**	$\frac{W}{A_b P_s}$*** (No Circ)	$\frac{W}{A_b P_s}$*** (Circ
5	.49	.36	.11	.30	.35	.285	.10
2	4.93	.50	.275	.55	.66	.531	.35
1.71	8.11	.495	.29	.59	.68	.543	.37
1.67	8.80	.49	.29	.59	.68	.543	.37
1.43	16.04	.455	.285	.63	.71	.513	.36
1.25	31.6	.375	.26	.69	.78	.426	.33
1.11	80.8	.24	.18	.75	.82	.264	.22

*From Figure 9a

**From Figure 9b

***From Figure 5

APPENDIX D

FLOW CHARACTERISTICS OF CAPILLARY, ORIFICE, AND BEARING FOR INCOMPRESSIBLE FLUID

Capillary Tube

The volumetric flow rate for a capillary tube can be expressed as:[7]

$$Q_{RC} = \frac{\pi r_t^4 (P_s - P_{bo})}{8 \mu L_t} \tag{128}$$

Orifice

The volumetric flow rate for a sharp-edged orifice can be expressed as:[10]

$$Q_{RO} = C A_o \sqrt{\frac{2 (P_s - P_{bo})}{\rho}} \tag{129}$$

where C = coefficient of discharge for V.D.I. sharp-edged orifice determined from Reference 10.

$A_o = \frac{\pi d_o^2}{4}$, in^2.

ρ = mass density of fluid, lb. $sec.^2/in^4$.

Four Pad Bearing

The volumetric flow rate for the bearing for the no-load condition can be determined by considering the flow to be like

parallel flat plate flow, hence the flow expression can be written[7] as:

$$Q_B = \frac{\pi D h_o^3 P_{bo}}{24 \mu L_e} \qquad (130)$$

where Q_B is the flow through one pressure pad, that is flow through a quarter of the bearing. Also the total flow is $4Q_B$, hence the total flow is

$$Q_T = \frac{\pi D h_o^3 P_{bo}}{6 \mu L_e} \qquad (26)$$

Determination of Capillary Tube Length for Externally Pressurized Bearing With Fixed External Capillary Restriction

Here $Q_{RC} = Q_B$,

hence $$L_t = \frac{3 L_e r_t^4}{D h_o^3} (\beta_3 - 1) \qquad (25)$$

Determination of Orifice Diameter for Externally Pressurized Bearing With Fixed External Orifice Restriction

Here $Q_{RO} = Q_B$,

hence $$d_o = \left\{ \frac{D h_o^3}{6 \mu L_e C} \sqrt{\frac{\rho P_s}{2 \beta_3 (\beta_3 - 1)}} \right\}^{\frac{1}{2}} \qquad (27)$$

APPENDIX E

FLOW CHARACTERISTICS OF SPOOL VALVE CONTROLLER FOR INCOMPRESSIBLE FLUID

The volumetric flow rate through one side of the spool valve controller for the central spool valve position can be expressed as:

$$Q_c = \frac{\pi\, d_c\, h_c^3 \left(P_s - P_{bo}\right)}{12\, \mu\, \ell} \tag{131}$$

The determination of the spool valve radial clearance for the externally pressurized bearing with spool valve controller is as follows:

Here $Q_c = Q_B$,

hence $$h_c = \left[\frac{D\, \ell\, P_{bo}}{2\, d_c\, L_e \left(P_s - P_{bo}\right)}\right]^{\frac{1}{3}} h_o$$

$$= \left[\frac{D\, \ell}{2\, d_c\, L_e \left(\beta_3 - 1\right)}\right]^{\frac{1}{3}} h_o \tag{36}$$

APPENDIX F

CALCULATION OF N_{TRANS} FOR AIR BEARING WITH D = 0.75" AND $2h_o$ = .001" WHEN $\nu = 2.45 \times 10^{-2}$ in.^{2}/sec. AND $W_T = 80 \times 10^{-6}$ lb./sec.

For Transition

$$v'_{crit} = \frac{R'_{e_{crit}}\,\nu}{2h_o} = \frac{(1500 \text{ to } 2500)\ 2.45 \times 10^{-2}}{.001}$$

$$= 36{,}700 \text{ to } 61{,}200 \text{ in/sec}$$

and for $W_T = 80 \times 10^{-6}$ lb./sec.

$$v = \frac{\left(\frac{W_T}{\rho_b g}\right)}{2h_o \pi D} = \frac{\left(\frac{W_T}{\rho_a g\left(\frac{P_b}{P_a}\right)}\right)}{2h_o \pi D}$$

$$= \frac{\left(\frac{80 \times 10^{-6}}{4.32 \times 10^{-5}\left(\frac{19.7}{14.7}\right)}\right)}{.001\,\pi\,(.75)} = .293 \text{ in/sec}$$

where the mean bearing pressure is taken as 5 psig or 19.7 psia.

From equation (38), it is thus seen that

$$N_{trans} = \frac{120}{\pi D}\, v'_{crit} = \frac{120}{\pi(.75)}(36{,}700 \text{ to } 61{,}200)$$

$$= 187{,}000 \text{ to } 312{,}000 \text{ rpm}$$

since $(v/v'_{crit}) \approx 0$.

APPENDIX G

DETERMINATION OF ORIFICE DIAMETER FOR EXTERNALLY PRESSURIZED BEARING WITH FIXED EXTERNAL ORIFICE RESTRICTIONS FOR THE CASE WHEN THE FLUID IS AIR

The expression for W_{out} is given by equation (72) and W_{in} is given by equation (64). Making use of the steady-state continuity relationship of $W_{in} = W_{out}$, the value of d_o can be written as

$$d_o = \left\{ \frac{\left(\frac{B_A}{L_2 \ln\left(\frac{L_2}{L_1}\right)} + \frac{B_B}{L_3 \ln\left(\frac{L_3}{L_1}\right)} \right) h_o^3 \, \frac{P_a \rho_a}{12 \mu} \left(\left(\frac{P_{bo}}{P_a} \right)^2 - 1 \right)}{.0703 \, C \, P_s \, z^{.715} \left(1 - z^{.286} \right)^{\frac{1}{2}}} \right\}^{\frac{1}{2}}$$

$$= \left\{ \frac{50.5 \left(\frac{B_A}{L_2 \ln\left(\frac{L_2}{L_1}\right)} + \frac{B_B}{L_3 \ln\left(\frac{L_3}{L_1}\right)} \right) \frac{h_o^3}{C} q \left(\left(\frac{z}{q} \right)^2 - 1 \right)}{z^{.715} \left(1 - z^{.286} \right)^{\frac{1}{2}}} \right\}^{\frac{1}{2}} \quad (132)$$

Here it was assumed that the supply air is at a temperature of 70°F.

APPENDIX H

THEORETICAL BEARING STATIC STIFFNESS FOR EXTERNALLY PRESSURIZED SQUARE BEARING WITH VARIABLE EXTERNAL SPOOL VALVE RESTRICTION WITH STABILIZING FIXED EXTERNAL RESTRICTION

This bearing arrangement is shown in Fig. 31. The journal load is again expressed by equation (1). And if the stabilizing fixed external restriction is assumed to be a linear flow restriction or a linearized orifice, then p_{b2} and p_{b1} are again given by equation (28) and (29) respectively. Also the flow ratios Q_{b2}/Q_{bo} and Q_{b1}/Q_{bo} are again related to h_2/h_o and h_1/h_o by equations (4) and (5) respectively, and h_2/h_o and h_1/h_o are again in turn related to ϵ/h_o by equations (8) and (9) respectively. The definitions of β_2 and β_3 given by equation (30) and (31) respectively can also be employed.

The only real variation from the derivation for the journal static load-displacement relation for the bearing arrangement of Fig. 10 is the expression for x. Here no longer is x given by equation (32) but instead by

$$x = \frac{(p'_{s2} - p'_{s1}) A_c}{2 K_c} \tag{133}$$

where p'_{s2} and p'_{s1} are as defined in Fig. 31 and $(p'_{s2} - p'_{s1})$ can be obtained from equations (28) and (29) as

Finally by substituting equations (4), (5), (8), (9), (30), (31) and (138) into equations (28) and (29) and by substituting equations (28) and (29) into equation (1) and by making use of the relationships of

$$\frac{A_c P_0'''}{2K_c \ell} = C_c \left[1 - \left(\frac{\beta_2 + 1}{\beta_3} \right) \right] \tag{139}$$

and

$$|1 + \beta_4| = |\beta_3 - \beta_2| \quad , \tag{140}$$

equation (92) can be obtained.

BIBLIOGRAPHY

1. "National Machine Tool Show at Chicago," Engineer, London, Vol. 200, no. 5206, 5207, 5208, 5209; November 4, 1955, p. 676-3; November 11, 1955, p. 707-9; November 18, 1955, p. 743-5; November 25, 1955, p. 778-81

2. "Selected Designs of Machine Elements," Product Engineering, Vol. 26, no. 12, November 1955, p. 129-44.

3. "Plain Bearings for Machine Tools," Tool Engineer, Vol. 33, December 1954, p. 195-6.

4. Helmke, E. C., "Lubrication in the Machine Tool Field," ASME Paper No. 54-F-38.

5. The M.I.T. Observer, Vol. 6, No. 6, March 1960, M.I.T.

6. Fuller, D. D., "Theory and Practice of Lubrication for Engineers," J. Wiley and Sons, Inc., 1956.

7. Shaw, M. C. and Macks, E. F., "Analysis and Lubrication of Bearings," McGraw-Hill, New York, 1949.

8. Raimondi, A. A. and Boyd, J., "An Analysis of Orifice- and Capillary-Compensated Hydrostatic Journal Bearing," Lubrication Engineering, Vol. 13, No. 1, January, 1957, p. 28.

9. "Weatherhead Yellow Book," Industrial Catalog C-100, Weatherhead Company, Cleveland, Ohio, p. 39-54.

10. Hunsaker, J. C. and Rightmire, B. G., "Engineering Applications of Fluid Mechanics," McGraw-Hill, New York, 1947.

11. Mayer, J. E., Jr., "Externally Pressurized Spindle Bearing," Report of Metals Processing Division, Mechanical Engineering Department, M.I.T., October 1958.

12. Scher, R. S., "Theoretical and Laboratory Performance of a Pressurized Journal Bearing with Positional Feedback Control," S. M. Thesis, M.I.T., 1958.

13. Tao, L. N. and Donovan, W. F., "Through Flow in Concentric and Eccentric Annuli of Fine Clearance With and Without Relative Motion of the Boundaries," ASME Trans., Vol. 77, November, 1955, p. 1291-1301.

14. Croft, H. O., "Thermodynamic, Fluid Flow and Heat Transmission," McGraw-Hill, New York, 1938, p. 116.

15. Richardson, H. H., "Static and Dynamic Characteristics of Compensated Gas Bearings," ASME Trans., Vol. 80, No. 7, October, 1958, page 1503.

16. Rightmire, B. G., "Parallel-Surface Bearing Compressibility Effects," Bearing Technology (Special Summer Session Notes) Materials Processing Division, Mechanical Engineering Department, M.I.T., Chapter VI, 1959.

17. Faires, V. M., "Applied Thermodynamics," MacMillan Company, New York, 1950.

18. Fischer, G. K., Cherubim, J. L., and Fuller, D. D., "Some Instabilities and Operating Characteristics of High-Speed Gas-Lubricated Journal Bearings." ASME Paper No. 58-A-231, September 24, 1958.